

# A scalable estimate of the out-of-sample prediction error via approximate leave-one-out

Kamiar Rahnema Rad

Baruch College, City University of New York

and

Arian Maleki \*

Columbia University

## Abstract

The paper considers the problem of out-of-sample risk estimation under the high dimensional settings where standard techniques such as  $K$ -fold cross validation suffer from large biases. Motivated by the low bias of the leave-one-out cross validation (LO) method, we propose a computationally efficient closed-form approximate leave-one-out formula (ALO) for a large class of regularized estimators. Given the regularized estimate, calculating ALO requires minor computational overhead. With minor assumptions about the data generating process, we obtain a finite-sample upper bound for  $|\text{LO} - \text{ALO}|$ . Our theoretical analysis illustrates that  $|\text{LO} - \text{ALO}| \rightarrow 0$  with overwhelming probability, when  $n, p \rightarrow \infty$ , where the dimension  $p$  of the feature vectors may be comparable with or even greater than the number of observations,  $n$ . Our extensive numerical experiments show that  $|\text{LO} - \text{ALO}|$  decreases as  $n, p$  increase, revealing the excellent finite sample performance of ALO. We further illustrate the usefulness of our proposed out-of-sample risk estimation method by an example of real recordings from spatially sensitive neurons (grid cells) in the medial entorhinal cortex of a rat.

*Keywords:* High-dimensional statistics, Regularized estimation, Out-of-sample risk estimation, Cross validation, Generalized linear models.

## 1 Introduction

### 1.1 Main objectives

Consider a dataset  $\mathcal{D} = \{(y_1, \mathbf{x}_1), (y_2, \mathbf{x}_2), \dots, (y_n, \mathbf{x}_n)\}$  where  $\mathbf{x}_i \in \mathbb{R}^p$  and  $y_i \in \mathbb{R}$ . In many applications, we model these observations as independent and identically distributed draws from some joint distribution  $q(y_i | \mathbf{x}_i^\top \boldsymbol{\beta}^*) p(\mathbf{x}_i)$  where the superscript  $\top$  denotes the transpose of a vector. To estimate the parameter  $\boldsymbol{\beta}^*$

---

\*A.M. gratefully acknowledges NSF DMS grant 1810888.

in such models, researchers often use the optimization problem

$$\hat{\beta} \triangleq \arg \min_{\beta \in \mathbb{R}^p} \left\{ \sum_{i=1}^n \ell(y_i | \mathbf{x}_i^\top \beta) + \lambda r(\beta) \right\}, \quad (1)$$

where  $\ell$  is called the loss function, and is typically set to  $-\log q(y_i | \mathbf{x}_i^\top \beta)$  when  $q$  is known, and  $r(\beta)$  is called the regularizer. In many applications, such as parameter tuning or model selection, one would like to estimate the *out-of-sample prediction error*, defined as

$$\text{Err}_{\text{extra}} \triangleq \mathbb{E}[\phi(y_{\text{new}}, \mathbf{x}_{\text{new}}^\top \hat{\beta}) | \mathcal{D}], \quad (2)$$

where  $(y_{\text{new}}, \mathbf{x}_{\text{new}})$  is a new sample from the distribution  $q(y | \mathbf{x}^\top \beta^*)p(\mathbf{x})$  independent of  $\mathcal{D}$ , and  $\phi$  is a function that measures the closeness of  $y_{\text{new}}$  to  $\mathbf{x}_{\text{new}}^\top \hat{\beta}$ . A standard choice for  $\phi$  is  $-\log q(y | \mathbf{x}^\top \beta)$ . However, in general we may use other functions too. Since  $\text{Err}_{\text{extra}}$  depends on the rarely known joint distribution of  $(y_i, \mathbf{x}_i)$ , a core problem in model assessment is to estimate it from data.

This paper considers a computationally efficient approach to the problem of estimating  $\text{Err}_{\text{extra}}$  under the high-dimensional setting, where both  $n$  and  $p$  are large, but  $n/p$  is a fixed number, possibly less than one. This high dimensional setting has received a lot of attention [El Karoui, 2018, El Karoui et al., 2013, Bean et al., 2013, Donoho and Montanari, 2016, Nevo and Ritov, 2016, Su et al., 2017, Dobriban and Wager, 2018]. But the problem of estimating  $\text{Err}_{\text{extra}}$  has not been carefully studied in generality, and as a result the issues of the existing techniques and their remedies have not been explored. For instance, a popular technique in practice is the  $K$ -fold cross validation, where  $K$  is a small number, e.g. 3 or 5. Figure 1 compares the performance of the  $K$ -fold cross validation for 4 different values of  $K$  on a LASSO linear regression problem. This figure implies that in high-dimensional settings,  $K$ -fold cross validation suffers from a large bias, unless  $K$  is a large number. This bias is due to the fact that in high-dimensional settings the fold that is removed in the training phase, may have a major effect on the solution of (1). This claim can be easily seen for LASSO linear regression with an IID design matrix using phase transition diagrams [Donoho et al., 2011]. To summarize, as the number of folds increases, the bias of the estimates reduces at the expense of a higher computational complexity.

In this paper, we consider the most extreme form of cross validation, namely leave-one-out cross-validation (LO), which according to Figure 1 is the least biased cross validation based estimate of the out-of-sample error. We will use the fact that both  $n$  and  $p$  are large numbers to approximate LO for both smooth and non-smooth regularizers. Our estimate, called approximate leave-one-out (ALO), requires solving the optimization problem (1) once. Then, it uses  $\hat{\beta}$  to approximate LO without solving the optimization problem again. In addition to obtaining  $\hat{\beta}$ , ALO requires a matrix inversion and two matrix-matrix multiplications. Despite these extra steps ALO offers a significant computational saving

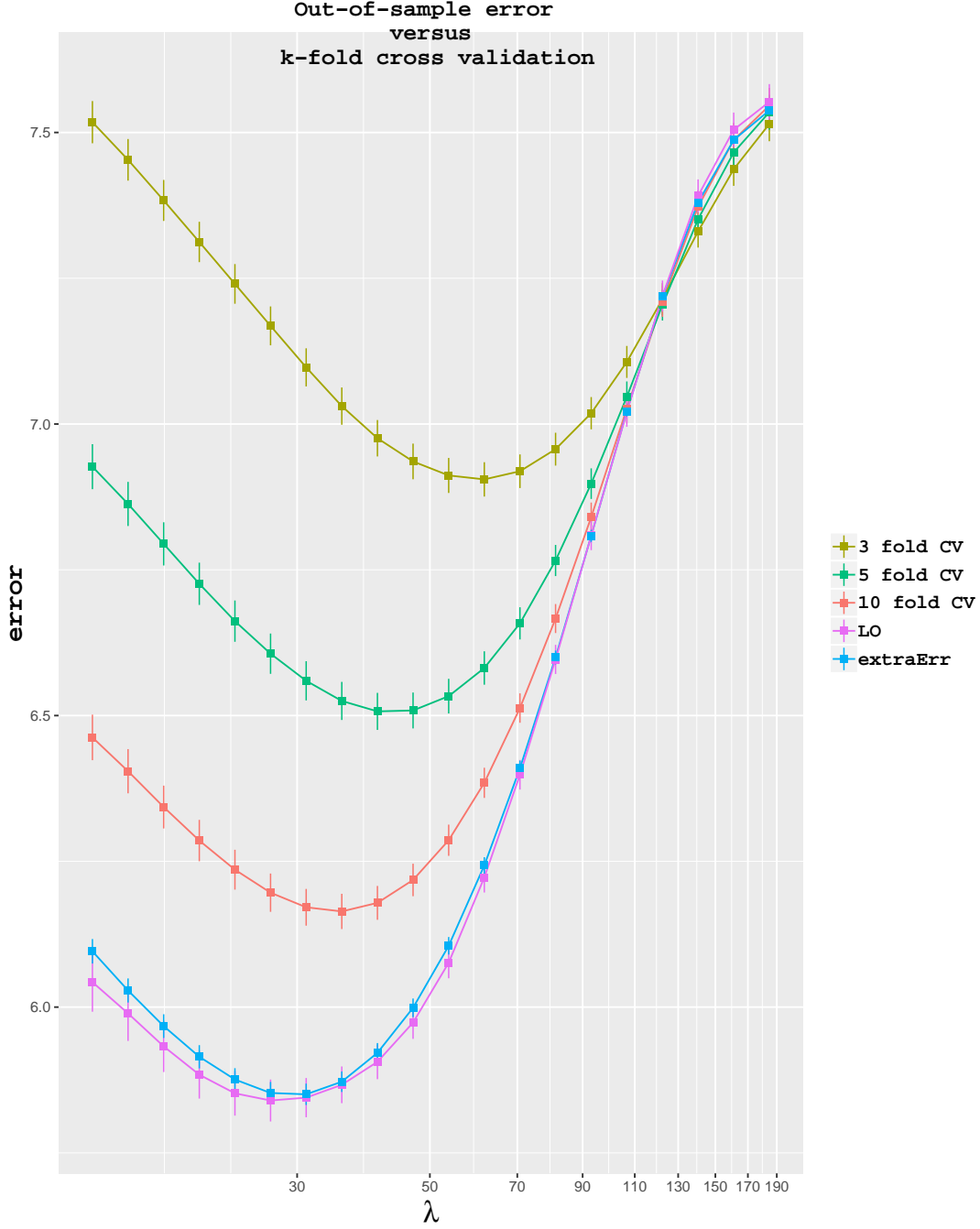


Figure 1: Comparison of  $K$ -fold cross validation (for  $K = 3, 5, 10$ ) and leave-one-out cross validation with the true (oracle-based) out-of-sample error for the LASSO problem where  $\ell(y|\mathbf{x}^\top \boldsymbol{\beta}) = \frac{1}{2}(y - \mathbf{x}^\top \boldsymbol{\beta})^2$  and  $r(\boldsymbol{\beta}) = \|\boldsymbol{\beta}\|_1$ . In high-dimensional settings the upward bias of  $K$ -fold CV clearly decreases as number of folds increase. Data is  $\mathbf{y} \sim N(\mathbf{X}\boldsymbol{\beta}^*, \sigma^2 \mathbf{I})$  where  $\mathbf{X} \in \mathbb{R}^{p \times n}$ . The number of nonzero elements of the true  $\boldsymbol{\beta}^*$  is set to  $k$  and their values is set to  $1/3$ . Dimensions are  $(p, n, k) = (1000, 250, 50)$  and  $\sigma = 2$ . The rows of  $\mathbf{X}$  are independent  $N(\mathbf{0}, \mathbf{I})$ . Extra-sample test data is  $y_{\text{new}} \sim N(\mathbf{x}_{\text{new}}^\top \boldsymbol{\beta}^*, \sigma^2)$  where  $\mathbf{x}_{\text{new}} \sim N(\mathbf{0}, \mathbf{I})$ . The true (oracle-based) out-of-sample prediction error is  $\text{Err}_{\text{extra}} = E[(y_{\text{new}} - \mathbf{x}_{\text{new}}^\top \hat{\boldsymbol{\beta}})^2 | \mathbf{y}, \mathbf{X}] = \sigma^2 + \|\hat{\boldsymbol{\beta}} - \boldsymbol{\beta}^*\|_2^2$ . All depicted quantities are averages based on 500 random independent samples, and error bars depict one standard error.

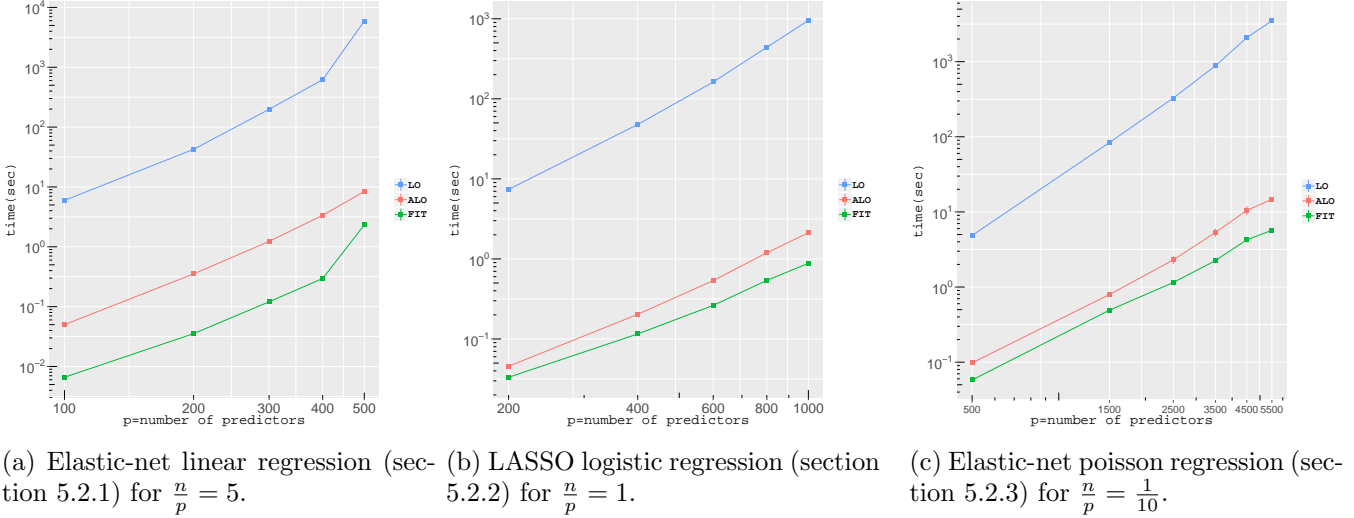


Figure 2: The time to compute ALO and LO. FIT refers to the time to fit  $\hat{\beta}$  and the ALO time includes computing  $\hat{\beta}$ . Calculating LO takes orders of magnitude longer than ALO.

compared to LO. This point is illustrated Figure 2 by comparing the computational complexity of ALO with that of LO and a single fit as both  $n$  and  $p$  increase for various data shapes, that is  $n > p$ ,  $n = p$ , and  $n < p$ . Details of this simulation are given in Section 5.2.4. Note that a readily usable R implementation of ALO is available online; see <https://github.com/Francis-Hsu/alocv> and the `alocv` package in R [He et al., 2018]. Moreover, all the codes for the figures presented in this paper are available here <https://github.com/RahnamaRad/ALO>.

Finally, to summarize a major point of this paper, we emphasize that despite the major reduction in the computational complexity of estimating the out-of-sample risk, the theoretical and empirical results presented in this paper reveal that under the high-dimensional settings ALO presents a sensible approximation of LO.

## 1.2 Relevant work

The problem of estimating  $\text{Err}_{\text{extra}}$  from  $\mathcal{D}$  has been studied for (at least) the past 50 years. Methods such as cross validation (CV) [Stone, 1974, Geisser, 1975], Allen’s PRESS statistic [Allen, 1974], generalized cross validation (GCV) [Craven and Wahba, 1979, Golub et al., 1979], and bootstrap [Efron, 1983] have been proposed for this purpose. In the high dimensional setting, employing LO or bootstrap is computationally infeasible and the less computationally demanding approaches such as 5-fold (or 10-fold) CV suffer from high bias as illustrated in Figure 1.

As for the computationally efficient approaches, extensions of Allen’s PRESS [Allen, 1974], and generalized cross validation (GCV) [Craven and Wahba, 1979, Golub et al., 1979] to non-linear models and classifiers with ridge penalty are well known: smoothing splines for generalized linear models in [O’Sullivan et al., 1986], spline estimation of generalized additive models [Burman, 1990], ridge estimators in logistic

regression in [Cessie and Houwelingen, 1992], smoothing splines with non-Gaussian data using various extensions of GCV in [Gu, 1992, Xiang and Wahba, 1996, Gu and Xiang, 2001], support vector machines [Opper and Winther, 2000], kernel logistic regression in [Cawley and Talbot, 2008], and Cox’s proportional hazard model with a ridge penalty in [Meijer and Goeman, 2013]. Despite the existence of this vast literature, the performance of such approximations in high-dimensional settings is unknown except for the straightforward linear ridge regression framework. Moreover, past heuristic approaches have only considered the ridge regularizer. The results of this paper include a much broader set of regularizers; examples include but are not limited to LASSO [Tibshirani, 1996], elastic net [Zou and Hastie, 2005] and bridge [Frank and Friedman, 1993], just to name a few.

More recently, a few papers have studied the problem of estimating  $\text{Err}_{\text{extra}}$  under high-dimensional settings [Mousavi et al., 2018, Obuchi and Kabashima, 2016]. The approximate message passing framework introduced in [Maleki, 2011, Donoho et al., 2009] was used in [Mousavi et al., 2018] to obtain an estimate of  $\text{Err}_{\text{extra}}$  for LASSO linear regression. In another related paper, [Obuchi and Kabashima, 2016] obtained similar results using approximations popular in statistical physics. The results of [Mousavi et al., 2018] and [Obuchi and Kabashima, 2016] are only valid for cases where the design matrix has IID entries and the empirical distribution of the regression coefficients converges weakly to a distribution with a bounded second moment. In this paper, our theoretical analysis includes correlated design matrices, and regularized estimators beyond LASSO linear regression.

In addition to these approaches, another contribution has been to study GCV and  $\text{Err}_{\text{extra}}$  for restricted least-squares estimators of submodels of the overall model without regularization [Breiman and Freedman, 1983, Leeb, 2008, Leeb, 2009]. In [Leeb, 2008] it was shown that a variant of GCV converges to  $\text{Err}_{\text{extra}}$  uniformly over a collection of candidate models provided that there are not too many candidate models, ruling out complete subset selection. Moreover, since restricted least-squares estimators are studied, the conclusions exclude the regularized problems considered in this paper.

Finally, it is worth mentioning that in another line of work, strategies have been proposed to obtain unbiased estimates of the in-sample error. In contrast to the out-of-sample error, the in-sample error is about the prediction of new responses for the same explanatory variables as in the training data. The literature of in-sample error estimation is too vast to be reviewed here. Mallows’s  $C_p$  [Mallows, 1973], Akaike’s Information Criterion (AIC) [Akaike, 1974, Hurvich and Tsai, 1989], Stein’s Unbiased Risk Estimate (SURE) [Stein, 1981, Zou et al., 2007, Tibshirani and Taylor, 2012] and Efron’s Covariance Penalty [Efron, 1986] are seminal examples of in-sample error estimators. When  $n$  is much larger than  $p$ , the in-sample prediction error is expected to be close to the out-of-sample prediction error. The problem is that in high-dimensional settings, where  $n$  is of the same order as (or even smaller than)  $p$ , the in-sample and out-of-sample errors are different.

The rest of the paper is organized as follows. After introducing the notations, we first present the

approximate leave-one-out formula (ALO) for twice differentiable regularizers in Section 2.1. In Section 2.2 we show how ALO can be extended to nonsmooth regularizers such as LASSO using Theorem 1 and Theorem 2. In Section 3, we compare the computational complexity and memory requirements of ALO and LO. In Section 4, we present Theorem 3, illustrating with minor assumptions about the data generating process that  $|\text{LO} - \text{ALO}| \rightarrow 0$  with overwhelming probability, when  $n, p \rightarrow \infty$ , where  $p$  may be comparable with or even greater than  $n$ . The numerical examples in Section 5 study the statistical accuracy and computational efficiency of the approximate leave-one-out approach. To illustrate the accuracy and computational efficiency of ALO we apply it to synthetic and real data in Section 5. We generate synthetic data, and compare ALO and LO for elastic-net linear regression in Section 5.2.1, LASSO logistic regression in Section 5.2.2, and elastic-net poisson regression in Section 5.2.3. For real data we apply LASSO, elastic-net and ridge logistic regression to sonar returns from two undersea targets in Section 5.3.1, and we apply LASSO poisson regression to real recordings from spatially sensitive neurons (grid cells) in Section 5.3.2. Our synthetic and real data examples cover various data shapes, that is  $n > p$ ,  $n = p$  and  $n < p$ . In Section 6 we discuss directions for future work. Technical proofs are collected in Section A, the appendix.

### 1.3 Notation

We first review the notations that will be used in the rest of the paper. Let  $\mathbf{x}_i^\top \in \mathbb{R}^{1 \times p}$  stand for the  $i$ th row of  $\mathbf{X} \in \mathbb{R}^{n \times p}$ .  $\mathbf{y}_{/i} \in \mathbb{R}^{(n-1) \times 1}$  and  $\mathbf{X}_{/i} \in \mathbb{R}^{(n-1) \times p}$  stand for  $\mathbf{y}$  and  $\mathbf{X}$ , excluding the  $i$ th entry  $y_i$  and the  $i$ th row  $\mathbf{x}_i^\top$ , respectively. The vector  $\mathbf{a} \odot \mathbf{b}$  stands for the entry-wise product of two vectors  $\mathbf{a}$  and  $\mathbf{b}$ . For two vectors  $\mathbf{a}$  and  $\mathbf{b}$ , we use  $\mathbf{a} < \mathbf{b}$  to indicate element-wise inequalities. Moreover,  $|\mathbf{a}|$  stands for the vector obtained by applying the element-wise absolute value to every element of  $\mathbf{a}$ . For a set  $S \subset \{1, 2, 3, \dots, p\}$ , let  $\mathbf{X}_S$  stand for the submatrix of  $\mathbf{X}$  restricted to *columns* indexed by  $S$ . Likewise, we let  $\mathbf{x}_{i,S} \in \mathbb{R}^{|S| \times 1}$  stand for subvector of  $\mathbf{x}_i$  restricted to the entries indexed by  $S$ . For a vector  $\mathbf{a}$ , depending on which notation is easier to read, we may use  $[\mathbf{a}]_i$  or  $a_i$  to denote the  $i$ th entry of  $\mathbf{a}$ . The diagonal matrix with elements of the vector  $\mathbf{a}$  is referred to as  $\text{diag}[\mathbf{a}]$ . Moreover, define

$$\begin{aligned} \dot{\phi}(y, z) &\triangleq \frac{\partial \phi(y, z)}{\partial z}, \quad \dot{\ell}_i(\boldsymbol{\beta}) \triangleq \frac{\partial \ell(y_i | z)}{\partial z} \Big|_{z=\mathbf{x}_i^\top \boldsymbol{\beta}}, \quad \ddot{\ell}_i(\boldsymbol{\beta}) \triangleq \frac{\partial^2 \ell(y_i | z)}{\partial z^2} \Big|_{z=\mathbf{x}_i^\top \boldsymbol{\beta}} \\ \dot{\boldsymbol{\ell}}_{/i}(\cdot) &\triangleq [\dot{\ell}_1(\cdot), \dots, \dot{\ell}_{i-1}(\cdot), \dot{\ell}_{i+1}(\cdot), \dots, \dot{\ell}_n(\cdot)]^\top, \\ \ddot{\boldsymbol{\ell}}_{/i}(\cdot) &\triangleq [\ddot{\ell}_1(\cdot), \dots, \ddot{\ell}_{i-1}(\cdot), \ddot{\ell}_{i+1}(\cdot), \dots, \ddot{\ell}_n(\cdot)]^\top. \end{aligned}$$

The notation  $\text{poly log } n$  denotes polynomial of  $\log n$  with a finite degree. Finally, let  $\sigma_{\max}(\mathbf{A})$  and  $\sigma_{\min}(\mathbf{A})$  stand for the largest and smallest singular values of  $\mathbf{A}$ , respectively.

## 2 Approximate leave-one-out

### 2.1 Twice differentiable losses and regularizers

The leave-one-out cross validation estimate is defined through the following formula:

$$\text{LO} \triangleq \frac{1}{n} \sum_{i=1}^n \phi(y_i, \mathbf{x}_i^\top \hat{\boldsymbol{\beta}}_{/i}), \quad (3)$$

where

$$\hat{\boldsymbol{\beta}}_{/i} \triangleq \arg \min_{\boldsymbol{\beta} \in \mathbb{R}^p} \left\{ \sum_{j \neq i} \ell(y_j | \mathbf{x}_j^\top \boldsymbol{\beta}) + \lambda r(\boldsymbol{\beta}) \right\}, \quad (4)$$

is the leave- $i$ -out estimate. If done naively, the calculation of LO asks for the optimization problem (4) to be solved  $n$  times, a computationally demanding task when  $p$  and  $n$  are large. To resolve this issue, we use the following simple strategy: Instead of solving (4) accurately, we use one step of the Newton method for solving (4) with initialization  $\hat{\boldsymbol{\beta}}$ . Note that this step requires both  $\ell$  and  $r$  to be twice differentiable. We will explain how this limitation can be lifted in the next section. The Newton step leads to the following simple approximation of  $\hat{\boldsymbol{\beta}}_{/i}$ :<sup>1</sup>

$$\tilde{\boldsymbol{\beta}}_{/i} = \hat{\boldsymbol{\beta}} + \left( \sum_{j \neq i} \mathbf{x}_j \mathbf{x}_j^\top \ddot{\ell}(y_j | \mathbf{x}_j^\top \hat{\boldsymbol{\beta}}) + \lambda \text{diag}[\ddot{\mathbf{r}}(\hat{\boldsymbol{\beta}})] \right)^{-1} \mathbf{x}_i \dot{\ell}(y_i | \mathbf{x}_i^\top \hat{\boldsymbol{\beta}}),$$

where  $\hat{\boldsymbol{\beta}}$  is defined in (1). Note that  $\sum_{j \neq i} \mathbf{x}_j \mathbf{x}_j^\top \ddot{\ell}(y_j | \mathbf{x}_j^\top \hat{\boldsymbol{\beta}}) + \lambda \text{diag}[\ddot{\mathbf{r}}(\hat{\boldsymbol{\beta}})]$  is still dependent on the observation that is removed. Hence, its inverse has to be calculated  $n$  times which is still computationally demanding.

We use the Woodberry lemma to reduce the computational cost:

$$\left( \sum_{j \neq i} \mathbf{x}_j \mathbf{x}_j^\top \ddot{\ell}(y_j | \mathbf{x}_j^\top \hat{\boldsymbol{\beta}}) + \lambda \text{diag}[\ddot{\mathbf{r}}(\hat{\boldsymbol{\beta}})] \right)^{-1} = \mathbf{J}^{-1} + \frac{\mathbf{J}^{-1} \mathbf{x}_i \ddot{\ell}(y_i | \mathbf{x}_i^\top \hat{\boldsymbol{\beta}}) \mathbf{x}_i^\top \mathbf{J}^{-1}}{1 - \mathbf{x}_i^\top \mathbf{J}^{-1} \mathbf{x}_i \ddot{\ell}(y_i | \mathbf{x}_i^\top \hat{\boldsymbol{\beta}})}, \quad (5)$$

where  $\mathbf{J} = (\sum_{j=1}^n \mathbf{x}_j \mathbf{x}_j^\top \ddot{\ell}(y_j | \mathbf{x}_j^\top \hat{\boldsymbol{\beta}}) + \lambda \text{diag}[\ddot{\mathbf{r}}(\hat{\boldsymbol{\beta}})])$ . Following this approach we define ALO as

$$\text{ALO} \triangleq \frac{1}{n} \sum_{i=1}^n \phi(y_i, \mathbf{x}_i^\top \tilde{\boldsymbol{\beta}}_{/i}) = \frac{1}{n} \sum_{i=1}^n \phi \left( y_i, \mathbf{x}_i^\top \hat{\boldsymbol{\beta}} + \left( \frac{\dot{\ell}_i(\hat{\boldsymbol{\beta}})}{\ddot{\ell}_i(\hat{\boldsymbol{\beta}})} \right) \left( \frac{H_{ii}}{1 - H_{ii}} \right) \right), \quad (6)$$

where

$$\mathbf{H} \triangleq \mathbf{X} \left( \lambda \text{diag}[\ddot{\mathbf{r}}(\hat{\boldsymbol{\beta}})] + \mathbf{X}^\top \text{diag}[\ddot{\boldsymbol{\ell}}(\hat{\boldsymbol{\beta}})] \mathbf{X} \right)^{-1} \mathbf{X}^\top \text{diag}[\ddot{\boldsymbol{\ell}}(\hat{\boldsymbol{\beta}})]. \quad (7)$$

Algorithm 1 summarizes how one should obtain an ALO estimate of the  $\text{Err}_{\text{extra}}$ . We will show that under the high-dimensional settings one Newton step is sufficient for obtaining a good approximation of  $\hat{\boldsymbol{\beta}}_{/i}$ , and

---

<sup>1</sup>Note that in the rest of the paper for notational simplicity of our theoretical results we have assumed that  $r(\boldsymbol{\beta}) = \sum_{i=1}^p r(\beta_i)$ . However, the extension to non-separable regularizers is straightforward.

the difference  $|\text{ALO} - \text{LO}|$  is small when either  $n$  or both  $n, p$  are large. However, before that we resolve the differentiability issue of the approach we discussed above.

---

**Algorithm 1** Risk estimation with ALO for twice differentiable losses and regularizers

---

**Input.**  $(\mathbf{x}_1, y_1), (\mathbf{x}_2, y_2), \dots, (\mathbf{x}_n, y_n)$ .

**Goal.** Estimating  $\text{Err}_{\text{extra}}$

1. Calculate  $\hat{\beta} = \arg \min_{\beta \in \mathbb{R}^p} \left\{ \sum_{i=1}^n \ell(y_i | \mathbf{x}_i^\top \beta) + \lambda r(\beta) \right\}$ .
  2. Obtain  $\mathbf{H} = \mathbf{X} \left( \lambda \text{diag}[\ddot{\mathbf{r}}(\hat{\beta})] + \mathbf{X}^\top \text{diag}[\ddot{\ell}(\hat{\beta})] \mathbf{X} \right)^{-1} \mathbf{X}^\top \text{diag}[\ddot{\ell}(\hat{\beta})]$ .
  3. The estimate of  $\text{Err}_{\text{extra}}$  is given by  $\frac{1}{n} \sum_{i=1}^n \phi \left( y_i, \mathbf{x}_i^\top \hat{\beta} + \left( \frac{\dot{\ell}_i(\hat{\beta})}{\ddot{\ell}_i(\hat{\beta})} \right) \left( \frac{H_{ii}}{1 - H_{ii}} \right) \right)$ .
- 

## 2.2 Nonsmooth regularizers

The Newton step, used in the derivation of ALO, requires the twice differentiability of the loss function and regularizer. However, in many modern applications non-smooth regularizers, such as LASSO, are preferable. In this section, we explain how ALO can be used for non-smooth regularizers. We start with the  $\ell_1$ -regularizer, and then extend it to the other bridge estimators. A similar approach can be used for other non-smooth regularizers. Consider

$$\hat{\beta} \triangleq \arg \min_{\beta \in \mathbb{R}^p} \left\{ \sum_{i=1}^n \ell(y_i | \mathbf{x}_i^\top \beta) + \lambda \|\beta\|_1 \right\}. \quad (8)$$

Let  $\hat{\mathbf{g}}$  be a subgradient of  $\|\beta\|_1$  at  $\hat{\beta}$ , denoted by  $\hat{\mathbf{g}} \in \partial \|\hat{\beta}\|_1$ . Then, the pair  $(\hat{\beta}, \hat{\mathbf{g}})$  must satisfy the zero-subgradient condition

$$\sum_{i=1}^n \mathbf{x}_i \dot{\ell}(y_i | \mathbf{x}_i^\top \hat{\beta}) + \lambda \hat{\mathbf{g}} = 0.$$

As a starting point we use a smooth approximation of the function  $\|\beta\|_1$  in our ALO formula. For instance, we can use the following approximation introduced in [Schmidt et al., 2007]:

$$r^\alpha(\beta) = \sum_{i=1}^p \frac{1}{\alpha} \left( \log(1 + e^{\alpha \beta_i}) + \log(1 + e^{-\alpha \beta_i}) \right).$$

Since  $\lim_{\alpha \rightarrow \infty} r^\alpha(\beta) = \|\beta\|_1$ , we can use

$$\hat{\beta}^\alpha \triangleq \arg \min_{\beta \in \mathbb{R}^p} \left\{ \sum_{i=1}^n \ell(y_i | \mathbf{x}_i^\top \beta) + \lambda \sum_{i=1}^p r^\alpha(\beta_i) \right\}, \quad (9)$$

to obtain the following formula for ALO:

$$\text{ALO}^\alpha \triangleq \frac{1}{n} \sum_{i=1}^n \phi \left( y_i, \mathbf{x}_i^\top \hat{\beta}^\alpha + \left( \frac{\dot{\ell}_i(\hat{\beta}^\alpha)}{\ddot{\ell}_i(\hat{\beta}^\alpha)} \right) \left( \frac{H_{ii}^\alpha}{1 - H_{ii}^\alpha} \right) \right) \quad (10)$$



where  $\mathbf{H}^\alpha \triangleq \mathbf{X} \left( \lambda \text{diag}[\ddot{\mathbf{r}}(\hat{\boldsymbol{\beta}}^\alpha)] + \mathbf{X}^\top \text{diag}[\ddot{\boldsymbol{\ell}}(\hat{\boldsymbol{\beta}}^\alpha)] \mathbf{X} \right)^{-1} \mathbf{X}^\top \text{diag}[\ddot{\boldsymbol{\ell}}(\hat{\boldsymbol{\beta}}^\alpha)]$ . Note that  $\|\hat{\boldsymbol{\beta}}^\alpha - \hat{\boldsymbol{\beta}}\|_2 \rightarrow 0$  as  $\alpha \rightarrow \infty$ , according to Lemma 3 in Section A.1. Therefore, we take the  $\alpha \rightarrow \infty$  limit in (10), yielding a simplification of  $\text{ALO}^\alpha$  in this limit. To prove this claim, we denote the active set of  $\hat{\boldsymbol{\beta}}$  with  $S$ , and we suppose the following:

**Assumption 1.**  $\hat{\boldsymbol{\beta}}$  is the unique global minimizer of (1).

**Assumption 2.**  $\hat{\boldsymbol{\beta}}^\alpha$  is the unique global minimizer of (9) for every value of  $\alpha$ .

**Assumption 3.**  $\ddot{\ell}(y|\mathbf{x}^\top \boldsymbol{\beta})$  is a continuous function of  $\boldsymbol{\beta}$ .

**Assumption 4.** The strict dual feasibility condition  $\|\hat{\mathbf{g}}_{S^c}\|_\infty < 1$  holds.

**Theorem 1.** If Assumptions 1,2,3 and 4 hold, then

$$\lim_{\alpha \rightarrow \infty} \text{ALO}^\alpha = \frac{1}{n} \sum_{i=1}^n \phi \left( y_i, \mathbf{x}_i^\top \hat{\boldsymbol{\beta}} + \left( \frac{\dot{\ell}_i(\hat{\boldsymbol{\beta}})}{\ddot{\ell}_i(\hat{\boldsymbol{\beta}})} \right) \left( \frac{H_{ii}}{1 - H_{ii}} \right) \right),$$

where  $\mathbf{H} = \mathbf{X}_S \left( \mathbf{X}_S^\top \text{diag}[\ddot{\boldsymbol{\ell}}(\hat{\boldsymbol{\beta}})] \mathbf{X}_S \right)^{-1} \mathbf{X}_S^\top \text{diag}[\ddot{\boldsymbol{\ell}}(\hat{\boldsymbol{\beta}})]$ .

The proof of this theorem is presented in Section A.1. In the simulation section, we show that the formula we obtain in Theorem 1 offers an accurate estimate of the out-of-sample prediction error. For instance, in the standard LASSO problem, where  $\ell(u, v) = (u - v)^2/2$  and  $r(\boldsymbol{\beta}) = \|\boldsymbol{\beta}\|_1$ , Theorem 1 gives the following estimate of the out-of-sample prediction error:

$$\lim_{\alpha \rightarrow \infty} \text{ALO}^\alpha = \frac{1}{n} \sum_{i=1}^n \frac{(y_i - \mathbf{x}_i^\top \hat{\boldsymbol{\beta}})^2}{(1 - H_{ii})^2}, \quad (11)$$

where  $\mathbf{H} = \mathbf{X}_S (\mathbf{X}_S^\top \mathbf{X}_S)^{-1} \mathbf{X}_S^\top$ . Figure 3 compares this estimate with the oracle estimate of the out-of-sample prediction error on a LASSO example. More extensive simulations are reported in Section 5.

Note that Assumptions 1,2 and 3 hold for most of the practical problems. For instance, to study the conditions under which Assumption 1 holds refer to [Tibshirani et al., 2013]. Moreover, for  $\ell(u, v) = (u - v)^2/2$ , Assumption 1 is a consequence of Assumption 4 [Wainwright, 2009]. Assumption 4 also holds in many cases with probability one with respect to the randomness of the dataset [Wainwright, 2009, Tibshirani and Taylor, 2012]. Even if this assumption is violated in a specific problem (note that checking this assumption is straightforward), we can use the following theorem to evaluate the accuracy of the ALO formula in Theorem 1.

**Theorem 2.** Let  $S$  and  $T$  denote the active set of  $\hat{\boldsymbol{\beta}}$ , and the set of zero coefficients at which the subgradient

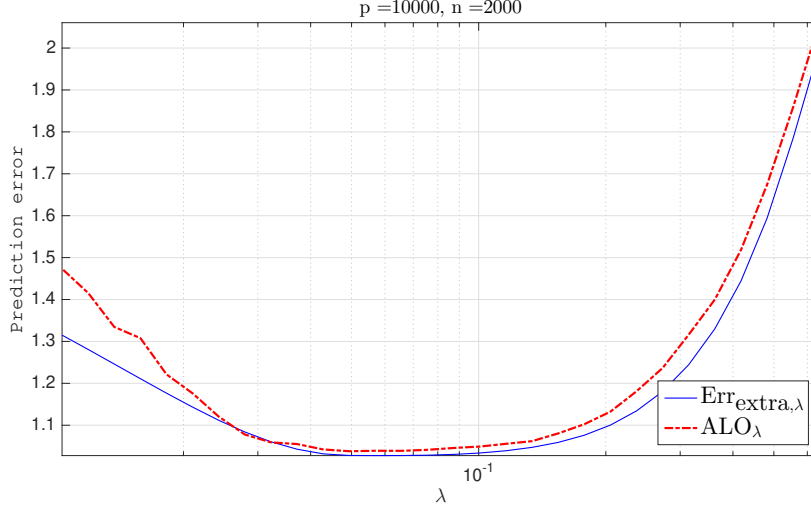


Figure 3: Out-of-sample prediction error versus ALO. Data is  $\mathbf{y} \sim \mathcal{N}(\mathbf{X}\beta^*, \sigma^2 \mathbf{I})$  where  $\sigma^2 = 1$  and  $\mathbf{X} \in \mathbb{R}^{p \times n}$  with  $p = 10000$  and  $n = 2000$ . The number of nonzero elements of the true  $\beta^*$  is set to  $k = 400$  and their values is set to 1. The rows  $\mathbf{x}_i^\top$  of the predictor matrix are generated randomly as  $\mathcal{N}(0, \Sigma)$  with correlation structure  $\text{cor}(X_{ij}, X_{ij'}) = 0.3$  for all  $i = 1, \dots, n$  and  $j, j' = 1, \dots, p$ . The covariance matrix  $\Sigma$  is scaled such the signal variance  $\text{var}(\mathbf{x}^\top \beta^*) = 1$ . Out-of-sample test data is  $y_{\text{new}} \sim \mathcal{N}(\mathbf{x}_{\text{new}}^\top \beta^*, \sigma^2)$  where  $\mathbf{x}_{\text{new}} \sim \mathcal{N}(0, \Sigma)$ . Out-of-sample error is calculated as  $E_{(y_{\text{new}}, \mathbf{x}_{\text{new}})}[(y_{\text{new}} - \mathbf{x}_{\text{new}}^\top \hat{\beta})^2 | \mathbf{y}, \mathbf{X}] = \sigma^2 + \|\Sigma^{1/2}(\hat{\beta} - \beta^*)\|_2^2$  and ALO is calculated using equation (11).

vector is equal to 1 or  $-1$ . Then,

$$\begin{aligned} \mathbf{x}_{i,S}^\top \left( \mathbf{X}_S^\top \text{diag}[\ddot{\ell}(\hat{\beta})] \mathbf{X}_S \right)^{-1} \mathbf{x}_{i,S} \ddot{\ell}_i(\hat{\beta}) &< \liminf_{\alpha \rightarrow \infty} H_{ii}^\alpha \\ \limsup_{\alpha \rightarrow \infty} H_{ii}^\alpha &< \mathbf{x}_{i,S \cup T}^\top \left( \mathbf{X}_{S \cup T}^\top \text{diag}[\ddot{\ell}(\hat{\beta})] \mathbf{X}_{S \cup T} \right)^{-1} \mathbf{x}_{i,S \cup T} \ddot{\ell}_i(\hat{\beta}) \end{aligned}$$

This Theorem is proved in A.2. A simple implication of this theorem is that

$$\limsup_{\alpha \rightarrow \infty} \text{ALO}^\alpha \leq \frac{1}{n} \sum_{i=1}^n \phi \left( y_i, \mathbf{x}_i^\top \hat{\beta} + \left( \frac{\dot{\ell}_i(\hat{\beta})}{\ddot{\ell}_i(\hat{\beta})} \right) \left( \frac{H_{ii}^h}{1 - H_{ii}^h} \right) \right), \quad (12)$$

and

$$\liminf_{\alpha \rightarrow \infty} \text{ALO}^\alpha \geq \frac{1}{n} \sum_{i=1}^n \phi \left( y_i, \mathbf{x}_i^\top \hat{\beta} + \left( \frac{\dot{\ell}_i(\hat{\beta})}{\ddot{\ell}_i(\hat{\beta})} \right) \left( \frac{H_{ii}^l}{1 - H_{ii}^l} \right) \right), \quad (13)$$

where

$$\begin{aligned} \mathbf{H}^l &= \mathbf{X}_S \left( \mathbf{X}_S^\top \text{diag}[\ddot{\ell}(\hat{\beta})] \mathbf{X}_S \right)^{-1} \mathbf{X}_S^\top \text{diag}[\ddot{\ell}(\hat{\beta})], \\ \mathbf{H}^h &= \mathbf{X}_{S \cup T} \left( \mathbf{X}_{S \cup T}^\top \text{diag}[\ddot{\ell}(\hat{\beta})] \mathbf{X}_{S \cup T} \right)^{-1} \mathbf{X}_{S \cup T}^\top \text{diag}[\ddot{\ell}(\hat{\beta})]. \end{aligned} \quad (14)$$

By comparing (12) and (13) we can evaluate the error in our simple formula of the risk, presented in Theorem 1. The approach we proposed above can be extended to other non-differentiable regularizers too. Below we consider two other popular classes of estimators: (i) bridge and (ii) elastic net, and show how we can derive ALO formulas for each estimator.

*Bridge estimators:* Consider the class of bridge estimators

$$\hat{\beta} \triangleq \arg \min_{\beta \in \mathbb{R}^p} \left\{ \sum_{i=1}^n \ell(y_i | \mathbf{x}_i^\top \beta) + \lambda \|\beta\|_q^q \right\}, \quad (15)$$

where  $q$  is a number between  $(1, 2)$ . Note that these regularizers are only one time differentiable at zero. Hence, the Newton method introduced in Section 2.1 is not directly applicable. One can argue intuitively that since the regularizer is differentiable at zero, none of the regression coefficients will be zero. Hence, the regularizer is locally twice differentiable and formula (6) works well. While this argument is often correct, we can again use the idea introduced above for LASSO to obtain the following ALO formula that can be used even when an estimate of 0 is observed:

$$\frac{1}{n} \sum_{i=1}^n \phi \left( y_i, \mathbf{x}_i^\top \hat{\beta} + \left( \frac{\dot{\ell}_i(\hat{\beta})}{\ddot{\ell}_i(\hat{\beta})} \right) \left( \frac{H_{ii}}{1 - H_{ii}} \right) \right), \quad (16)$$

where if we define  $S \triangleq \{i : \beta_i \neq 0\}$  and for  $u \neq 0$ ,  $\ddot{r}^q(u) \triangleq q(q-1)|u|^{q-2}$ , then

$$\mathbf{H} = \mathbf{X}_S \left( \mathbf{X}_S^\top \text{diag}[\ddot{\ell}(\hat{\beta})] \mathbf{X}_S + \lambda \text{diag}[\ddot{r}_S^q(\hat{\beta})] \right)^{-1} \mathbf{X}_S^\top \text{diag}[\ddot{\ell}(\hat{\beta})]. \quad (17)$$

This formula is derived in Section A.3.

*Elastic-net:* Finally, we consider the following elastic-net estimator

$$\hat{\beta} \triangleq \arg \min_{\beta \in \mathbb{R}^p} \left\{ \sum_{i=1}^n \ell(y_i | \mathbf{x}_i^\top \beta) + \lambda_1 \|\beta\|_2^2 + \lambda_2 \|\beta\|_1 \right\}. \quad (18)$$

Again by smoothing the  $\ell_1$ -regularizer (similar to what we did for LASSO) we obtain the following ALO formula for the out-of-sample predictor error:

$$\frac{1}{n} \sum_{i=1}^n \phi \left( y_i, \mathbf{x}_i^\top \hat{\beta} + \left( \frac{\dot{\ell}_i(\hat{\beta})}{\ddot{\ell}_i(\hat{\beta})} \right) \left( \frac{H_{ii}}{1 - H_{ii}} \right) \right),$$

where  $S = \{i : \hat{\beta}_i \neq 0\}$ , and

$$\mathbf{H} = \mathbf{X}_S \left( \mathbf{X}_S^\top \text{diag}[\ddot{\ell}(\hat{\beta})] \mathbf{X}_S + 2\lambda_1 \mathbf{I} \right)^{-1} \mathbf{X}_S^\top \text{diag}[\ddot{\ell}(\hat{\beta})]. \quad (19)$$

We do not derive this formula, since it follows exactly the same lines as those of LASSO and bridge. Algorithm 2 summarizes all the calculations required for the calculation of ALO for elastic-net.

---

**Algorithm 2** Risk estimation with ALO for elastic-net regularizer

---

**Input.**  $(\mathbf{x}_1, y_1), (\mathbf{x}_2, y_2), \dots, (\mathbf{x}_n, y_n)$ .

**Goal.** Estimating  $\text{Err}_{\text{extra}}$

1. Calculate  $\hat{\beta} = \arg \min_{\beta \in \mathbb{R}^p} \left\{ \sum_{i=1}^n \ell(y_i | \mathbf{x}_i^\top \beta) + \lambda_1 \|\beta\|_2^2 + \lambda_2 \|\beta\|_1 \right\}$ .
  2. Calculate  $S = \{i : \hat{\beta}_i \neq 0\}$ .
  3. Obtain  $\mathbf{H} = \mathbf{X}_S \left( \mathbf{X}_S^\top \text{diag}[\ddot{\ell}(\hat{\beta})] \mathbf{X}_S + 2\lambda_1 \mathbf{I} \right)^{-1} \mathbf{X}_S^\top \text{diag}[\ddot{\ell}(\hat{\beta})]$ , where  $\mathbf{X}_S$  only includes the columns of  $\mathbf{X}$  that are in  $S$ .
  4. The estimate of  $\text{Err}_{\text{extra}}$  is given by  $\frac{1}{n} \sum_{i=1}^n \phi \left( y_i, \mathbf{x}_i^\top \hat{\beta} + \left( \frac{\dot{\ell}_i(\hat{\beta})}{\ddot{\ell}_i(\hat{\beta})} \right) \left( \frac{H_{ii}}{1-H_{ii}} \right) \right)$ .
- 

### 3 Computational complexity and memory requirements of ALO

Counting the number of floating point operations algorithms require is a standard approach for comparing their computational complexities. In this section, we calculate and compare the number of operations required by ALO and LO. We first start with Algorithm 1 and then discuss Algorithm 2.

#### Algorithm 1

Before we start the calculations, we should warn the reader that in many cases the specific structure of the loss and/or the regularizer enables more efficient implementation of the formulas. However, here we consider the worst case scenario.

The first step of Algorithm 1 requires solving an optimization problem. Several different methods exist for solving this optimization problem. Here, we discuss the interior point method and the accelerated gradient descent algorithm. Suppose that our goal is to reach accuracy  $\epsilon$ . Then, interior point method requires  $O(\log(1/\epsilon))$  iterations to reach this accuracy, while accelerated gradient descent requires  $O(\frac{1}{\sqrt{\epsilon}})$  iterations [Nesterov, 2013]. Furthermore, each iteration of the accelerated gradient descent requires  $O(np)$  operations, while each iteration of the interior point method requires  $O(p^3)$  operations.

Regarding the memory usage of these two algorithms, note that in the accelerated gradient descent algorithm the memory is mainly used for storing matrix  $\mathbf{X}$ . Hence, the amount of memory that is required by this algorithm is  $O(np)$ . On the other hand, interior point method uses  $O(p^3)$  of memory.

The second step of Algorithm 1 is to calculate the matrix  $\mathbf{H}$ . This requires inverting the matrix  $\left( \lambda \text{diag}[\ddot{\ell}(\hat{\beta})] + \mathbf{X}^\top \text{diag}[\ddot{\ell}(\hat{\beta})] \mathbf{X} \right)^{-1}$ . In general, this inversion requires  $O(p^3)$  (e.g. by using Cholesky factorization). However, if  $n$  is much smaller than  $p$ , then one can use a better trick for performing the matrix inversion; suppose that both  $\ell$  and  $r$  are strongly convex at  $\hat{\beta}$  and define  $\mathbf{\Gamma} \triangleq (\text{diag}[\ddot{\ell}(\hat{\beta})])^{\frac{1}{2}}$ , and  $\mathbf{\Lambda} \triangleq \lambda \text{diag}[\ddot{\ell}(\hat{\beta})]$ . Then, from the matrix inversion lemma we have

$$\mathbf{X}(\mathbf{X}^\top \mathbf{\Gamma}^2 \mathbf{X} + \mathbf{\Lambda})^{-1} \mathbf{X}^\top = \mathbf{X} \mathbf{\Lambda}^{-1} \mathbf{X}^\top - \mathbf{X} \mathbf{\Lambda}^{-1} \mathbf{X}^\top \mathbf{\Gamma} (\mathbf{I} + \mathbf{\Gamma} \mathbf{X} \mathbf{\Lambda}^{-1} \mathbf{X}^\top \mathbf{\Gamma})^{-1} \mathbf{\Gamma} \mathbf{X} \mathbf{\Lambda}^{-1} \mathbf{X}^\top. \quad (20)$$

The inversion  $(\mathbf{I} + \mathbf{\Gamma}\mathbf{X}\mathbf{\Lambda}^{-1}\mathbf{X}^\top\mathbf{\Gamma})^{-1}$  requires  $O(n^3)$  operations and  $O(np)$  of memory (the main memory usage is for storing  $\mathbf{X}$ ). Also, the other matrix-matrix multiplications require  $O(n^2p+n^3)$  operations. Hence, overall if we use the matrix inversion lemma, then the calculation of  $\mathbf{H}$  requires  $O(n^3 + n^2p)$  operations. In summary, the calculation of  $\mathbf{H}$  requires  $O(\min(p^3 + np^2, n^3 + n^2p))$ . Also, the amount of memory that is required by the algorithm is  $O(np)$ . The last step of ALO, i.e. Step 3 in Algorithm 1, requires only  $O(np)$  operations. Hence, the calculations of ALO in Algorithm 1 requires

1. Through interior point method:  $O(\min(p^3 \log(1/\epsilon) + p^3 + np^2, p^3 \log(1/\epsilon) + n^3 + n^2p))$
2. Through accelerated gradient descent:  $O(\min(np\frac{1}{\sqrt{\epsilon}} + p^3 + np^2, np\frac{1}{\sqrt{\epsilon}} + n^3 + n^2p))$

Similarly, the calculation of the LO requires solving  $n$  optimization problem of the form (4). Hence, the number of floating point operations that are required for LO are:

1. Through interior point method:  $O(np^3 \log(1/\epsilon))$ .
2. Through accelerated gradient descent:  $O(n^2p\frac{1}{\sqrt{\epsilon}})$ .

## Algorithm 2

Note that in Algorithm 2, we have used the specific form of the regularizer and simplified the form of  $\mathbf{H}$ . Hence, this allows for faster calculation of  $\mathbf{H}$  and equivalently faster calculation of the ALO estimate. Again the first step of calculating ALO is to solve the optimization problem. Solving this optimization problem by the interior point method or accelerated proximal gradient descent requires  $O(p^3 \log(1/\epsilon))$  and  $O(np\frac{1}{\sqrt{\epsilon}})$  floating point operations respectively. The next step is to calculate  $\mathbf{H}$ . If  $\hat{\beta}$  is  $s$ -sparse, i.e., has only  $s$  non-zero coefficients, then the calculation of  $\mathbf{H}$  requires  $O(s^3 + ns^2)$  floating point operations. Also, the amount of memory required for this inversion is  $O(s^2)$ . Finally, the last step requires  $O(np)$  operations. Hence, calculating an ALO estimate of the risk requires:

1. Through interior point method:  $O(p^3 \log(1/\epsilon) + s^3 + ns^2 + np)$ .
2. Through accelerated proximal gradient descent:  $O(np\frac{1}{\sqrt{\epsilon}} + s^3 + ns^2 + np)$

The calculations of LO in the worst case is similar to what we had in the previous section:<sup>2</sup>

1. Through interior point method:  $O(np^3 \log(1/\epsilon))$ .
2. Through accelerated proximal gradient descent:  $O(n^2p\frac{1}{\sqrt{\epsilon}})$ .

In this section, we used the number of floating point operations to compare the computational complexity of ALO and LO. However, since this approach is based on the worst case scenarios and is not capable of

---

<sup>2</sup>It is known that after a finite number of iterations the estimates of proximal gradient descent becomes sparse, and hence the iterations require less operations. Hence, in practice the sparsity can reduce the computational complexity of calculating LO even though this gain is not captured in the worst case analysis of this section.

capturing the constants, it is less accurate than comparing the timing of algorithms through simulations. Hence, Section 5 compares the performance of ALO and LO through simulations.

## Memory usage

First, we discuss Algorithm 1. We only consider the accelerated gradient descent algorithm. As discussed above, the amount of memory that is required for Step 1 of ALO is  $O(np)$  (the main memory usage is for storing matrix  $\mathbf{X}$ ). For the second step, direct inversion of  $\left(\lambda \text{diag}[\ddot{\mathbf{r}}(\hat{\beta})] + \mathbf{X}^\top \text{diag}[\ddot{\ell}(\hat{\beta})]\mathbf{X}\right)^{-1}$  requires  $O(p^2)$  of memory. However, by using the formula derived in (20) the memory usage reduces to  $O(n^2)$  (for inverting  $(\mathbf{I} + \mathbf{\Gamma}\mathbf{X}\mathbf{\Lambda}^{-1}\mathbf{X}^\top\mathbf{\Gamma})^{-1}$ ). Hence, the total amount of memory required for the second step of Algorithm 1 is  $O(\min(np+n^2, np+p^2))$ :  $np$  for storing  $\mathbf{X}$  and  $n^2$  or  $p^2$  for calculating  $\left(\lambda \text{diag}[\ddot{\mathbf{r}}(\hat{\beta})] + \mathbf{X}^\top \text{diag}[\ddot{\ell}(\hat{\beta})]\mathbf{X}\right)^{-1}$ . The last step of ALO requires negligible amount of memory. Hence, the total amount of memory ALO requires especially when  $n < p$ , is  $O(np + n^2)$ , which is the same as  $O(np)$ . Note that the amount of memory required by LO is also  $O(np)$ , since it requires to store  $\mathbf{X}$ .

The situation is even more favorable for ALO in Algorithm 2; all the memory requirements are the same as before, except that the amount of memory that is required for the calculation and storing of  $\left(\mathbf{X}_S^\top \text{diag}[\ddot{\ell}(\hat{\beta})]\mathbf{X}_S + 2\lambda_1\mathbf{I}\right)^{-1}$  is  $O(s^2)$ .

## 4 Theoretical Results in High Dimensions

Below we mention three assumptions later used in our theoretical results. While all the assumptions and the theoretical results that will follow are mentioned for finite sample sizes, and can be used in different asymptotic settings, in our presentation we consider the high-dimensional asymptotic setting in which  $n, p \rightarrow \infty$  and  $n/p \rightarrow \delta_o$ , where  $\delta_o$  is a finite number bounded away from zero. Hence, if we write a constant as  $c(n)$ , it may be the case that the constant depends on both  $n$  and  $p$ , but since  $p \sim n/\delta_o$ , we drop the dependance on  $p$ . This simplification enables us to present our results with more readable notations. However, it is straightforward to remove this assumption and obtain more general results that can be useful for other asymptotic settings too.

**Assumption 5.** *The rows of  $\mathbf{X} \in \mathbb{R}^{n \times p}$  are independent zero mean Gaussian vectors with covariance  $\mathbf{\Sigma}$ . Let  $\rho_{\max}$  denote the largest eigenvalue of  $\mathbf{\Sigma}$ .*

**Assumption 6.** *There exist finite constants  $c_1(n)$  and  $c_2(n)$ , functions of  $n$ , such that for all  $i = 1, \dots, n$*

$$c_1(n) > \left\| \dot{\ell}(\hat{\beta}) \right\|_{\infty}, \quad (21)$$

$$c_2(n) > \sup_{t \in [0,1]} \frac{\|\ddot{\ell}_{/i}((1-t)\hat{\beta}_{/i} + t\hat{\beta}) - \ddot{\ell}_{/i}(\hat{\beta})\|_2}{\|\hat{\beta}_{/i} - \hat{\beta}\|_2}. \quad (22)$$

$$c_2(n) > \sup_{t \in [0,1]} \frac{\|\ddot{r}((1-t)\hat{\beta}_{/i} + t\hat{\beta}) - \ddot{r}(\hat{\beta})\|_2}{\|\hat{\beta}_{/i} - \hat{\beta}\|_2}. \quad (23)$$

**Assumption 7.** *There exists a constant  $\nu > 0$  such that for all  $i = 1, \dots, n$*

$$\inf_{t \in [0,1]} \sigma_{\min} \left( \lambda \operatorname{diag}[\ddot{r}(t\hat{\beta} + (1-t)\hat{\beta}_{/i})] + \mathbf{X}_{/i}^{\top} \operatorname{diag}[\ddot{\ell}_{/i}(t\hat{\beta} + (1-t)\hat{\beta}_{/i})] \mathbf{X}_{/i} \right) \geq \nu \quad (24)$$

where  $\sigma_{\min}(\mathbf{A})$  stands for the smallest singular value of  $\mathbf{A}$ .

All these assumptions can be weakened at the expense of making our final result look more complicated. For instance, the Gaussianity of the rows of  $X$  can be replaced with the subgaussianity assumption with minor changes in our final result. We expect our results (or slightly weaker ones) to hold even when the rows of  $X$  have heavier tails. However, for the sake of brevity we do not study such matrices in the current paper. Furthermore, the smoothness of the second derivatives of the loss function and the regularizer that is assumed in (22) and (23) can be weakened at the expense of slower convergence in Theorem 3. We will clarify this point in a footnote after (107) in the proof. Now based on these results we bound the difference  $|\text{ALO} - \text{LO}|$ . The proof is given in Section A.4.

**Theorem 3.** *If Assumptions 5, 6, and 7 are satisfied, then with probability at least  $1 - 2ne^{-p} - \frac{2n}{p^3} - \frac{2n}{(n-1)^3}$  the following bound is valid:*

$$\left| \mathbf{x}_i^{\top} \hat{\beta}_{/i} - \mathbf{x}_i^{\top} \hat{\beta} - \left( \frac{\dot{\ell}_i(\hat{\beta})}{\ddot{\ell}_i(\hat{\beta})} \right) \left( \frac{H_{ii}}{1 - H_{ii}} \right) \right| \leq \frac{C_o}{\sqrt{p}}, \quad (25)$$

where

$$\begin{aligned} C_o &\triangleq 32\sqrt{5} \left( \frac{c_1^2(n)c_2(n)(p\rho_{\max})^{3/2}}{\nu^3} \right) \left( 1 + \left( \sqrt{\frac{n}{p}} + 3 \right)^2 p\rho_{\max} \sqrt{\frac{n-1}{p} \frac{\log(n-1)}{\log p}} \right) \\ &\times \left( 1 + \frac{2c_1(n)c_2(n)\sqrt{5} \left( 1 + \left( \sqrt{\frac{n}{p}} + 3 \right)^2 p\rho_{\max} \right) \sqrt{p\rho_{\max}}}{\nu^2} \right). \end{aligned} \quad (26)$$

Moreover, if

$$c_3 \triangleq \max_{i=1,2,\dots,n} \sup_{|b_i| < \frac{C_o}{\sqrt{p}}} \left| \dot{\phi} \left( y_i, \mathbf{x}_i^{\top} \hat{\beta}_{/i} + b_i \right) \right|$$

then,

$$|\text{ALO} - \text{LO}| \leq \frac{c_3 C_o}{\sqrt{p}}. \quad (27)$$

In many high-dimensional problems, under the asymptotic setting  $n/p \rightarrow \delta_o$  for some  $\delta_o$  bounded away from zero, a refinement of the arguments presented in [El Karoui, 2018, Donoho and Montanari, 2016, Donoho et al., 2011, Bayati and Montanari, 2012, Weng et al., 2018] will offer  $C_o = O(\text{poly log } n)$ , and in turn  $|\text{ALO} - \text{LO}| = o_p(1)$ .<sup>3</sup> We clarify this point, through the ridge regression example in Appendix A.6.

Note that in the  $p$  fixed,  $n \rightarrow \infty$  regime, Theorem 3 fails to yield  $|\text{ALO} - \text{LO}| = o_p(1)$ . This is just an artifact of our proof. In Theorem 8 presented in Section A.7 we prove that under mild regularity conditions, error between ALO and LO is  $o_p(1/n)$  when  $n \rightarrow \infty$  and  $p$  is fixed. For the sake of brevity details are presented in Section A.7.

## 5 Numerical Experiments

### 5.1 Summary

To illustrate the accuracy and computational efficiency of ALO we apply it to synthetic and real data. We generate synthetic data, and compare ALO and LO for elastic-net linear regression in Section 5.2.1, LASSO logistic regression in Section 5.2.2, and elastic-net poisson regression in Section 5.2.3. For real data we apply LASSO, elastic-net and ridge logistic regression to sonar returns from two undersea targets in Section 5.3.1, and we apply LASSO poisson regression to real recordings from spatially sensitive neurons in Section 5.3.2. Our synthetic and real data examples cover various data shapes where  $n > p$ ,  $n = p$  and  $n < p$ .

Figures 4, 5, 6, 7, and the middle-lower panel of Figure 10 reveal that ALO offers a reasonably accurate estimate of LO for a large range of  $\lambda$ . These figures show that ALO deteriorates for extremely small values of  $\lambda$ , specially when  $p > n$ . This is not a serious issue because the  $\lambda$ s minimizing LO and ALO tend to be far from those small values.

The real data example in Section 5.3.1, illustrating ALO and LO in Figure 7, is about classifying sonar returns from two undersea targets using penalized logistic regression. The neuroscience example in Section 5.3.2 is about estimating an inhomogeneous spatial point process using an over-complete basis from a sparsely sampled two-dimensional space. Given the spatial nature of the problem, the design matrix  $\mathbf{X}$  is very sparse, which fails to satisfy the dense Gaussian design assumption we made in Theorem 3. Nevertheless, the lower middle panel of Figure 10 illustrates the excellent performance of ALO in approximating LO in an example where  $p = 10000$  and  $n = 3133$ .

Figure 2 compares the computational complexity(time) of a single fit, ALO and LO, as we increase

---

<sup>3</sup>The scaling of the design matrix  $\mathbf{X}$  and the regression coefficients will also be clarified in Appendix A.6.



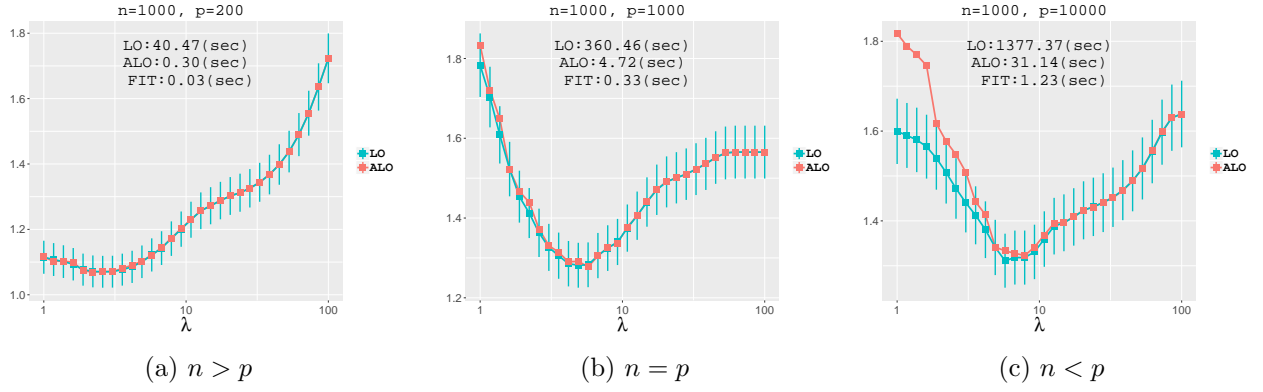


Figure 4: The ALO and LO mean square error for elastic-net linear regression. The red error bars identify the one standard error interval of LO.

$p$  while we keep the ratio  $\frac{n}{p}$  fixed. We consider various data shapes, models, and penalties. Figure 2a shows time versus  $p$  for elastic-net linear regression when  $\frac{n}{p} = 5$ . Figure 2b shows time versus  $p$  for LASSO logistic regression when  $\frac{n}{p} = 1$ . Figure 2c shows time versus  $p$  for elastic-net poisson regression when  $\frac{n}{p} = \frac{1}{10}$ . Finally, the middle-lower panel of Figure 10 shows that for the neuroscience example ALO takes 7 seconds in comparison to the 60428 seconds required by LO. All these numerical experiments illustrate the significant computational saving offered by ALO. As it pertains to the reported run times, all fittings in this paper were performed using a 3.1 GHz Intel Core i7 MacBook Pro with 16 GB of memory.

## 5.2 Simulations

In all the examples in this section (5.2.1, 5.2.2, 5.2.3 and 5.2.4), we let the true unknown parameter vector  $\beta^* \in \mathbb{R}^p$  to have  $k = n/10$  non-zero coefficients. The  $k$  non-zero coefficients are randomly selected, and their values are independently drawn from a zero mean unit variance Laplace distribution. The rows  $\mathbf{x}_1^\top, \dots, \mathbf{x}_n^\top$  of the design matrix  $\mathbf{X}$  are independently drawn from  $N(0, \Sigma)$ . We consider two correlation structures: 1) *Spiked*:  $\text{cor}(X_{ij}, X_{ij'}) = 0.5$ , and 2) *Toeplitz*:  $\text{cor}(X_{ij}, X_{ij'}) = 0.9^{|j'-j|}$ .  $\Sigma$  is scaled such that the signal variance  $\text{var}(\mathbf{x}_i^\top \beta^*) = 1$  regardless of the problem dimension. In this section, all the fittings and calculations of LO (and the one standard error interval of LO) were computed using the `glmnet` package in R [Friedman et al., 2010], and ALO was computed using the `alocv` package in R [He et al., 2018].

### 5.2.1 Linear regression with elastic-net penalty

We set  $\ell(y|\mathbf{x}^\top \beta) = \frac{1}{2}(y - \mathbf{x}^\top \beta)^2$ ,  $r(\beta) = \frac{(1-\alpha)}{2}\|\beta\|_2^2 + \alpha\|\beta\|_1$  and  $\alpha = 0.5$ . We let the rows  $\mathbf{x}_1^\top, \dots, \mathbf{x}_n^\top$  of  $\mathbf{X}$  to have a *Spiked* covariance and to generate data, we sample  $\mathbf{y} \sim N(\mathbf{X}\beta^*, \mathbf{I})$ . Moreover,  $\phi(y, \mathbf{x}^\top \beta) = (y - \mathbf{x}^\top \beta)^2$  so that  $\text{ALO} = \frac{1}{n} \sum_{i=1}^n \left( \frac{y_i - \mathbf{x}_i^\top \hat{\beta}}{1 - H_{ii}} \right)^2$  with  $\mathbf{H} = \mathbf{X}_S (\mathbf{X}_S^\top \mathbf{X}_S + \lambda(1-\alpha)\mathbf{I})^{-1} \mathbf{X}_S^\top$ . For various data shapes, that is  $\frac{n}{p} \in \{5, 1, \frac{1}{10}\}$ , we depict results in Figure 4 where reported times refer to the required time to fit the model, compute ALO and LO for a sequence of 30 logarithmically spaced tuning parameters from 1 to 100.

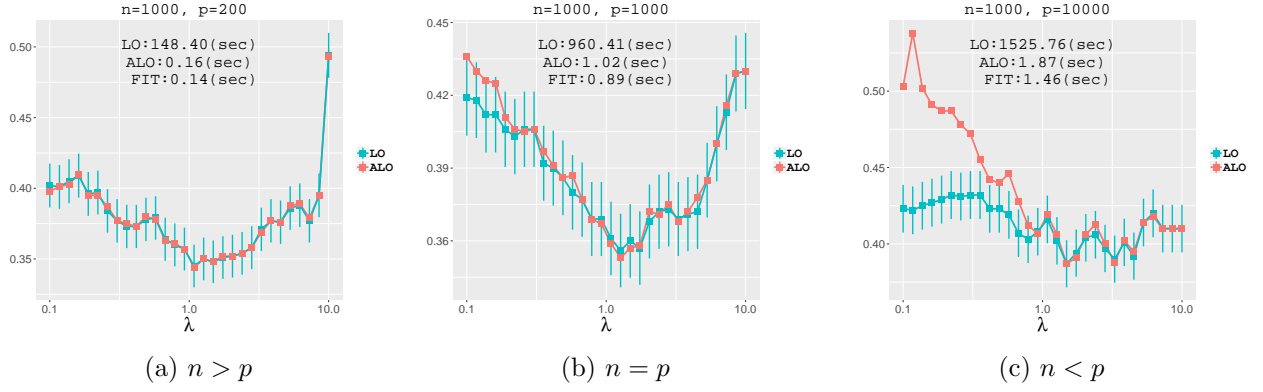


Figure 5: The ALO and LO misclassification errors (as a function of  $\lambda$ ) for LASSO logistic regression. The red error bars identify the one standard error interval of LO.

### 5.2.2 Logistic regression with LASSO penalty

We set  $\ell(y|\mathbf{x}^\top \boldsymbol{\beta}) = -y\mathbf{x}^\top \boldsymbol{\beta} + \log(1 + e^{\mathbf{x}^\top \boldsymbol{\beta}})$  (the negative logistic log-likelihood) and  $r(\boldsymbol{\beta}) = \|\boldsymbol{\beta}\|_1$ . We let the rows  $\mathbf{x}_1^\top, \dots, \mathbf{x}_n^\top$  of  $\mathbf{X}$  to have a *Toeplitz* covariance and to generate data, we sample  $y_i \sim \text{Binomial}\left(\frac{e^{\mathbf{x}_i^\top \boldsymbol{\beta}^*}}{1 + e^{\mathbf{x}_i^\top \boldsymbol{\beta}^*}}\right)$ . We take the misclassification rate as our measure of error, and  $1_{\{\mathbf{x}^\top \boldsymbol{\beta} > 0\}}$  as prediction, where  $1_{\{\cdot\}}$  is the indicator function, so that

$$\text{ALO} = \frac{1}{n} \sum_{i=1}^n \left| y_i - 1_{\{\mathbf{x}_i^\top \hat{\boldsymbol{\beta}} + \frac{\dot{\ell}_i(\hat{\boldsymbol{\beta}})}{\dot{\ell}_i(\hat{\boldsymbol{\beta}})} \frac{H_{ii}}{1 - H_{ii}} > 0\}} \right|$$

where  $\mathbf{H} = \mathbf{X}_S \left( \mathbf{X}_S^\top \text{diag}[\ddot{\ell}(\hat{\boldsymbol{\beta}})] \mathbf{X}_S \right)^{-1} \mathbf{X}_S^\top \text{diag}[\ddot{\ell}(\hat{\boldsymbol{\beta}})]$ ,  $\dot{\ell}_i(\hat{\boldsymbol{\beta}}) = \left( 1 + e^{-\mathbf{x}_i^\top \hat{\boldsymbol{\beta}}} \right)^{-1} - y_i$  and  $\ddot{\ell}_i(\hat{\boldsymbol{\beta}}) = e^{\mathbf{x}_i^\top \hat{\boldsymbol{\beta}}} \left( 1 + e^{\mathbf{x}_i^\top \hat{\boldsymbol{\beta}}} \right)^{-2}$ . For various data shapes, that is  $\frac{n}{p} \in \{5, 1, \frac{1}{10}\}$ , we depict results in Figure 5 where reported times refer to the required time to fit the model, compute ALO and LO for a sequence of 30 logarithmically spaced tuning parameters from 0.1 to 10.

### 5.2.3 Poisson regression with elastic-net penalty

We set  $\ell(y|\mathbf{x}^\top \boldsymbol{\beta}) = e^{y\mathbf{x}^\top \boldsymbol{\beta}} - y\mathbf{x}^\top \boldsymbol{\beta}$  (the negative poisson log-likelihood),  $r(\boldsymbol{\beta}) = \frac{(1-\alpha)}{2} \|\boldsymbol{\beta}\|_2^2 + \alpha \|\boldsymbol{\beta}\|_1$  and  $\alpha = 0.5$ . We let the rows  $\mathbf{x}_1^\top, \dots, \mathbf{x}_n^\top$  of  $\mathbf{X}$  to have a *Spiked* covariance and to generate data, we sample  $y_i \sim \text{Poisson}\left(e^{\mathbf{x}_i^\top \boldsymbol{\beta}^*}\right)$ . We use the mean absolute error as our measure of error, and  $e^{\mathbf{x}^\top \boldsymbol{\beta}}$  as prediction, so that

$$\text{ALO} = \frac{1}{n} \sum_{i=1}^n \left| y_i - e^{\mathbf{x}_i^\top \hat{\boldsymbol{\beta}} + \frac{\dot{\ell}_i(\hat{\boldsymbol{\beta}})}{\dot{\ell}_i(\hat{\boldsymbol{\beta}})} \frac{H_{ii}}{1 - H_{ii}}} \right|$$

where  $\mathbf{H} = \mathbf{X}_S \left( \mathbf{X}_S^\top \text{diag}[\ddot{\ell}(\hat{\boldsymbol{\beta}})] \mathbf{X}_S + \lambda(1 - \alpha)\mathbf{I} \right)^{-1} \mathbf{X}_S^\top \text{diag}[\ddot{\ell}(\hat{\boldsymbol{\beta}})]$ ,  $\dot{\ell}_i(\hat{\boldsymbol{\beta}}) = e^{\mathbf{x}_i^\top \hat{\boldsymbol{\beta}}} - y_i$ , and  $\ddot{\ell}_i(\hat{\boldsymbol{\beta}}) = e^{\mathbf{x}_i^\top \hat{\boldsymbol{\beta}}}$ . For various data shapes, that is  $\frac{n}{p} \in \{5, 1, \frac{1}{10}\}$ , we depict results in Figure 6 where reported times refer to the required time to fit the model, compute ALO and LO for a sequence of 30 logarithmically spaced tuning parameters from 1 to 100.

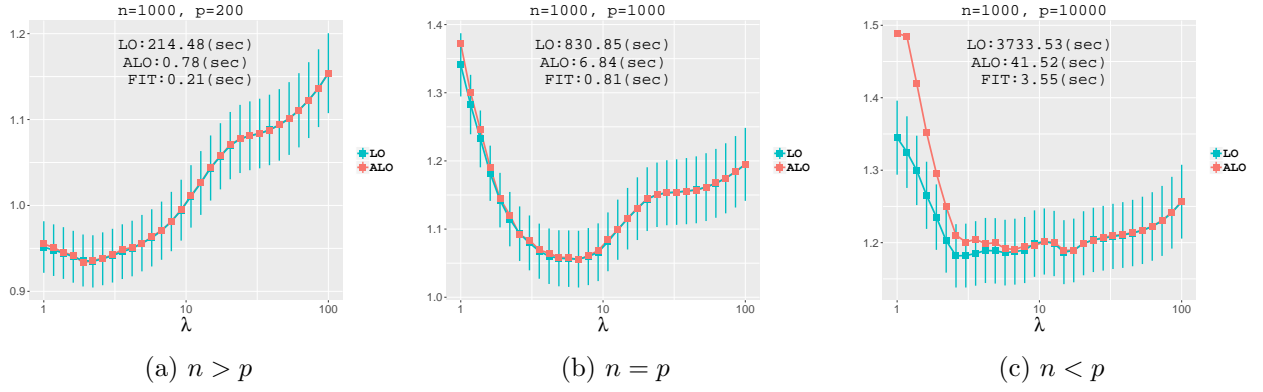


Figure 6: The ALO and LO mean absolute errors (as a function of  $\lambda$ ) for elastic-net poisson regression. The red error bars identify the one standard error interval of LO.

### 5.2.4 Timing simulations

To compare the timing of ALO with that of LO, we consider the following scenarios:

- Elastic-net linear regression, with rows of the design matrix having a *Spiked* covariance, data generated as described in Sections 5.2 and 5.2.1, and considered for a sequence of 10 logarithmically spaced tuning parameters from 1 to 100. We let  $\frac{n}{p} = 5$ .
- LASSO logistic regression, with rows of the design matrix having a *Toeplitz* covariance, data generated as described in Sections 5.2 and 5.2.2, and considered for a sequence of 10 logarithmically spaced tuning parameters from 0.1 to 10. We let  $\frac{n}{p} = 1$ .
- Elastic-net poisson regression, with rows of the design matrix having a *Spiked* covariance, data generated as described in Sections 5.2 and 5.2.3, and considered for a sequence of 10 logarithmically spaced tuning parameters from 1 to 100. We let  $\frac{n}{p} = \frac{1}{10}$ .

The timings of a single fit, ALO and LO versus model complexity  $p$  are illustrated in Figure 2. The reported timings are obtained by recording the time required to find a single fit and LO using the `glmnet` package in R [Friedman et al., 2010], and to find ALO using the `alocv` package in R [He et al., 2018], all along the tuning parameters above. This process is repeated 5 times to obtain the average timing.

## 5.3 Real Data

### 5.3.1 Sonar data

Here we use ridge, elastic-net and LASSO logistic regression to classify sonar returns collected from a metal cylinder and a cylindrically shaped rock positioned on a sandy ocean floor. The data consists of a set of  $n = 208$  returns, 111 cylinder returns and 97 rock returns, and  $p = 60$  spectral features extracted from the returning signals [Gorman and Sejnowski, 1988]. We use the misclassification rate as our measure of error. Numerical results comparing ALO and LO for ridge, elastic-net and LASSO logistic regression are depicted in Figure 7. The single fit and LO (and the one standard error interval of LO) were computed

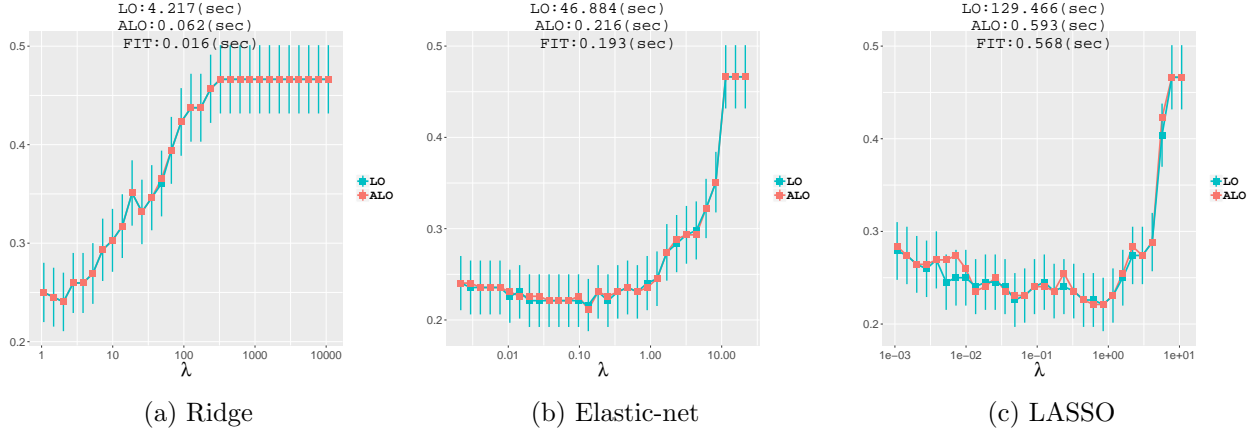


Figure 7: The ALO and LO deviances (as a function of  $\lambda$ ) for penalized logistic regression applied to the sonar data (Section 5.3.1) where  $n = 208$  and  $p = 60$ . The red error bars identify the one standard error interval of LO.

using the `glmnet` package in R [Friedman et al., 2010], and ALO was computed using the `alocv` package in R [He et al., 2018]. The values of the tuning parameters are a sequence of 30 logarithmically spaced tuning parameters between two value automatically selected by the `glmnet` package.

### 5.3.2 Spatial point process smoothing of grid cells: a neuroscience application

In this section, we compare ALO with LO on a real dataset. This dataset includes electrical recordings of single neurons in the entorhinal cortex, an area in the brain found to be particularly responsible for the navigation and perception of space in mammals [Moser et al., 2008]. The entorhinal cortex is also one of the areas pathologically affected in the early stages of Alzheimer’s disease, causing symptoms of spatial disorientation [Khan et al., 2014]. Moreover, the entorhinal cortex provides input to another area, the Hippocampus, which is involved in the cognition of space and the formation of episodic memory [Buzsaki and Moser, 2013].

Electrical recordings of single neurons in the medial domain of the entorhinal cortex (MEC) of freely moving rodents have revealed spatially modulated neurons, called grid cells, firing action potentials only around the vertices of two dimensional hexagonal lattices covering the environment in which the animal navigates. The hexagonal firing pattern of a single grid cell is illustrated in the left panel of Figure 8. These grid cells can be categorized according to the orientation of their triangular grid, the wavelength (distance between the vertices), and the phase (shift of the whole lattice). See the right panel of Figure 8 for an illustration of the orientation and wavelength of a single grid cell.

The data we analyze here consists of extra cellular recordings of several grid cells, and the simultaneously recorded location of the rat within a  $300\text{cm} \times 300\text{cm}$  box for roughly 20 minutes<sup>4</sup>. Since the number of

<sup>4</sup>The source of the data is [Stensola et al., 2012]. For a video of a single grid cell recorded in the MEC see the clip <https://www.youtube.com/watch?v=i9GiLBXWAHI>.

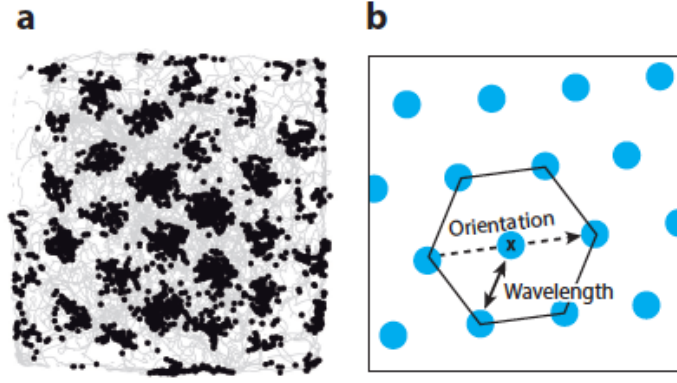


Figure 8: Left: Spike locations (black) are superimposed on the animal’s trajectory (grey). Firing fields are areas covered by a cluster of action potentials. Right: The firing fields of a grid cell form a periodic triangular matrix tiling the entire environment available to the animal. Figure is adapted from [Moser et al., 2014].

spikes fired by a grid cell depends mainly on the location of the animal, regardless of the animal’s speed and running direction [Hafting et al., 2005], it is reasonable to summarize this spatial dependency in terms of a rate map  $\eta(\mathbf{r})$ , where  $\eta(\mathbf{r})dt$  is the expected number of spikes emitted by the grid cell in a fixed time interval  $dt$ , given that the animal is located at position  $\mathbf{r}$  during this time interval [Rahnema Rad and Paninski, 2010, Pnevmatikakis et al., 2014, Dunn et al., 2015]. In other words, if the rat passes the same location again, we again expect the grid cell to fire at more or less the same rate<sup>5</sup>, specifically according to a Poisson distribution with mean  $\eta(\mathbf{r})dt$ . For each grid cell, the estimation of the rate map  $\eta(\mathbf{r})$  is a first step toward understanding the cortical circuitry underlying spatial cognition [Rowland et al., 2016]. Consequently, the estimation of firing fields without contamination from measurement noise or bias from over-smoothing will help to clarify important questions about neuronal algorithms underlying navigation in real and mental spaces [Buzsaki and Moser, 2013].

To be concrete, we discretize the two dimensional space into an  $m \times m$  grid, and discretize time into bins with width  $dt$ . In this example,  $dt$  is 0.4 seconds and  $m$  is 50. The experiment is 1252.9 seconds long, and therefore we have  $\lceil \frac{1252.9}{0.4} \rceil = 3133$  time bins. In other words,  $n = 3133$ . We use  $y_i \in \{0, 1, 2, 3, \dots\}$  to denote the number of action potentials observed in time interval  $[(i-1)dt, idt)$ , where  $i = 1, \dots, n$ . Moreover, we use  $\mathbf{r}_i \in \mathbb{R}^{m^2}$  to denote a vector composed of zeros except for a single +1 at the entry corresponding to the animal’s location within the  $m \times m$  grid during the time interval  $[(i-1)dt, idt)$ . We assume a log-linear model  $\log \eta(\mathbf{r}) = \mathbf{r}^\top \mathbf{z}$ , relating the firing rate at location  $\mathbf{r} \in \mathbb{R}^{m^2}$  to the latent vector  $\mathbf{z}$  where the  $m \times m$  latent spatial process responsible for the observed spiking activity is unraveled into  $\mathbf{z} \in \mathbb{R}^{m^2}$ . The firing rate can be written as  $\eta(\mathbf{r}_i) = \exp(\mathbf{r}_i^\top \mathbf{z})$ . Due to this notation,  $\mathbf{r}_i^\top \mathbf{z}$  is the value of  $\mathbf{z}$  at the animal’s location during the time interval  $[(i-1)dt, idt)$ . In this vein, the distribution of observed spiking activity can be written as

$$p(y_i | \mathbf{r}_i) = \frac{e^{-\eta(\mathbf{r}_i)} \eta(\mathbf{r}_i)^{y_i}}{y_i!}. \quad (28)$$

As mentioned earlier, the main goal is to estimate the two dimensional rate map  $\eta(\cdot)$ . Since it is known

<sup>5</sup>It is known that these rate maps can in some cases change with time but in most cases it is reasonable to assume them to be constant. Moreover, the two dimensional surface represented by  $\eta(\mathbf{r})$  is not the same for different grid cells.

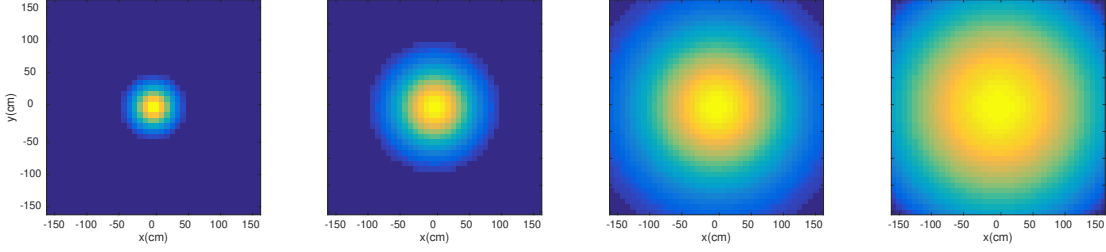


Figure 9: The four truncated Gaussian bumps

that the rate map of any single grid cell consists of bumps of elevated firing rates, located at various points in the two dimensional space, as illustrated in the left panel of Figure 8, it is reasonable to represent  $\mathbf{z}$  as a linear combination of  $\{\psi_1, \dots, \psi_p\}$ , an over-complete basis in  $\mathbb{R}^p$  [Brown et al., 2001, Pnevmatikakis et al., 2014, Dunn et al., 2015]. We compose the over-complete basis using truncated Gaussian bumps with various scales, distributed at all pixels. The four basic Gaussian bumps we use are depicted in Figure 9. Since we use four truncated Gaussian bumps for each pixel, in this example, we have a total of  $p = 4m^2 = 10000$  basis functions. We employ the truncated Gaussian bumps  $e^{-\frac{1}{2\sigma^2}(u_x^2 + u_y^2)} 1_{\left\{\exp\left(-\frac{1}{2\sigma^2}(u_x^2 + u_y^2)\right) > 0.05\right\}}$  where  $u_x$  and  $u_y$  are the horizontal and vertical coordinates. Define  $\Psi \in \mathbb{R}^{m^2 \times p}$  as a matrix composed of columns  $\{\psi_1, \dots, \psi_p\}$ . Furthermore, define  $\tilde{\mathbf{x}}_i \in \mathbb{R}^p$  as

$$\tilde{\mathbf{x}}_i \triangleq \Psi^\top \mathbf{r}_i,$$

and define  $\tilde{\mathbf{X}} \in \mathbb{R}^{n \times p}$  as a matrix composed of rows  $\{\tilde{\mathbf{x}}_1^\top, \dots, \tilde{\mathbf{x}}_n^\top\}$ . We normalize the columns of  $\tilde{\mathbf{X}}$ , calling the resulting matrix  $\mathbf{X}$ . The columns of  $\mathbf{X} \in \mathbb{R}^{n \times p}$  are unit normed. Formally,  $\mathbf{X} = \tilde{\mathbf{X}}\Gamma^{-1}$  where  $\Gamma \in \mathbb{R}^{p \times p}$  is a diagonal matrix filled with the column-norms of  $\tilde{\mathbf{X}}$ . We use  $\{\mathbf{x}_1^\top, \dots, \mathbf{x}_n^\top\}$  to refer to the rows of  $\mathbf{X}$ , yielding  $\eta(\mathbf{r}_i) = \exp(\mathbf{x}_i^\top \beta)$ . Note that due to the above mentioned rescaling, we have the following relationship between the latent map  $\mathbf{z}$  and  $\beta$ :  $\mathbf{z} = \Psi\Gamma\beta$ .

Sparsity of  $\beta$  refers to our prior understanding that the rate map of a grid cells consists of some bumps of elevated firing rates, located at various points in the two dimensional space, and therefore, our estimation problem is as follows:

$$\begin{aligned} \hat{\beta} &\triangleq \arg \min_{\beta \in \mathbb{R}^p} \left\{ \sum_{i=1}^n [\eta(\mathbf{r}_i) - y_i \log \eta(\mathbf{r}_i)] + \lambda \|\beta\|_1 \right\}, \\ &= \arg \min_{\beta \in \mathbb{R}^p} \left\{ \sum_{i=1}^n \left[ \exp(\mathbf{x}_i^\top \beta) - y_i \mathbf{x}_i^\top \beta \right] + \lambda \|\beta\|_1 \right\}. \end{aligned}$$

Here we use the negative log-likelihood in equation (28) as the cost function, that is,  $\phi(y, \mathbf{x}^\top \beta) = y\mathbf{x}^\top \beta - \exp(\mathbf{x}^\top \beta) + \log y!$ . We remind the reader that we will use ALO formula that was obtained in Theorem 1. Figures 10 illustrate that ALO is reasonable approximation of LO, allowing computationally efficient tuning of  $\lambda$ . To see the effect of  $\lambda$  of the rate map, we also present the maps resulting from small and large values of  $\lambda$ , leading to under and over smooth rate maps, respectively. As it pertains to the reported run times,

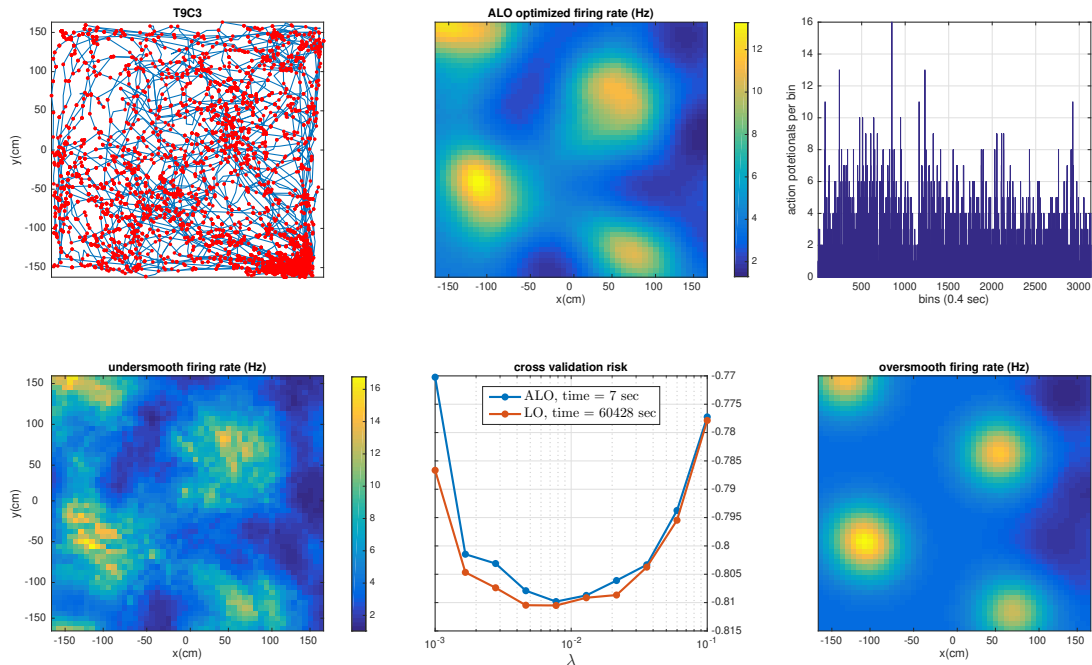


Figure 10: Top left: Spike locations (red) are superimposed on the animal’s trajectory (black). Firing fields are areas covered by a cluster of action potentials. The firing fields of a grid cell form a periodic triangular matrix tiling the entire environment available to the animal. Top middle: ALO-based firing rate. Top right: LO-based firing rate. Bottom left:  $\lambda = 0.001$ -based firing rate. Bottom middle: ALO and LO over a wide range of  $\lambda$ s. Bottom right:  $\lambda = 0.1$ -based firing rate.

all fittings in this section were performed using the `glmnet` package [Qian et al., 2013] in MATLAB.

## 6 Concluding Remarks

Leave-one-out cross validation (LO) is an intuitive and conceptually simple risk estimation technique. Despite its low bias in estimating the extra-sample prediction error, the high computational complexity of LO has limited its applications for high-dimensional problems. In this paper, by combining a single step of the Newton method with low-rank matrix identities, we obtained an approximate formula for LO, called ALO. We showed how ALO can be applied to popular non-differentiable regularizers, such as LASSO. With the aid of theoretical results and numerical experiments, we showed that ALO offers a computationally efficient and statistically accurate estimate of the extra-sample prediction error in high-dimensions.

Important directions for future work involve various approximations that further reduce the computational complexity. The computational bottleneck of ALO is the inversion of the large generalized hat matrix  $\mathbf{H}$ . This can make the application of ALO to ultra high dimensional problems computationally challenging. Since the diagonals of our  $\mathbf{H}$  matrix can be represented as leverage scores of an augmented  $\mathbf{X}$  matrix, scalable methods to approximately compute the leverage score may offer a promising avenue for future work. For example [Drineas and Woodruff, 2012] offers a randomized method to estimate the leverage scores. However, the randomized algorithm presented in [Drineas and Woodruff, 2012] applies to the  $p \ll n$  case, making it challenging to apply these methods to high-dimensional settings where  $p$  is also very large. Nevertheless this is certainly a promising direction for speeding up ALO.

In another line of work, the generalized cross-validation approach [Craven and Wahba, 1979, Golub et al., 1979] approximates the diagonal elements of  $\mathbf{H}$  with  $\text{tr}(\mathbf{H})/n$ . Computationally efficient randomized estimates of  $\text{tr}(\mathbf{H})$  can be produced without having any explicit calculations of this matrix [Deshpande and Girard, 1991, Wahba et al., 1995, Girard, 1998, Lin et al., 2000]. The theoretical study of the additional errors introduced by these randomized approximations, and the scalable implementations of them is another promising avenue for future work.

## References

- [Akaike, 1974] Akaike, H. (1974). A new look at the statistical model identification. *IEEE transactions on automatic control*, 19(6):716–723.
- [Allen, 1974] Allen, D. (1974). The relationship between variable selection and data augmentation and a method for prediction. *Technometrics*, 16:125–127.
- [Bayati and Montanari, 2012] Bayati, M. and Montanari, A. (2012). The lasso risk for gaussian matrices. *IEEE Transactions on Information Theory*, 58(4):1997–2017.
- [Bean et al., 2013] Bean, D., Bickel, P. J., El Karoui, N., and Yu, B. (2013). Optimal m-estimation in high-dimensional regression. *Proceedings of the National Academy of Sciences*, 110(36):14563–14568.
- [Boucheron et al., 2013] Boucheron, S., Lugosi, G., and Massart, P. (2013). *Concentration inequalities: A nonasymptotic theory of independence*. Oxford University Press.
- [Breiman and Freedman, 1983] Breiman, L. and Freedman, D. (1983). How many variables should be entered in a regression equation? *Journal of American Statistical Association*, 78(381):131–136.
- [Brown et al., 2001] Brown, E., Nguyen, D., Frank, L., Wilson, M., and Solo, V. (2001). An analysis of neural receptive field plasticity by point process adaptive filtering. *PNAS*, 98:12261–12266.
- [Burman, 1990] Burman, P. (1990). Estimation of generalized additive models. *Journal of Multivariate Analysis*, 32:230–255.
- [Buzsaki and Moser, 2013] Buzsaki, G. and Moser, E. (2013). Memory, navigation and theta rhythm in the hippocampal-entorhinal system. *Nat Neurosci*, 16(2):130–138.
- [Cawley and Talbot, 2008] Cawley, G. and Talbot, N. (2008). Efficient approximate leave-one-out cross-validation for kernel logistic regression. *Machine Learning*, 71:243–264.
- [Cessie and Houwelingen, 1992] Cessie, S. and Houwelingen, J. (1992). Ridge estimators in logistic regression. *Applied Statistics*, 41(1):191–201.
- [Craven and Wahba, 1979] Craven, P. and Wahba, G. (1979). Estimating the correct degree of smoothing by the method of generalized cross-validation. *Numerische Mathematik*, 31:377–403.
- [Deshpande and Girard, 1991] Deshpande, L. and Girard, D. (1991). Fast computation of cross-validated robust Splines and other non-linear smoothing Splines. *Curves and Surfaces*, pages 143–148.



- [Dobriban and Wager, 2018] Dobriban, E. and Wager, S. (2018). High-dimensional asymptotics of prediction: Ridge regression and classification. *Ann. Stat.*, 46(1):247–279.
- [Donoho et al., 2011] Donoho, D., Maleki, A., and Montanari, A. (2011). Noise sensitivity phase transition. *IEEE Trans. Inform. Theory*, 57(10).
- [Donoho and Montanari, 2016] Donoho, D. and Montanari, A. (2016). High dimensional robust m-estimation: Asymptotic variance via approximate message passing. *Probab Theory Relat Fields*, 166(3-4):935–969.
- [Donoho et al., 2009] Donoho, D. L., Maleki, A., and Montanari, A. (2009). Message passing algorithms for compressed sensing. *Proc. Natl. Acad. Sci.*, 106(45):18914–18919.
- [Drineas and Woodruff, 2012] Drineas, P., M.-I. M. M. M. and Woodruff, D. (2012). Fast approximation of matrix coherence and statistical leverage. *Journal of Machine Learning Research*, 13:3475–3506.
- [Dunn et al., 2015] Dunn, B., Morreaunet, M., and Roudi, Y. (2015). Correlations and functional connections in a population of grid cells. *PLOS Computational Biology*, 11(2):e1004052.
- [Efron, 1983] Efron, B. (1983). Estimating the error rate of a prediction rule: Improvement on cross-validation. *JASA*, 78(382):316–331.
- [Efron, 1986] Efron, B. (1986). How biased is the apparent error rate of a prediction rule? *JASA*, 81:461–470.
- [El Karoui, 2018] El Karoui, N. (2018). On the impact of predictor geometry on the performance on high-dimensional ridge-regularized generalized robust regression estimators. *Probab. Theory Relat. Fields*, 170:95–175.
- [El Karoui et al., 2013] El Karoui, N., Bean, D., Bickel, P., Lim, C., and Yu, B. (2013). On robust regression with high-dimensional predictors. *PNAS*, 110(36):14557–14562.
- [Frank and Friedman, 1993] Frank, I. and Friedman, J. (1993). A statistical view of some chemometric regression tools (with discussion). *Technometrics*, 35:109–148.
- [Friedman et al., 2010] Friedman, F., Hastie, T., and Tibshirani, R. (2010). Regularization paths for generalized linear models via coordinate descent. *Journal of Statistical Software*, 33(1):1–22.
- [Geisser, 1975] Geisser, S. (1975). The predictive sample reuse method with applications. *Journal of American Statistical Association*, 70(350):320–328.
- [Girard, 1998] Girard, D. (1998). Asymptotic comparison of (partial) cross-validation, GCV and randomized GCV in nonparametric regression. *Ann. Statist.*, 26(1):315–334.
- [Golub et al., 1979] Golub, G., Heath, M., and Wahba, G. (1979). Generalized cross-validation as a method for choosing a good ridge parameter. *Technometrics*, 21(2):215–223.
- [Gorman and Sejnowski, 1988] Gorman, R. and Sejnowski, T. (1988). Analysis of hidden units in a layered network trained to classify sonar targets. *Neural Networks*, 1:75–89.
- [Gu, 1992] Gu, C. (1992). Cross-validating non-gaussian data. *J. Comp. Graph. Stat.*, 1(2):169–179.
- [Gu and Xiang, 2001] Gu, C. and Xiang, D. (2001). Cross-validating non-gaussian data: Generalized approximate cross-validation revisited. *J. Comp. Graph. Stat.*, 10(3):581–591.

- [Hafting et al., 2005] Hafting, T., Fyhn, M., Molden, S., Moser, M., and Moser, E. (2005). Microstructure of a spatial map in the entorhinal cortex. *Nature*, 436:801–806.
- [He et al., 2018] He, L., Qin, W., Xu, P., and Zhou, Y. (2018). *alocv: Approximate Leave-One-Out Risk Estimation*. R package version 0.02.
- [Hurvich and Tsai, 1989] Hurvich, C. and Tsai, C. (1989). Regression and time series model selection in small samples. *Biometrika*, 76(2).
- [Khan et al., 2014] Khan, U., Liu, L., Provenzano, F. A., Berman, D., Profacia, C., Sloa, R., Mayeux, R., Duff, K., and Small, S. (2014). Molecular drivers and cortical spread of lateral entorhinal cortex dysfunction in preclinical alzheimer’s disease. *Nat. Neurosci.*, 17:304–311.
- [Leeb, 2008] Leeb, H. (2008). Evaluation and selection of models for out-of-sample prediction when the sample size is small relative to the complexity of the data-generating process. *Bernoulli*, pages 661–690.
- [Leeb, 2009] Leeb, H. (2009). Conditional predictive inference post model selection. *Ann. Stat.*, 37(5B):2838–2876.
- [Lin et al., 2000] Lin, X., Wahba, G., Xiang, D., Gao, F., Klein, R., and Klein, B. (2000). Smoothing spline ANOVA models for large data sets with Bernoulli observations and the randomized GACV. *Ann. Stat.*, 28(6):1570–1600.
- [Maleki, 2011] Maleki, A. (2011). Approximate message passing algorithm for compressed sensing. *Stanford University PhD Thesis*.
- [Mallows, 1973] Mallows, C. (1973). Some comments on  $c_p$ . *Technometrics*, 15:661–675.
- [Meijer and Goeman, 2013] Meijer, R. and Goeman, J. (2013). Efficient approximate k-fold and leave-one-out cross-validation for ridge regression. *Biometrical Journal*, 55(2):141–155.
- [Moser et al., 2008] Moser, E., Kropff, E., and Moser, M. (2008). Place cells, grid cells, and the brain’s spatial representation system. *Ann. Rev. Neurosci.*, 31:69–89.
- [Moser et al., 2014] Moser, E., Moser, M., and Roudi, Y. (2014). Network mechanisms of grid cells. *Phil. Trans. R. Soc. B*, 369(1635).
- [Mousavi et al., 2018] Mousavi, A., Maleki, A., Baraniuk, R. G., et al. (2018). Consistent parameter estimation for lasso and approximate message passing. *The Annals of Statistics*, 46(1):119–148.
- [Nesterov, 2013] Nesterov, Y. (2013). *Introductory lectures on convex optimization: A basic course*, volume 87. Springer Science & Business Media.
- [Nevo and Ritov, 2016] Nevo, D. and Ritov, Y. (2016). On Bayesian robust regression with diverging number of predictors. *Electron. J. Statist.*, 10(2):3045–3062.
- [Obuchi and Kabashima, 2016] Obuchi, T. and Kabashima, Y. (2016). Cross validation in lasso and its acceleration. *J. Stat. Mech. Theor. Exp.*, 53(304):1–36.
- [Opper and Winther, 2000] Opper, M. and Winther, O. (2000). Gaussian processes and SVM: Mean field results and leave-one-out. In Smola, A., Bartlett, P., Scholkopf, B., and Schuurmans, D., editors, *Advances Large Margin Classifiers*, pages 43–56. MIT Press, Cambridge, MA.

- [O’Sullivan et al., 1986] O’Sullivan, F., Yandell, B., and Raynor, W. (1986). Automatic smoothing of regression functions in generalized linear models. *JASA*, 81(393):96–103.
- [Pnevmatikakis et al., 2014] Pnevmatikakis, E., Rahnema Rad, K., Huggins, J., and Paninski, L. (2014). Fast Kalman filtering and forward-backward smoothing via low-rank perturbative approach. *J. Comp. Graph. Stat.*, 23(316-339).
- [Qian et al., 2013] Qian, J., Hastie, T., Friedman, J., Tibshirani, R., and Simon, N. (2013). Glmnet for Matlab.
- [Rahnema Rad and Paninski, 2010] Rahnema Rad, K. and Paninski, L. (2010). Efficient estimation of two-dimensional firing rate surfaces via Gaussian process methods. *Computation in Neural Systems*, 21:142–168.
- [Rowland et al., 2016] Rowland, D., Roudi, Y., Moser, M., and Moser, E. (2016). Ten years of grid cells. *Ann. Rev. Neurosci.*, 39:19–40.
- [Schmidt et al., 2007] Schmidt, M., Fung, G., and Rosales, R. (2007). Fast optimization methods for l1 regularization: A comparative study and two new approaches. In *ECML*, pages 286–297. Springer.
- [Stein, 1981] Stein, C. (1981). Estimation of the mean of a multivariate normal. *Ann. Stat.*, 9(6):1135–1151.
- [Stensola et al., 2012] Stensola, H., Stensola, T., Solstad, T., Froland, K., Moser, M., and Moser, E. (2012). The entorhinal grid map is discretized. *Nature*, 492(7427):72–80.
- [Stone, 1974] Stone, M. (1974). Cross-validatory choice and assesment of statistical predictions. *J R Stat Soc Series B*, 36(2):111–147.
- [Stone, 1977] Stone, M. (1977). An asymptotic equivalence of choice of model by cross-validation and akaike’s criterion. *J R Stat Soc Series B*, pages 44–47.
- [Su et al., 2017] Su, W., Bogdan, M., and Candes, E. (2017). False discoveries occur early on the Lasso path. *Ann. Stat.*, 45(5):2133–2150.
- [Tibshirani, 1996] Tibshirani, R. (1996). Regression shrinkage and selection via the lasso. *Journal of the Royal Statistical Society. Series B*, 58:267–288.
- [Tibshirani and Taylor, 2012] Tibshirani, R. and Taylor, J. (2012). Degrees of freedom in lasso problems. *Annals of Statistics*, 40(2):1198–1232.
- [Tibshirani et al., 2013] Tibshirani, R. J. et al. (2013). The lasso problem and uniqueness. *Electronic Journal of Statistics*, 7:1456–1490.
- [Van der Vaart, 2000] Van der Vaart, A. W. (2000). *Asymptotic statistics*, volume 3. Cambridge university press.
- [Wahba et al., 1995] Wahba, G., Johnson, D., Gao, F., and Gong, J. (1995). Adaptive tuning of numerical weather prediction models: Randomized GCV in three- and four-dimensionalassimilation. *Monthly Weather Review*, 123:3358–3369.
- [Wainwright, 2009] Wainwright, M. (2009). Sharp thresholds for high-dimensional and noisy sparsity recovery using  $ell_1$ -constrained quadratic programming (lasso). *IEEE Trans. Inf. Theory*, 55(5):2183–2202.
- [Weng et al., 2018] Weng, H., Maleki, A., and Zheng, L. (2018). Overcoming the limitations of phase transition by higher order analysis of regularization techniques. *Annals of Statistics*.

- [Xiang and Wahba, 1996] Xiang, D. and Wahba, G. (1996). A generalized approximate cross validation for smoothing splines with non-gaussian data. *Statistica Sinica*, 6:675–692.
- [Zou and Hastie, 2005] Zou, H. and Hastie, T. (2005). Regularization and variable selection via the elastic net. *J. R. Statist. Soc. B.*, 67(2):301–320.
- [Zou et al., 2007] Zou, H., Hastie, T., and Tibshirani, R. (2007). On the “degrees of freedom” of the lasso. *Ann. Stat.*, 35(5):2173–2192.

# A Proofs (FOR ON-LINE PUBLICATION ONLY)

## A.1 Proof of Theorem 1

### A.1.1 Roadmap of the proof

We first remind the reader that  $r_\alpha(z) \triangleq \frac{1}{\alpha}(\log(1 + e^{-\alpha z}) + \log(1 + e^{\alpha z}))$ . Before we discuss the proof, let us mention the following definitions:

$$h_\alpha(\boldsymbol{\beta}) \triangleq \sum_{i=1}^n \ell(y_i | \mathbf{x}_i^\top \boldsymbol{\beta}) + \lambda \sum_{i=1}^p r_\alpha(\beta_i), \quad h(\boldsymbol{\beta}) \triangleq \sum_{i=1}^n \ell(y_i | \mathbf{x}_i^\top \boldsymbol{\beta}) + \lambda \sum_{i=1}^p |\beta_i|, \quad (29)$$

$$\hat{\boldsymbol{\beta}}^\alpha \triangleq \arg \min_{\boldsymbol{\beta}} h_\alpha(\boldsymbol{\beta}), \quad \hat{\boldsymbol{\beta}} \triangleq \arg \min_{\boldsymbol{\beta}} h(\boldsymbol{\beta}). \quad (30)$$

Note that according to Assumptions 1 and 2,  $\hat{\boldsymbol{\beta}}^\alpha$  and  $\hat{\boldsymbol{\beta}}$  are unique. We first mention a few structural properties of  $r_\alpha(z)$  that will be used throughout our proof. Since the proofs of these results are straightforward, we skip them.

**Lemma 1.** *For any  $\alpha > 0$  we have  $r_\alpha(z) \geq |z|$ , and*

$$\sup_z |r_\alpha(z) - |z|| \leq \frac{2 \log 2}{\alpha}.$$

*In particular, as  $\alpha \rightarrow \infty$ ,  $r_\alpha(z)$  uniformly converges to  $|z|$ .*

**Lemma 2.**  *$r_\alpha(z)$  is infinitely many times differentiable, and*

$$\begin{aligned} \dot{r}_\alpha(z) &= \frac{e^{\alpha z} - e^{-\alpha z}}{e^{\alpha z} + e^{-\alpha z} + 2} \\ \ddot{r}_\alpha(z) &= \frac{2\alpha}{(e^{\alpha z} + e^{-\alpha z} + 2)}. \end{aligned} \quad (31)$$

*Furthermore, if  $|z_\alpha| < \frac{\zeta_1}{\alpha}$  for a constant  $\zeta_1 > 0$ , then  $\lim_{\alpha \rightarrow \infty} \ddot{r}_\alpha(z_\alpha) = +\infty$ . Finally, if  $|z_\alpha| > \zeta_2$  for a constant  $\zeta_2 > 0$ , then  $\lim_{\alpha \rightarrow \infty} \ddot{r}_\alpha(z_\alpha) = 0$  and  $\lim_{\alpha \rightarrow \infty} \dot{r}_\alpha(z_\alpha) = 1$ .*

Now, we show the main steps for finding the following limit

$$\lim_{\alpha \rightarrow \infty} \mathbf{H}^\alpha \triangleq \lim_{\alpha \rightarrow \infty} \mathbf{X} \left( \lambda \text{diag}[\ddot{\mathbf{r}}_\alpha(\hat{\boldsymbol{\beta}}^\alpha)] + \mathbf{X}^\top \text{diag}[\ddot{\boldsymbol{\ell}}(\hat{\boldsymbol{\beta}}^\alpha)] \mathbf{X} \right)^{-1} \mathbf{X}^\top \text{diag}[\ddot{\boldsymbol{\ell}}(\hat{\boldsymbol{\beta}}^\alpha)].$$

In that vein, let

$$\begin{aligned} \mathbf{A} &\triangleq \mathbf{X}_{S^c}^\top \text{diag}[\ddot{\boldsymbol{\ell}}(\hat{\boldsymbol{\beta}}^\alpha)] \mathbf{X}_{S^c} + \text{diag}[\ddot{\mathbf{r}}_{S^c}^\alpha(\hat{\boldsymbol{\beta}}^\alpha)], & \mathbf{B} &\triangleq \mathbf{X}_{S^c}^\top \text{diag}[\ddot{\boldsymbol{\ell}}(\hat{\boldsymbol{\beta}}^\alpha)] \mathbf{X}_S, \\ \mathbf{C} &\triangleq \mathbf{X}_S^\top \text{diag}[\ddot{\boldsymbol{\ell}}(\hat{\boldsymbol{\beta}}^\alpha)] \mathbf{X}_S + \text{diag}[\ddot{\mathbf{r}}_S^\alpha(\hat{\boldsymbol{\beta}}^\alpha)], & \mathbf{D} &\triangleq (\mathbf{C} - \mathbf{B}^\top \mathbf{A}^{-1} \mathbf{B})^{-1}, \end{aligned} \quad (32)$$

where  $S = \{i : |\hat{\beta}_i| \neq 0\}$ . Based on Theorem 4 in Section A.1.3, for large enough  $\alpha$ , there exist fixed numbers  $\zeta_1, \zeta_2 > 0$  such that

$$\max_{i \in S^c} |\hat{\beta}_i^\alpha| < \frac{\zeta_1}{\alpha}, \text{ and } \min_{i \in S} |\hat{\beta}_i^\alpha| > \zeta_2,$$

which with Lemma 2 implies  $\ddot{r}_\alpha(\hat{\beta}_i^\alpha) \rightarrow \infty$  for  $i \in S^c$  and  $\ddot{r}_\alpha(\hat{\beta}_i^\alpha) \rightarrow 0$  for  $i \in S$ , as  $\alpha \rightarrow \infty$ . Since the diagonal elements

of  $\text{diag}[\ddot{\mathbf{r}}_{\mathcal{S}^c}^\alpha(\hat{\boldsymbol{\beta}}^\alpha)]$  go off to infinity,  $\mathbf{A}^{-1} \rightarrow 0$ , as  $\alpha \rightarrow \infty$ . Furthermore, since the diagonal elements of  $\text{diag}[\ddot{\mathbf{r}}_{\mathcal{S}}^\alpha(\hat{\boldsymbol{\beta}}^\alpha)]$  converge to zero,  $\lim_{\alpha \rightarrow \infty} \mathbf{D} = (\mathbf{X}_S^\top \text{diag}[\ddot{\boldsymbol{\ell}}(\hat{\boldsymbol{\beta}}^\alpha)] \mathbf{X}_S)^{-1}$ . Therefore, by using the following identity

$$\begin{bmatrix} \mathbf{A} & \mathbf{B} \\ \mathbf{B}^\top & \mathbf{C} \end{bmatrix}^{-1} = \begin{bmatrix} \mathbf{A}^{-1} + \mathbf{A}^{-1} \mathbf{B} \mathbf{D} \mathbf{B}^\top \mathbf{A}^{-1} & -\mathbf{A}^{-1} \mathbf{B} \mathbf{D} \\ -\mathbf{D} \mathbf{B}^\top \mathbf{A}^{-1} & \mathbf{D} \end{bmatrix}, \quad (33)$$

and noting that  $\lim_{\alpha \rightarrow \infty} \mathbf{A}^{-1} + \mathbf{A}^{-1} \mathbf{B} \mathbf{D} \mathbf{B}^\top \mathbf{A}^{-1} = 0$ ,  $\lim_{\alpha \rightarrow \infty} -\mathbf{A}^{-1} \mathbf{B} \mathbf{D} = 0$ , we obtain

$$\begin{aligned} \lim_{\alpha \rightarrow \infty} \mathbf{H}^\alpha &= \lim_{\alpha \rightarrow \infty} \mathbf{X} \left( \lambda \text{diag}[\ddot{\mathbf{r}}(\hat{\boldsymbol{\beta}}^\alpha)] + \mathbf{X}^\top \text{diag}[\ddot{\boldsymbol{\ell}}(\hat{\boldsymbol{\beta}}^\alpha)] \mathbf{X} \right)^{-1} \mathbf{X}^\top \text{diag}[\ddot{\boldsymbol{\ell}}(\hat{\boldsymbol{\beta}}^\alpha)] \\ &= \mathbf{X}_S \left( \mathbf{X}_S^\top \text{diag}[\ddot{\boldsymbol{\ell}}(\hat{\boldsymbol{\beta}})] \mathbf{X}_S \right)^{-1} \mathbf{X}_S^\top \text{diag}[\ddot{\boldsymbol{\ell}}(\hat{\boldsymbol{\beta}})]. \end{aligned}$$

Note that in Lemma 3 in Section A.1.2 we prove that  $\|\hat{\boldsymbol{\beta}}^\alpha - \hat{\boldsymbol{\beta}}\|_2 \rightarrow 0$  as  $\alpha \rightarrow \infty$ . Hence, from the continuity of the second derivative of  $\ell$  (Assumption 3) we have  $\ddot{\boldsymbol{\ell}}(\hat{\boldsymbol{\beta}}^\alpha) \rightarrow \ddot{\boldsymbol{\ell}}(\hat{\boldsymbol{\beta}})$  as  $\alpha \rightarrow \infty$ .

### A.1.2 Proof of $\|\hat{\boldsymbol{\beta}}^\alpha - \hat{\boldsymbol{\beta}}\|_2 \rightarrow 0$

**Lemma 3.** *If Assumptions 1 and 2 hold, i.e. uniqueness of  $\hat{\boldsymbol{\beta}}$  and  $\hat{\boldsymbol{\beta}}^\alpha$ , then  $\lim_{\alpha \rightarrow \infty} \|\hat{\boldsymbol{\beta}}^\alpha - \hat{\boldsymbol{\beta}}\|_2 = 0$ .*

**Proof.** First note that according to Lemma 1, we have

$$|h(\boldsymbol{\beta}) - h_\alpha(\boldsymbol{\beta})| \leq \frac{2p \log 2}{\alpha}.$$

Hence, we have

$$h_\alpha(\hat{\boldsymbol{\beta}}^\alpha) \geq h(\hat{\boldsymbol{\beta}}^\alpha) - \frac{2p \log 2}{\alpha} \geq h(\hat{\boldsymbol{\beta}}) - \frac{2p \log 2}{\alpha}, \quad (34)$$

and

$$h_\alpha(\hat{\boldsymbol{\beta}}) \leq h(\hat{\boldsymbol{\beta}}) + \frac{2p \log 2}{\alpha}. \quad (35)$$

Suppose that  $\|\hat{\boldsymbol{\beta}}^\alpha - \hat{\boldsymbol{\beta}}\|_2$  does not go to zero as  $\alpha \rightarrow \infty$ . Then, there exists an  $\epsilon > 0$  for which we can find a sequence  $\alpha_1, \alpha_2, \dots$ , such that

$$\|\hat{\boldsymbol{\beta}}^{\alpha_i} - \hat{\boldsymbol{\beta}}\|_2 > \epsilon. \quad (36)$$

According to Lemma 1, we have

$$\lambda \|\hat{\boldsymbol{\beta}}^{\alpha_i}\|_1 \stackrel{(a)}{\leq} \lambda \sum_{j=1}^p r_{\alpha_i}(\hat{\beta}_j^{\alpha_i}) \stackrel{(b)}{\leq} h_{\alpha_i}(\hat{\boldsymbol{\beta}}^{\alpha_i}) \stackrel{(c)}{\leq} h_{\alpha_i}(0) = \sum_{j=1}^n \ell(y_j|0) + \frac{2p \log 2}{\alpha_i}. \quad (37)$$

Note that Inequality (a) uses Lemma 1 which proves  $|\hat{\beta}_j^{\alpha_i}| \leq r_{\alpha_i}(\hat{\beta}_j^{\alpha_i})$ . Inequality (b) is due to the fact that  $h_\alpha(\boldsymbol{\beta}) = \sum_{i=1}^n \ell(y_i|\mathbf{x}_i^\top \boldsymbol{\beta}) + \sum_{i=1}^p r_\alpha(\beta_i)$  and we assume that the loss function returns positive numbers. Inequality (c) is due to the fact that  $\hat{\boldsymbol{\beta}}^{\alpha_i}$  is the minimizer of  $h_{\alpha_i}(\boldsymbol{\beta})$ .

According to (37) the sequence  $\hat{\boldsymbol{\beta}}^{\alpha_1}, \hat{\boldsymbol{\beta}}^{\alpha_2}, \dots$  belongs to a compact set, and hence has a converging subsequence, called  $\hat{\boldsymbol{\beta}}^{\tilde{\alpha}_1}, \hat{\boldsymbol{\beta}}^{\tilde{\alpha}_2}, \dots$ . Suppose that  $\hat{\boldsymbol{\beta}}^{\tilde{\alpha}_1}, \hat{\boldsymbol{\beta}}^{\tilde{\alpha}_2}, \dots$  converges to  $\tilde{\boldsymbol{\beta}}$ . Therefore,

$$h(\hat{\boldsymbol{\beta}}^{\tilde{\alpha}_j}) \stackrel{(d)}{\leq} h_{\tilde{\alpha}_j}(\hat{\boldsymbol{\beta}}^{\tilde{\alpha}_j}) + \frac{2p \log 2}{\tilde{\alpha}_j} \stackrel{(e)}{\leq} h_{\tilde{\alpha}_j}(\tilde{\boldsymbol{\beta}}) + \frac{2p \log 2}{\tilde{\alpha}_j} \stackrel{(f)}{\leq} h(\tilde{\boldsymbol{\beta}}) + \frac{4p \log 2}{\tilde{\alpha}_j}. \quad (38)$$

Inequality (d) is due to (34). Inequality (e) is true because  $\hat{\beta}^{\tilde{\alpha}_j}$  is the minimizer of  $h_{\tilde{\alpha}_j}(\beta)$ , and finally Inequality (f) is due to (35). By taking the limit  $j \rightarrow \infty$  from both sides of (38), we have

$$h(\tilde{\beta}) \leq h(\hat{\beta}).$$

But  $\tilde{\beta}$  is different from  $\hat{\beta}$ , according to (36), contradicting the uniqueness of  $\hat{\beta}$  in Assumption 1.  $\square$ .

### A.1.3 Bounds for regression coefficients in smoothed LASSO

**Theorem 4.** *Let  $S$  denote the active set of  $\hat{\beta}$ , i.e., the location of its non-zero coefficients. Under assumptions 1, 2, 3, and 4, there exists a fixed numbers  $\zeta_1, \zeta_2 > 0$ , such that for  $\alpha$  large enough, we have*

$$\begin{aligned} \max_{i \in S^c} |\hat{\beta}_i^\alpha| &< \frac{\zeta_1}{\alpha} \\ \min_{i \in S} |\hat{\beta}_i^\alpha| &> \zeta_2. \end{aligned}$$

**Proof.** The optimality conditions

$$\sum_{i=1}^n \mathbf{x}_i \dot{\ell}(y_i | \mathbf{x}_i^\top \hat{\beta}^\alpha) + \lambda \dot{\mathbf{r}}_\alpha(\hat{\beta}^\alpha) = 0, \quad (39)$$

$$\sum_{i=1}^n \mathbf{x}_i \dot{\ell}(y_i | \mathbf{x}_i^\top \hat{\beta}^\alpha) + \lambda \hat{\mathbf{g}} = 0, \quad (40)$$

lead to

$$\left\| \lambda \dot{\mathbf{r}}_\alpha(\hat{\beta}^\alpha) - \lambda \hat{\mathbf{g}} \right\|_2 = \left\| - \sum_{i=1}^n \mathbf{x}_i \dot{\ell}(y_i | \mathbf{x}_i^\top \hat{\beta}^\alpha) + \sum_{i=1}^n \mathbf{x}_i \dot{\ell}(y_i | \mathbf{x}_i^\top \hat{\beta}) \right\|_2. \quad (41)$$

We know  $\|\hat{\beta}^\alpha - \hat{\beta}\|_2 \rightarrow 0$  from Lemma 3. And since  $\ell$  is twice differentiable (Assumption 3), we can argue that  $\left\| - \sum \mathbf{x}_i \dot{\ell}(y_i | \mathbf{x}_i^\top \hat{\beta}^\alpha) + \sum \mathbf{x}_i \dot{\ell}(y_i | \mathbf{x}_i^\top \hat{\beta}) \right\|_2 \rightarrow 0$  as  $\alpha \rightarrow \infty$ . Hence,

$$\|\lambda \dot{\mathbf{r}}_\alpha(\hat{\beta}^\alpha) - \lambda \hat{\mathbf{g}}\|_\infty \leq \|\lambda \dot{\mathbf{r}}_\alpha(\hat{\beta}^\alpha) - \lambda \hat{\mathbf{g}}\|_2 \rightarrow 0, \quad (42)$$

as  $\alpha \rightarrow \infty$ . This shows that for every  $i \in S^c$ ,  $|\alpha \hat{\beta}_i^\alpha|$  should remain bounded as  $\alpha \rightarrow \infty$ . Suppose that this is not true. Then we find a subsequence that  $\alpha_j \hat{\beta}_i^{\alpha_j} \rightarrow \infty$  as  $j \rightarrow \infty$ . Then

$$\lim_{j \rightarrow \infty} \dot{r}_{\alpha_j}(\hat{\beta}_i^{\alpha_j}) = \lim_{j \rightarrow \infty} \frac{e^{\alpha_j \hat{\beta}_i^{\alpha_j}} - e^{-\alpha_j \hat{\beta}_i^{\alpha_j}}}{e^{\alpha_j \hat{\beta}_i^{\alpha_j}} + e^{-\alpha_j \hat{\beta}_i^{\alpha_j}} + 2} = 1.$$

If we combine this with Assumption 4, we conclude that  $\|\lambda \dot{\mathbf{r}}_\alpha(\hat{\beta}^\alpha) - \lambda \hat{\mathbf{g}}\|_\infty$  will be a constant due to the assumption  $\sup_{i \in S^c} |\hat{g}_i| < 1$ . This is in contradiction with (42). Hence, we have proved that for every  $i \in S^c$ ,  $|\alpha \hat{\beta}_i^\alpha|$  remains bounded.

Next, we show that  $\min_{i \in S} |\hat{\beta}_i^\alpha|$  is bounded away from zero in the limit  $\alpha \rightarrow \infty$ . Define  $\min_{i \in S} |\hat{\beta}_i| = \gamma > 0$ . Lemma 3 implies  $\max_{i \in S} |\hat{\beta}_i^\alpha - \hat{\beta}_i| \rightarrow 0$ , and therefore, for  $\alpha$  large enough, we have

$$\max_{i \in S} |\hat{\beta}_i^\alpha - \hat{\beta}_i| < \gamma/2,$$

leading to

$$\min_{i \in S} |\hat{\beta}_i^\alpha| > \min_{i \in S} |\hat{\beta}_i| - \max_{i \in S} |\hat{\beta}_i^\alpha - \hat{\beta}_i| > \zeta_2 \triangleq \gamma/2.$$

□

## A.2 Proof of Theorem 2

The following lemma plays a critical role in our proof of Theorem 2.

**Lemma 4.** *Consider a class of symmetric positive definite matrices of the form*

$$\mathbf{\Gamma}_\delta \triangleq \begin{bmatrix} a + \delta & \mathbf{b}^\top \\ \mathbf{b} & \mathbf{C} \end{bmatrix}, \quad (43)$$

where  $a > 0$ ,  $\delta \geq 0$  and  $\mathbf{C} \in \mathbb{R}^{n-1 \times n-1}$ . Then, for any vector  $\mathbf{v} \in \mathbb{R}^n$  we have

$$\lim_{\delta \rightarrow \infty} \mathbf{v}^\top \mathbf{\Gamma}_\delta^{-1} \mathbf{v} \leq \mathbf{v}^\top \mathbf{\Gamma}_\delta^{-1} \mathbf{v} \leq \mathbf{v}^\top \mathbf{\Gamma}_0^{-1} \mathbf{v}.$$

Furthermore, if we define  $\mathbf{v}_{/1} \triangleq (v_2, v_3, \dots, v_n)^\top$ , then  $\lim_{\delta \rightarrow \infty} \mathbf{v}^\top \mathbf{\Gamma}_\delta^{-1} \mathbf{v} = \mathbf{v}_{/1}^\top \mathbf{C}^{-1} \mathbf{v}_{/1}$ .

**Proof:** Define  $\kappa \triangleq a + \delta - \mathbf{b}^\top \mathbf{C}^{-1} \mathbf{b}$ . Note that since the matrix  $\mathbf{\Gamma}_\delta$  is always positive definite, for any value of  $\delta$ ,  $\kappa > 0$ . By using the formulas for the inverse of block matrices we have

$$\mathbf{\Gamma}_\delta^{-1} = \begin{bmatrix} \frac{1}{\kappa} & -\frac{\mathbf{b}^\top \mathbf{C}^{-1}}{\kappa} \\ -\frac{\mathbf{C}^{-1} \mathbf{b}}{\kappa} & \frac{\mathbf{C}^{-1} \mathbf{b} \mathbf{b}^\top \mathbf{C}^{-1}}{\kappa} + \mathbf{C}^{-1} \end{bmatrix}. \quad (44)$$

Define  $\mathbf{v}_{/1} \triangleq (v_2, v_3, \dots, v_n)^\top$ .

$$\begin{aligned} \mathbf{v}^\top \mathbf{\Gamma}_\delta^{-1} \mathbf{v} &= \frac{v_1^2}{\kappa} + \mathbf{v}_{/1}^\top \mathbf{C}^{-1} \mathbf{v}_{/1} + \frac{\mathbf{v}_{/1}^\top \mathbf{C}^{-1} \mathbf{b} \mathbf{b}^\top \mathbf{C}^{-1} \mathbf{v}_{/1}}{\kappa} - 2 \frac{\mathbf{v}_{/1}^\top \mathbf{C}^{-1} \mathbf{b} v_1}{\kappa} \\ &= \mathbf{v}_{/1}^\top \mathbf{C}^{-1} \mathbf{v}_{/1} + \frac{1}{\kappa} (v_1 - \mathbf{b}^\top \mathbf{C}^{-1} \mathbf{v}_{/1})^2. \end{aligned} \quad (45)$$

Lemma 4 follows from the monotonicity of  $\mathbf{v}^\top \mathbf{\Gamma}_\delta^{-1} \mathbf{v}$  in terms of  $\kappa$ . □

*Proof of Theorem 2.* Before we start the proof, let us emphasize on the following facts that will be used later in the proof.

1. Consider an index  $i \in (S \cup T)^c$ . We know that  $\hat{\beta}_i = 0$  and the subgradient  $|\hat{g}_i| < 1$ . Hence, according to the proof of Theorem 4 we have  $\alpha \hat{\beta}_i^\alpha < \zeta$ . Therefore, according to Lemma 2 we have  $\ddot{r}(\hat{\beta}_i^\alpha) \rightarrow \infty$  as  $\alpha \rightarrow \infty$ .
2. Consider  $i \in S$ . Then by definition  $\hat{\beta}_i \neq 0$ . Similar to the proof of Theorem 1, we have  $\ddot{r}(\hat{\beta}_i^\alpha) \rightarrow 0$  as  $\alpha \rightarrow \infty$ .

Hence, we already know the limiting behavior of  $\ddot{r}(\hat{\beta}_i^\alpha)$  for  $i \in S$  and  $i \in (S \cup T)^c$  as  $\alpha \rightarrow \infty$ . The only remaining index set is  $T$ . Unfortunately, for  $i \in T$  we can not specify the limiting behavior of  $\ddot{r}(\hat{\beta}_i^\alpha)$ . Hence, our goal is to use



Lemma 4 to get around this issue. Set  $U \triangleq (S \cup T)^c$  and define the matrices

$$\begin{aligned}\tilde{\mathbf{A}}^\alpha &\triangleq \mathbf{X}_S^\top \text{diag}[\ddot{\ell}(\hat{\beta}^\alpha)] \mathbf{X}_S + \text{diag}[\ddot{\mathbf{r}}_S^\alpha(\hat{\beta}^\alpha)], & \tilde{\mathbf{B}}^\alpha &\triangleq \mathbf{X}_T^\top \text{diag}[\ddot{\ell}(\hat{\beta}^\alpha)] \mathbf{X}_T, \\ \tilde{\mathbf{C}}^\alpha &\triangleq \mathbf{X}_U^\top \text{diag}[\ddot{\ell}(\hat{\beta}^\alpha)] \mathbf{X}_U + \text{diag}[\ddot{\mathbf{r}}_U^\alpha(\hat{\beta}^\alpha)], & \tilde{\mathbf{D}}^\alpha &\triangleq \mathbf{X}_S^\top \text{diag}[\ddot{\ell}(\hat{\beta}^\alpha)] \mathbf{X}_T, \\ \tilde{\mathbf{E}}^\alpha &\triangleq \mathbf{X}_S^\top \text{diag}[\ddot{\ell}(\hat{\beta}^\alpha)] \mathbf{X}_U, & \tilde{\mathbf{F}}^\alpha &\triangleq \mathbf{X}_T^\top \text{diag}[\ddot{\ell}(\hat{\beta}^\alpha)] \mathbf{X}_U.\end{aligned}\quad (46)$$

Given this notation we have

$$H_{ii}^\alpha = \mathbf{x}_i^\top \begin{bmatrix} \tilde{\mathbf{A}}^\alpha & \tilde{\mathbf{D}}^\alpha & \tilde{\mathbf{E}}^\alpha \\ (\tilde{\mathbf{D}}^\alpha)^\top & \tilde{\mathbf{B}}^\alpha + \text{diag}[\ddot{\mathbf{r}}_T^\alpha(\hat{\beta}^\alpha)] & \tilde{\mathbf{F}}^\alpha \\ (\tilde{\mathbf{E}}^\alpha)^\top & (\tilde{\mathbf{F}}^\alpha)^\top & \tilde{\mathbf{C}}^\alpha \end{bmatrix}^{-1} \mathbf{x}_i \ddot{\ell}_i(\hat{\beta}^\alpha). \quad (47)$$

Here each element of  $\text{diag}[\ddot{\mathbf{r}}_T^\alpha(\hat{\beta}^\alpha)]$  may converge to any number in the range  $[0, \infty]$ . Hence we use Lemma 4 to find upper and lower bounds for  $H_{ii}^\alpha$ . According to Lemma 4 we have

$$H_{ii}^\alpha \leq \mathbf{x}_i^\top \begin{bmatrix} \tilde{\mathbf{A}}^\alpha & \tilde{\mathbf{D}}^\alpha & \tilde{\mathbf{E}}^\alpha \\ (\tilde{\mathbf{D}}^\alpha)^\top & \tilde{\mathbf{B}}^\alpha & \tilde{\mathbf{F}}^\alpha \\ (\tilde{\mathbf{E}}^\alpha)^\top & (\tilde{\mathbf{F}}^\alpha)^\top & \tilde{\mathbf{C}}^\alpha \end{bmatrix}^{-1} \mathbf{x}_i \ddot{\ell}_i(\hat{\beta}^\alpha), \quad (48)$$

and

$$\begin{aligned}H_{ii}^\alpha &\geq \lim_{\delta_{|T|} \rightarrow \infty} \dots \lim_{\delta_1 \rightarrow \infty} \mathbf{x}_i^\top \begin{bmatrix} \tilde{\mathbf{A}}^\alpha & \tilde{\mathbf{D}}^\alpha & \tilde{\mathbf{E}}^\alpha \\ (\tilde{\mathbf{D}}^\alpha)^\top & \tilde{\mathbf{B}}^\alpha + \text{diag}[\delta_1, \delta_2, \dots, \delta_{|T|}] & \tilde{\mathbf{F}}^\alpha \\ (\tilde{\mathbf{E}}^\alpha)^\top & (\tilde{\mathbf{F}}^\alpha)^\top & \tilde{\mathbf{C}}^\alpha \end{bmatrix}^{-1} \mathbf{x}_i \ddot{\ell}_i(\hat{\beta}^\alpha) \\ &= \mathbf{x}_{i, S \cup U}^\top \begin{bmatrix} \tilde{\mathbf{A}}^\alpha & \tilde{\mathbf{E}}^\alpha \\ (\tilde{\mathbf{E}}^\alpha)^\top & \tilde{\mathbf{C}}^\alpha \end{bmatrix}^{-1} \mathbf{x}_{i, S \cup U} \ddot{\ell}_i(\hat{\beta}^\alpha).\end{aligned}\quad (49)$$

The rest of the proof is similar to the proof of Theorem 1; we take the limit  $\alpha \rightarrow \infty$  from both sides of (48) and (49), and then use the block matrix inversion formulas (similar to those used in the proof of Theorem 1) and the fact that  $(\tilde{\mathbf{A}}^\alpha)^{-1} \rightarrow 0$  as  $\alpha \rightarrow \infty$  to complete the proof.  $\square$

### A.3 Derivation of (17)

#### A.3.1 Roadmap of the derivations

The goal of this section is to derive the ALO formula, presented in (17), for the following class of bridge estimators:

$$\hat{\beta} \triangleq \arg \min_{\beta \in \mathbb{R}^p} \left\{ \sum_{i=1}^n \ell(y_i | \mathbf{x}_i^\top \beta) + \lambda \|\beta\|_q^q \right\}, \quad (50)$$

where  $q \in (1, 2)$ . Since  $\|\beta\|_q^q$  is not twice differentiable at zero, similar to what we did for LASSO, we first consider a smoothed version of the bridge regularizer:

$$r_\gamma^q(z) = \frac{1}{\gamma} \int |u|^q \psi((z - u)/\gamma) du, \quad (51)$$

where  $\psi$  satisfies the following conditions:

- (i)  $\psi$  has a compact support, i.e.,  $\text{supp}(\psi) = [-1, 1]$ . Also,  $\psi(w) \geq 0$  for every  $w$ .
- (ii)  $\int \psi(w)dw = 1$  and  $\psi(0) > 0$ ;
- (iii)  $\psi$  is infinitely many times smooth and symmetric around 0 on  $\mathbb{R}$ ;

The two important properties of  $r_\gamma^q(z)$  are

1.  $r_\gamma^q(z)$  is infinitely many times differentiable for any nonzero value of  $\gamma$ .
2.  $|r_\gamma^q(z) - |z|^q| \rightarrow 0$  as  $\gamma \rightarrow 0$ . This claim will be proved in Lemma 5 below.

Hence, instead of finding the ALO formula directly for (50), we start with

$$\hat{\beta}^\gamma \triangleq \arg \min_{\beta} \sum_{i=1}^n \ell(y_i | \mathbf{x}_i^\top \beta) + \lambda \sum_{i=1}^p r_\gamma^q(\beta_i). \quad (52)$$

Given that both the loss function and the regularizer are smooth in (52), we can use (6) to obtain the following formula as the estimate of the out-of-sample prediction error of  $\hat{\beta}^\gamma$ :

$$\text{ALO}^\gamma \triangleq \frac{1}{n} \sum_{i=1}^n \phi \left( y_i, \mathbf{x}_i^\top \hat{\beta}^\gamma + \left( \frac{\dot{\ell}_i(\hat{\beta}^\gamma)}{\ddot{\ell}_i(\hat{\beta}^\gamma)} \right) \left( \frac{H_{ii}^\gamma}{1 - H_{ii}^\gamma} \right) \right), \quad (53)$$

where

$$\mathbf{H}^\gamma \triangleq \mathbf{X} \left( \lambda \text{diag}[\ddot{\mathbf{r}}_\gamma^q(\hat{\beta}^\gamma)] + \mathbf{X}^\top \text{diag}[\ddot{\ell}(\hat{\beta}^\gamma)] \mathbf{X} \right)^{-1} \mathbf{X}^\top \text{diag}[\ddot{\ell}(\hat{\beta}^\gamma)]. \quad (54)$$

Note that we are interested in  $\text{ALO}^\gamma$  for large values of  $\gamma$ . Hence, as suggested for the LASSO problem in Section 2.2, we calculate  $\lim_{\gamma \rightarrow 0} \text{ALO}^\gamma$ . In Section A.3.3 we prove the following theorem:

**Theorem 5.** *If the loss function is twice continuously differentiable with respect to its second argument, and the optimization problem in (52) has a unique solution for every  $\gamma$ , then*

$$\lim_{\gamma \rightarrow 0} \text{ALO}^\gamma \triangleq \frac{1}{n} \sum_{i=1}^n \phi \left( y_i, \mathbf{x}_i^\top \hat{\beta} + \left( \frac{\dot{\ell}_i(\hat{\beta})}{\ddot{\ell}_i(\hat{\beta})} \right) \left( \frac{H_{ii}}{1 - H_{ii}} \right) \right), \quad (55)$$

where

$$\mathbf{H} \triangleq \mathbf{X}_S \left( \mathbf{X}_S^\top \text{diag}[\ddot{\ell}(\hat{\beta})] \mathbf{X}_S + \lambda \text{diag}[\ddot{\mathbf{r}}_S^q(\hat{\beta})] \right)^{-1} \mathbf{X}_S^\top \text{diag}[\ddot{\ell}(\hat{\beta})], \quad (56)$$

$S$  is the active set of  $\hat{\beta}$ , and  $\ddot{r}^q(u) = q(q-1)|u|^{q-2}$ .

Proof of this Theorem is presented in Section A.3.3. We will first prove in Lemma 7 that

$$\|\hat{\beta}^\gamma - \hat{\beta}\|_2 \rightarrow 0.$$

Since,  $\|\hat{\beta}^\gamma - \hat{\beta}\|_2 \rightarrow 0$ , and  $\dot{\ell}$  and  $\ddot{\ell}$  functions are continuous, it is straightforward to prove that as  $\gamma \rightarrow 0$

$$\dot{\ell}_i(\hat{\beta}^\gamma) \rightarrow \dot{\ell}_i(\hat{\beta}), \quad \ddot{\ell}_i(\hat{\beta}^\gamma) \rightarrow \ddot{\ell}_i(\hat{\beta}).$$

Hence, the final remaining challenge in proving Theorem 5 is to calculate  $\lim_{\gamma \rightarrow 0} H_{ii}^\gamma$ . In Section A.3.3 we prove that

$$\lim_{\gamma \rightarrow 0} \mathbf{H}^\gamma = \mathbf{X}_S \left( \mathbf{X}_S^\top \text{diag}[\ddot{\ell}(\hat{\beta})] \mathbf{X}_S + \lambda \text{diag}[\ddot{\mathbf{r}}_S^q(\hat{\beta})] \right)^{-1} \mathbf{X}_S^\top \text{diag}[\ddot{\ell}(\hat{\beta})].$$

### A.3.2 Basic properties of $r_\gamma^q(\cdot)$

**Lemma 5.** *The smoothed regularizer  $r_\gamma^q(\cdot)$  satisfies*

$$\sup_{|z| < M} |r_\gamma^q(z) - |z|^q| \leq q(M + \gamma)^{q-1} \gamma.$$

*Proof.* According to the symmetry, we only consider  $z \geq 0$ . We have

$$\begin{aligned} |r_\gamma^q(z) - |z|^q| &= \frac{1}{\gamma} \left| \int_{-\gamma}^{\gamma} (|z - u|^q - |z|^q) \psi\left(\frac{u}{\gamma}\right) du \right| \\ &\stackrel{(a)}{\leq} (z + \gamma)^q - z^q \stackrel{(b)}{=} q \tilde{z}^{q-1} \gamma \leq q(M + \gamma)^{q-1} \gamma. \end{aligned} \quad (57)$$

Note that inequality (a) is due to the fact that since  $z > 0$ , the difference between  $|z - u|^q - |z|^q$  is maximized when  $u = -\gamma$ . In other words,

$$||z - u|^q - |z|^q| \leq (z + \gamma)^q - z^q, \quad \forall u \in [-\gamma, \gamma].$$

Furthermore, equality (b) is a result of the mean value theorem and  $\tilde{z} \in (z, z + \gamma)$ .  $\square$

### A.3.3 Proof of Theorem 5

Consider the following definitions:

$$h_\gamma^q(\beta) \triangleq \sum_{i=1}^n \ell(y_i | \mathbf{x}_i^\top \beta) + \lambda \sum_{i=1}^p r_\gamma^q(\beta_i), \quad h^q(\beta) \triangleq \sum_{i=1}^n \ell(y_i | \mathbf{x}_i^\top \beta) + \lambda \sum_{i=1}^p |\beta_i|^q, \quad (58)$$

As discussed in Lemma 5, the difference  $|r_\gamma^q(z) - |z|^q|$  is bounded by the maximum value that  $z$  takes. Our first lemma shows that  $\sup_{\gamma \in (0,1]} \|\hat{\beta}^\gamma\|_\infty < M$ . Hence, according to Lemma 5 the discrepancy between  $|r_\gamma^q(\hat{\beta}_i^\gamma) - |\hat{\beta}_i^\gamma|^q|$  goes to zero as  $\gamma \rightarrow 0$ .

**Lemma 6.** *There exists an  $M < \infty$  such that  $\sup_{\gamma \in [0,1]} \|\hat{\beta}^\gamma\|_\infty < M$  and  $\|\hat{\beta}\|_\infty < M$ .*

Here we only present the sketch of the proof, and skip the straightforward details. If  $\|\hat{\beta}^\gamma\|_\infty \rightarrow \infty$ , then  $h_\gamma^q(\hat{\beta}^\gamma) \rightarrow \infty$ . Hence, since  $h_\gamma^q(\mathbf{0})$  is bounded,  $\|\hat{\beta}^\gamma\|_\infty$  cannot go off to infinity. We can now use this lemma to prove that as  $\gamma \rightarrow 0$ ,  $\|\hat{\beta}^\gamma - \hat{\beta}\|_2 \rightarrow 0$ .

**Lemma 7.** *If the optimization problems in (58) have unique solutions, then as  $\gamma \rightarrow 0$*

$$\|\hat{\beta}^\gamma - \hat{\beta}\|_2 \rightarrow 0.$$

The proof of this lemma is similar to the proof of Lemma 3, and is hence skipped here. As mentioned in Section A.3.1, the main step in proving Theorem 5 is to find the limit of  $\lim_{\gamma \rightarrow 0} \mathbf{H}_\gamma$ . The main step in this calculation is to calculate  $\lim_{\gamma \rightarrow 0} \ddot{\mathbf{r}}(\hat{\beta}^\gamma)$ . The following lemma shows how this limit can be calculated.

**Lemma 8.** Let  $z_\gamma$  denote a function of  $\gamma$ . If  $z_\gamma \rightarrow 0$  as  $\gamma \rightarrow 0$ , then

$$\lim_{\gamma \rightarrow 0} \ddot{r}_\gamma^q(z_\gamma) = \infty.$$

*Proof.* Without loss of generality we consider the case  $z_\gamma \geq 0$ . We consider three different cases. Each case has a slightly different proof strategy.

1. Case I:  $\frac{z_\gamma}{\gamma} \rightarrow \infty$  or  $\frac{z_\gamma}{\gamma} \rightarrow c \geq 1$ .
2. Case II:  $\frac{z_\gamma}{\gamma} \rightarrow c$ , where  $c \in (0, 1)$ .
3. Case III:  $\frac{z_\gamma}{\gamma} \rightarrow 0$ .

It is straightforward to show that

$$\ddot{r}_\gamma^q(z_\gamma) = \int_{-\infty}^{\infty} q|z_\gamma - u|^{q-1} \text{sign}(z_\gamma - u) \frac{1}{\gamma^2} \dot{\psi}\left(\frac{u}{\gamma}\right) du. \quad (59)$$

Note that  $\dot{\psi}\left(\frac{u}{\gamma}\right) = 0$  for  $u$  outside the interval  $[-\gamma, \gamma]$ . Now we consider the three cases we described above.

Case I: We assume that for large enough values of  $\gamma$ ,  $z_\gamma > \gamma$ . Clearly, this holds when  $z_\gamma/\gamma \rightarrow c > 1$ . However, it may be violated when  $\frac{z_\gamma}{\gamma} \rightarrow 1$ . But, this special case can be handled with a similar approach and is hence skipped. We have

$$\begin{aligned} |\ddot{r}_\gamma^q(z_\gamma)| &= \left| \int_{-\gamma}^0 q(z_\gamma - u)^{q-1} \frac{1}{\gamma^2} \dot{\psi}\left(\frac{u}{\gamma}\right) du + \int_0^\gamma q(z_\gamma - u)^{q-1} \frac{1}{\gamma^2} \dot{\psi}\left(\frac{u}{\gamma}\right) du \right| \\ &= \left| \int_0^\gamma q[(z_\gamma - u)^{q-1} - (z_\gamma + u)^{q-1}] \frac{1}{\gamma^2} \dot{\psi}\left(\frac{u}{\gamma}\right) dt \right| \\ &\stackrel{(a)}{=} 2q(q-1) \left| \int_0^\gamma \tilde{z}_u^{q-2} u \frac{1}{\gamma^2} \dot{\psi}\left(\frac{u}{\gamma}\right) du \right| \\ &\stackrel{(b)}{\geq} 2q(q-1)(z_\gamma + \gamma)^{q-2} \left| \int_0^\gamma u \frac{1}{\gamma^2} \dot{\psi}\left(\frac{u}{\gamma}\right) du \right| \\ &\stackrel{(c)}{=} q(q-1)(z_\gamma + \gamma)^{q-2}. \end{aligned} \quad (60)$$

Equality (a) is due to the mean-value theorem. To obtain (b) we used the fact that  $\tilde{z}_u \in [z_\gamma - \gamma, z_\gamma + \gamma]$ , and that  $z_\gamma - \gamma > 0$  (hence  $\tilde{z}_u > 0$ ). The last equality is the result of integration by parts. Note that since  $z_\gamma \rightarrow 0$  as  $\gamma \rightarrow 0$ ,  $q(q-1)(z_\gamma + \gamma)^{q-2} \rightarrow \infty$ .

Case II:  $\frac{z_\gamma}{\gamma} \rightarrow c$ , where  $c \in (0, 1)$ . For large enough values of  $\gamma$ , we know that  $z_\gamma < \gamma$ . Hence, according to (59) we have

$$\begin{aligned} \ddot{r}_\gamma^q(z_\gamma) &= - \int_0^\gamma q(z_\gamma + u)^{q-1} \frac{1}{\gamma^2} \dot{\psi}\left(\frac{u}{\gamma}\right) du + \int_0^{z_\gamma} q(z_\gamma - u)^{q-1} \frac{1}{\gamma^2} \dot{\psi}\left(\frac{u}{\gamma}\right) du \\ &\quad - \int_{z_\gamma}^\gamma q|z_\gamma - u|^{q-1} \frac{1}{\gamma^2} \dot{\psi}\left(\frac{u}{\gamma}\right) du \\ &\geq - \int_{z_\gamma}^\gamma q(z_\gamma + u)^{q-1} \frac{1}{\gamma^2} \dot{\psi}\left(\frac{u}{\gamma}\right) du \\ &\geq -q(2z_\gamma)^{q-1} \int_{z_\gamma}^\gamma \frac{1}{\gamma^2} \dot{\psi}\left(\frac{u}{\gamma}\right) du = \frac{q(2z_\gamma)^{q-1}}{\gamma} \psi\left(\frac{z_\gamma}{\gamma}\right). \end{aligned} \quad (61)$$

It is straightforward to confirm that  $\frac{q(2z_\gamma)^{q-1}}{\gamma} \psi(\frac{z_\gamma}{\gamma}) \rightarrow \infty$ .

Case III: First note that since  $z_\gamma/\gamma \rightarrow 0$ , for large enough  $\gamma$ ,  $z_\gamma < \gamma/2$ . Similar to the derivation in (61), we have

$$\begin{aligned}
\ddot{r}_\gamma^q(z_\gamma) &\geq - \int_{z_\gamma}^\gamma q|z_\gamma - u|^{q-1} \frac{1}{\gamma^2} \dot{\psi}\left(\frac{u}{\gamma}\right) du \\
&\geq - \int_{z_\gamma}^\gamma q(z_\gamma + u)^{q-1} \frac{1}{\gamma^2} \dot{\psi}\left(\frac{u}{\gamma}\right) du \\
&\geq - \int_{\gamma/2}^\gamma q(z_\gamma + u)^{q-1} \frac{1}{\gamma^2} \dot{\psi}\left(\frac{u}{\gamma}\right) du \\
&\geq q(z_\gamma + \frac{\gamma}{2})^{q-1} \frac{r(0.5)}{\gamma}.
\end{aligned} \tag{62}$$

Again, it is straightforward to see that the last expression goes to  $\infty$  as  $\gamma \rightarrow 0$ .  $\square$

We remind the reader that our goal is to show that

$$\lim_{\gamma \rightarrow 0} \mathbf{H}^\gamma = \mathbf{X}_S \left( \mathbf{X}_S^\top \text{diag}[\ddot{\ell}(\hat{\beta})] \mathbf{X}_S + \lambda \text{diag}[\ddot{r}_S^q(\hat{\beta})] \right)^{-1} \mathbf{X}_S^\top \text{diag}[\ddot{\ell}(\hat{\beta})],$$

where  $S$  denotes the active set of  $\hat{\beta}$ . Since,  $\|\hat{\beta}^\gamma - \hat{\beta}\|_2 \rightarrow 0$ , and  $\dot{\ell}$  and  $\ddot{\ell}$  functions are continuous, it is straightforward to prove that

$$\dot{\ell}_i(\hat{\beta}^\gamma) \rightarrow \dot{\ell}_i(\hat{\beta}), \quad \ddot{\ell}_i(\hat{\beta}^\gamma) \rightarrow \ddot{\ell}_i(\hat{\beta}).$$

Let  $S$  denote the set of indices of the non-zero elements of  $\hat{\beta}$ , and define

$$\begin{aligned}
\mathbf{A} &= \mathbf{X}_{S^c}^\top \text{diag}[\ddot{\ell}(\hat{\beta}^\gamma)] \mathbf{X}_{S^c} + \text{diag}[\ddot{r}_{\gamma, S^c}^q(\hat{\beta}^\gamma)], & \mathbf{B} &= \mathbf{X}_{S^c}^\top \text{diag}[\ddot{\ell}(\hat{\beta}^\gamma)] \mathbf{X}_S, \\
\mathbf{C} &= \mathbf{X}_S^\top \text{diag}[\ddot{\ell}(\hat{\beta}^\gamma)] \mathbf{X}_S + \text{diag}[\ddot{r}_{\gamma, S}^q(\hat{\beta}^\gamma)].
\end{aligned} \tag{63}$$

Also define  $\mathbf{D} \triangleq (\mathbf{C} - \mathbf{B}^\top \mathbf{A}^{-1} \mathbf{B})^{-1}$ . According to Lemmas 7 and 8, the diagonal elements of  $\text{diag}[\ddot{r}_{\gamma, S^c}^q(\hat{\beta}^\gamma)]$  go off to infinity. Hence, it is straightforward to show that  $\mathbf{A}^{-1} \rightarrow 0$ , as  $\gamma \rightarrow 0$ . By using the following identity

$$\begin{bmatrix} \mathbf{A} & \mathbf{B} \\ \mathbf{B}^\top & \mathbf{C} \end{bmatrix}^{-1} = \begin{bmatrix} \mathbf{A}^{-1} + \mathbf{A}^{-1} \mathbf{B} \mathbf{D} \mathbf{B}^\top \mathbf{A}^{-1} & -\mathbf{A}^{-1} \mathbf{B} \mathbf{D} \\ -\mathbf{D} \mathbf{B}^\top \mathbf{A}^{-1} & \mathbf{D} \end{bmatrix}, \tag{64}$$

and noting that  $\lim_{\gamma \rightarrow 0} \mathbf{A}^{-1} + \mathbf{A}^{-1} \mathbf{B} \mathbf{D} \mathbf{B}^\top \mathbf{A}^{-1} = 0$ ,  $\lim_{\gamma \rightarrow 0} -\mathbf{A}^{-1} \mathbf{B} \mathbf{D} = 0$ , and  $\lim_{\gamma \rightarrow 0} \mathbf{D} = (\mathbf{X}_S^\top \text{diag}[\ddot{\ell}(\hat{\beta})] \mathbf{X}_S)^{-1}$  we obtain

$$\lim_{\gamma \rightarrow 0} \mathbf{H}^\gamma = \mathbf{X}_S \left( \mathbf{X}_S^\top \text{diag}[\ddot{\ell}(\hat{\beta})] \mathbf{X}_S + \lambda \text{diag}[\ddot{r}_S^q(\hat{\beta})] \right)^{-1} \mathbf{X}_S^\top \text{diag}[\ddot{\ell}(\hat{\beta})].$$

## A.4 Proof of Theorem 3

We first present lemmas necessary for the proof of Theorem 3. Lemmas are proved in section A.5.

**Lemma 9.** *Let  $\mathbf{X} \in \mathbb{R}^{m \times p}$  be a matrix with  $m > p = \text{rank}(\mathbf{X})$ . Moreover, let  $\mathbf{D} \in \mathbb{R}^{m \times m}$  and  $\mathbf{D} + \mathbf{\Gamma} \in \mathbb{R}^{m \times m}$  be*

diagonal matrices with positive elements, then

$$\begin{aligned} & (\mathbf{X}^\top \mathbf{D} \mathbf{X})^{-1} - (\mathbf{X}^\top (\mathbf{D} + \mathbf{\Gamma}) \mathbf{X})^{-1} \\ &= \mathbf{A}^{-1} \mathbf{X}^\top \mathbf{\Gamma} \mathbf{X} \mathbf{A}^{-1} - \mathbf{A}^{-1} \mathbf{X}^\top \mathbf{\Gamma} \mathbf{X} (\mathbf{X}^\top (\mathbf{D} + \mathbf{\Gamma}) \mathbf{X})^{-1} \mathbf{X}^\top \mathbf{\Gamma} \mathbf{X} \mathbf{A}^{-1}, \end{aligned}$$

where  $\mathbf{A} \triangleq \mathbf{X}^\top \mathbf{D} \mathbf{X}$ .

**Lemma 10.** Assume that  $\mathbf{X}^\top (\mathbf{D} + \mathbf{\Gamma}) \mathbf{X}$  and  $\mathbf{X}^\top \mathbf{D} \mathbf{X}$  are positive definite, and define:

$$\mathbf{\Gamma} \triangleq \text{diag}(\boldsymbol{\gamma}), \quad (65)$$

$$\bar{\omega}_{\max} \triangleq \sigma_{\max}(\mathbf{X} \mathbf{X}^\top), \quad (66)$$

$$\nu_{\min} \triangleq \sigma_{\min}(\mathbf{X}^\top (\mathbf{D} + \mathbf{\Gamma}) \mathbf{X}), \quad (67)$$

$$\mathbf{A} \triangleq \mathbf{X}^\top \mathbf{D} \mathbf{X}. \quad (68)$$

Then,

$$\left| \mathbf{z}^\top (\mathbf{X}^\top (\mathbf{D} + \mathbf{\Gamma}) \mathbf{X})^{-1} \mathbf{z} - \mathbf{z}^\top (\mathbf{X}^\top \mathbf{D} \mathbf{X})^{-1} \mathbf{z} \right| \leq \left( \|\boldsymbol{\gamma}\|_2 + \left( \frac{\bar{\omega}_{\max}}{\nu_{\min}} \right) \|\boldsymbol{\gamma}\|_4^2 \right) \|\mathbf{X} \mathbf{A}^{-1} \mathbf{z}\|_4^2. \quad (69)$$

**Lemma 11.** Given Assumptions 6 and 7, we have

$$\left| \mathbf{x}_i^\top \boldsymbol{\Delta}_{/i}^* - \left( \frac{\dot{\ell}_i(\hat{\boldsymbol{\beta}})}{\ddot{\ell}_i(\hat{\boldsymbol{\beta}})} \right) \frac{H_{ii}}{1 - H_{ii}} \right| \leq \bar{C}_i \left( \|\mathbf{X}_{/i} \mathbf{J}_{/i}^{-1} \mathbf{x}_i\|_4^2 + \|\mathbf{J}_{/i}^{-1} \mathbf{x}_i\|_4^2 \right),$$

where

$$\begin{aligned} \boldsymbol{\Delta}_{/i}^* &\triangleq \hat{\boldsymbol{\beta}} - \hat{\boldsymbol{\beta}}_{/i}, \\ \mathbf{H} &\triangleq \mathbf{X} \left( \lambda \text{diag}[\dot{\mathbf{r}}(\hat{\boldsymbol{\beta}})] + \mathbf{X}^\top \text{diag}[\ddot{\boldsymbol{\ell}}(\hat{\boldsymbol{\beta}})] \mathbf{X} \right)^{-1} \mathbf{X}^\top \text{diag}[\ddot{\boldsymbol{\ell}}(\hat{\boldsymbol{\beta}})], \\ \mathbf{J}_{/i} &\triangleq \lambda \text{diag}[\dot{\mathbf{r}}(\hat{\boldsymbol{\beta}}_{/i})] + \mathbf{X}_{/i}^\top \text{diag}[\ddot{\boldsymbol{\ell}}_{/i}(\hat{\boldsymbol{\beta}}_{/i})] \mathbf{X}_{/i}, \\ \bar{C}_i &\triangleq 4 \|\mathbf{x}_i\|_2 \left( \frac{c_1^2(n) c_2(n)}{\nu} \right) \left( 1 + \frac{2c_1(n) c_2(n) (1 + \omega_{\max, i})}{\nu^2} \|\mathbf{x}_i\|_2 \right), \end{aligned}$$

and  $c_1(n)$  and  $c_2(n)$  are defined in Assumption 6,  $\nu$  is defined in Assumption 7, and  $\omega_{\max, i} \triangleq \sigma_{\max}(\mathbf{X}_{/i} \mathbf{X}_{/i}^\top)$ .

**Lemma 12.** Let  $\mathbf{x} \sim \mathcal{N}(0, \boldsymbol{\Sigma})$  with  $\rho_{\max} \triangleq \sigma_{\max}(\boldsymbol{\Sigma})$ , where  $\boldsymbol{\Sigma} \in \mathbb{R}^{p \times p}$  then

$$\Pr \left[ \|\mathbf{x}\|_4^2 > 2(1 + c) \rho_{\max} \sqrt{p} \log p \right] \leq \frac{2}{p^c}. \quad (70)$$

Moreover, if

$$\omega_{\max} \triangleq \sigma_{\max}(\mathbf{X} \mathbf{X}^\top), \quad (71)$$

$$\nu_{\min} \triangleq \sigma_{\min}(\mathbf{J}), \quad (72)$$

where  $\mathbf{x}$  is independent of the symmetric matrix  $\mathbf{J} \in \mathbb{R}^{p \times p}$  and  $\mathbf{X} \in \mathbb{R}^{m \times p}$ , then

$$\Pr \left[ \|\mathbf{J}^{-1} \mathbf{x}\|_4^2 > 2(1+c) \left( \frac{\rho_{\max}}{\nu_{\min}^2} \right) \sqrt{p} \log p \right] < \frac{2}{p^c}, \quad (73)$$

$$\Pr \left[ \|\mathbf{X} \mathbf{J}^{-1} \mathbf{x}\|_4^2 > 2(1+c) \left( \frac{\rho_{\max}}{\nu_{\min}^2} \omega_{\max} \right) \sqrt{m} \log m \right] < \frac{2}{m^c}. \quad (74)$$

**Lemma 13** (Due to [Boucheron et al., 2013]). Let  $\mathbf{x} \sim \mathcal{N}(0, \mathbf{\Sigma})$  with  $\rho_{\max} \triangleq \sigma_{\max}(\mathbf{\Sigma})$ , where  $\mathbf{\Sigma} \in \mathbb{R}^{p \times p}$  then

$$\Pr \left[ \|\mathbf{x}\|_2^2 > 5p\rho_{\max} \right] \leq e^{-p}. \quad (75)$$

Furthermore, if  $\mathbf{X} \in \mathbb{R}^{n \times p}$  is composed of independently distributed  $\mathcal{N}(0, \frac{1}{n})$  entries, then

$$\Pr \left[ \sqrt{\sigma_{\max}(\mathbf{X}^\top \mathbf{X})} \geq 1 + \sqrt{\frac{p}{n}} + t \right] \leq e^{-\frac{nt^2}{2}}. \quad (76)$$

**Lemma 14.**  $\mathbf{X} \in \mathbb{R}^{n \times p}$  is composed of independently distributed  $\mathcal{N}(0, \mathbf{\Sigma})$  rows, with  $\rho_{\max} \triangleq \sigma_{\max}(\mathbf{\Sigma})$ , where  $\mathbf{\Sigma} \in \mathbb{R}^{p \times p}$  then

$$\Pr \left[ \sigma_{\max}(\mathbf{X} \mathbf{X}^\top) \geq (\sqrt{n} + 3\sqrt{p})^2 \rho_{\max} \right] \leq e^{-p}. \quad (77)$$

*Proof of Theorem 3.* Define the following events:

$$E_i \triangleq \left\{ \left| \mathbf{x}_i^\top \mathbf{\Delta}_{/i}^* - \left( \frac{\dot{\ell}_i(\hat{\beta})}{\ddot{\ell}_i(\hat{\beta})} \right) \frac{H_{ii}}{1 - H_{ii}} \right| > C \frac{\log p}{\sqrt{p}} \right\}, \quad (78)$$

$$F_i \triangleq \left\{ \bar{C}_i \left( \|\mathbf{X}_{/i} \mathbf{J}_{/i}^{-1} \mathbf{x}_i\|_4^2 + \|\mathbf{J}_{/i}^{-1} \mathbf{x}_i\|_4^2 \right) > \bar{C}_i C_i \sqrt{p} \log p \right\}, \quad (79)$$

$$K_i \triangleq \left\{ \frac{C}{\sqrt{p}} \geq \bar{C}_i C_i \sqrt{p} \right\}, \quad (80)$$

$$W_i \triangleq \left\{ \|\mathbf{x}_i\|_2^2 > 5p\rho_{\max} \right\} \cup \left\{ \omega_{\max} > (\sqrt{n} + 3\sqrt{p})^2 \rho_{\max} \right\}, \quad (81)$$

where  $C$  in (78) is a positive constant (defined later in (86)), and

$$C_i \triangleq 2(1+c) \left( \frac{\rho_{\max}}{\nu^2} \right) \left( 1 + \omega_{\max} \sqrt{\frac{n-1}{p} \frac{\log(n-1)}{\log p}} \right), \quad (82)$$

$$\bar{C}_i \triangleq 4 \|\mathbf{x}_i\|_2 \left( \frac{c_1^2(n) c_2(n)}{\nu} \right) \left( 1 + \frac{2c_1(n) c_2(n) (1 + \omega_{\max})}{\nu^2} \|\mathbf{x}_i\|_2 \right), \quad (83)$$

$$\omega_{\max} \triangleq \sigma_{\max}(\mathbf{X} \mathbf{X}^\top). \quad (84)$$

The variable  $c$  in (82) is later set to 3, but for now all we need to know is that it is a positive constant. Note that the probability of  $\left| \mathbf{x}_i^\top \mathbf{\Delta}_{/i}^* - \left( \frac{\dot{\ell}_i(\hat{\beta})}{\ddot{\ell}_i(\hat{\beta})} \right) \frac{H_{ii}}{1 - H_{ii}} \right| > \bar{C}_i C_i \sqrt{p} \log p$  is greater than or equal to  $\Pr[E_i | K_i]$ . Moreover, due to Lemma 11, if Assumption 6 and Assumption 7 are valid, then

$$\bar{C}_i \left( \|\mathbf{X}_{/i} \mathbf{J}_{/i}^{-1} \mathbf{x}_i\|_4^2 + \|\mathbf{J}_{/i}^{-1} \mathbf{x}_i\|_4^2 \right) \geq \left| \mathbf{x}_i^\top \mathbf{\Delta}_{/i}^* - \left( \frac{\dot{\ell}_i(\hat{\beta})}{\ddot{\ell}_i(\hat{\beta})} \right) \frac{H_{ii}}{1 - H_{ii}} \right|.$$

In that vein,

$$\begin{aligned}
\Pr[E_i] &\leq \Pr[E_i|K_i] + \Pr[K_i^c], \\
&\stackrel{1}{\leq} \Pr[F_i] + \Pr[K_i^c] \leq \Pr\left[\left\|\mathbf{X}_{/i}\mathbf{J}_{/i}^{-1}\mathbf{x}_i\right\|_4^2 > 2(1+c)\left(\frac{\rho_{\max}}{\nu^2}\omega_{\max}\right)\sqrt{n-1}\log(n-1)\right] \\
&+ \Pr\left[\left\|\mathbf{J}_{/i}^{-1}\mathbf{x}_i\right\|_4^2 > 2(1+c)\left(\frac{\rho_{\max}}{\nu^2}\right)\sqrt{p}\log p\right] + \Pr[K_i^c] \\
&\stackrel{2}{\leq} \frac{2}{(n-1)^c} + \frac{2}{p^c} + \Pr[K_i^c],
\end{aligned} \tag{85}$$

where  $\stackrel{1}{\leq}$  is due to Lemma 11, and  $\stackrel{2}{\leq}$  is due to Inequality (74) from Lemma 12. To bound  $\Pr[K_i^c]$  we define

$$\begin{aligned}
C &\triangleq 32\sqrt{5}\left(\frac{c_1^2(n)c_2(n)(p\rho_{\max})^{3/2}}{\nu^3}\right)\left(1+\left(\sqrt{\frac{n}{p}}+3\right)^2 p\rho_{\max}\sqrt{\frac{n-1}{p}}\frac{\log(n-1)}{\log p}\right) \\
&\times \left(1+\frac{2c_1(n)c_2(n)\sqrt{5}\left(1+\left(\sqrt{\frac{n}{p}}+3\right)^2 p\rho_{\max}\right)\sqrt{p\rho_{\max}}}{\nu^2}\right)
\end{aligned} \tag{86}$$

obtained by setting  $c = 3$ , and computing  $p\bar{C}_i C_i$  after putting  $\sqrt{5p\rho_{\max}}$  and  $(\sqrt{n} + 3\sqrt{p})^2 \rho_{\max}$ , bounds in event  $W_i$ , into  $\|\mathbf{x}_i\|_2$  and  $\omega_{\max}$ , respectively. Next,

$$\begin{aligned}
\Pr[K_i^c] &= \Pr\left[\frac{C}{p} < \bar{C}_i C_i\right] \leq \Pr[C < p\bar{C}_i C_i | W_i] + \Pr[W_i] \\
&= \Pr[C < C] + \Pr[W_i] = \Pr[W_i].
\end{aligned}$$

The term  $\Pr[W_i]$  is exponentially small because  $\mathbf{x}_i$  is  $N(0, \Sigma)$  with  $\rho_{\max} = \sigma_{\max}(\Sigma)$ , leading to

$$\Pr[W_i] \leq \Pr[\|\mathbf{x}_i\|_2^2 > 5p\rho_{\max}] + \Pr[\sigma_{\max}(\mathbf{X}\mathbf{X}^\top) > (\sqrt{n} + 3\sqrt{p})^2 \rho_{\max}] \leq 2e^{-p}, \tag{87}$$

due to Lemma 13 and Lemma 14. To summarize

$$\Pr\left[\left|\mathbf{x}_i^\top \Delta_{/i}^* - \left(\frac{\dot{\ell}_i(\hat{\beta})}{\ddot{\ell}_i(\hat{\beta})}\right) \frac{H_{ii}}{1-H_{ii}}\right| > C \frac{\log p}{\sqrt{p}}\right] \leq \frac{2}{(n-1)^3} + \frac{2}{p^3} + 2e^{-p}. \tag{88}$$

Inequality (25) in Theorem 3 follows from the fact that  $\frac{C_o}{\sqrt{p}} > C \frac{\log p}{\sqrt{p}}$  where  $C_o$  is defined in (26). To bound  $|\text{LO} - \text{ALO}|$  we use the following variable

$$\kappa_i \triangleq \left(\frac{\dot{\ell}_i(\hat{\beta})}{\ddot{\ell}_i(\hat{\beta})}\right) \frac{H_{ii}}{1-H_{ii}} - \mathbf{x}_i^\top \Delta_{/i}^*$$

as follows:

$$\begin{aligned}
|\text{LO} - \text{ALO}| &= \left|\frac{1}{n} \sum_{i=1}^n \phi\left(y_i, \mathbf{x}_i^\top \hat{\beta}_{/i}\right) - \frac{1}{n} \sum_{i=1}^n \phi\left(y_i, \mathbf{x}_i^\top \hat{\beta} + \left(\frac{\dot{\ell}_i(\hat{\beta})}{\ddot{\ell}_i(\hat{\beta})}\right) \left(\frac{H_{ii}}{1-H_{ii}}\right)\right)\right| \\
&= \left|\frac{1}{n} \sum_{i=1}^n \phi\left(y_i, \mathbf{x}_i^\top \hat{\beta} + \mathbf{x}_i^\top \Delta_{/i}^*\right) - \frac{1}{n} \sum_{i=1}^n \phi\left(y_i, \mathbf{x}_i^\top \hat{\beta} + \left(\frac{\dot{\ell}_i(\hat{\beta})}{\ddot{\ell}_i(\hat{\beta})}\right) \left(\frac{H_{ii}}{1-H_{ii}}\right)\right)\right| \\
&= \left|\frac{1}{n} \sum_{i=1}^n \phi\left(y_i, \mathbf{x}_i^\top \hat{\beta}_{/i} + a_i \kappa_i\right) \kappa_i\right|.
\end{aligned} \tag{89}$$



where  $a_1, \dots, a_n$  denote  $n$  numbers between 0 and 1. Note that we have  $\kappa_i < \frac{C_o}{\sqrt{p}}$  with probability at least  $1 - \frac{2}{(n-1)^3} - \frac{2}{p^3} - 2e^{-p}$ . Therefore, with at least the same probability we have

$$|\text{LO} - \text{ALO}| \leq \frac{C_o}{\sqrt{p}} \times \max_{i=1, \dots, n} \sup_{|b_i| < \frac{C_o}{\sqrt{p}}} \left| \dot{\phi} \left( y_i, \mathbf{x}_i^\top \hat{\beta}_{/i} + b_i \right) \right| \quad (90)$$

□

## A.5 Proofs of lemmas 9, 10, 11, 12 and 14

*Proof of Lemma 9.* Let  $Q \triangleq \{i : \Gamma_{ii} \neq 0\}$ . Moreover, let  $\mathbf{X}_{Q,:} \in \mathbb{R}^{|Q| \times p}$  stand for the sub-matrix of  $\mathbf{X}$  restricted to the rows indexed by  $Q$ , and let  $\tilde{\mathbf{\Gamma}} \in \mathbb{R}^{|Q| \times |Q|}$  be the diagonal matrix with the diagonal elements of  $\mathbf{\Gamma}$  indexed by  $Q$ . Then,  $\mathbf{X}^\top \mathbf{\Gamma} \mathbf{X} = \mathbf{X}_{Q,:}^\top \tilde{\mathbf{\Gamma}} \mathbf{X}_{Q,:}$ , and in turn, the Woodbury inversion lemma yields

$$\begin{aligned} (\mathbf{X}^\top \mathbf{D} \mathbf{X} + \mathbf{X}^\top \mathbf{\Gamma} \mathbf{X})^{-1} &= (\mathbf{A} + \mathbf{X}_{Q,:}^\top \tilde{\mathbf{\Gamma}} \mathbf{X}_{Q,:})^{-1} \\ &= \mathbf{A}^{-1} - \mathbf{A}^{-1} \mathbf{X}_{Q,:}^\top (\tilde{\mathbf{\Gamma}}^{-1} + \mathbf{X}_{Q,:} \mathbf{A}^{-1} \mathbf{X}_{Q,:}^\top)^{-1} \mathbf{X}_{Q,:} \mathbf{A}^{-1}. \end{aligned} \quad (91)$$

Using the Woodbury lemma again we obtain

$$\begin{aligned} (\tilde{\mathbf{\Gamma}}^{-1} + \mathbf{X}_{Q,:} \mathbf{A}^{-1} \mathbf{X}_{Q,:}^\top)^{-1} &= \tilde{\mathbf{\Gamma}} - \tilde{\mathbf{\Gamma}} \mathbf{X}_{Q,:} (\mathbf{A} + \mathbf{X}_{Q,:}^\top \tilde{\mathbf{\Gamma}} \mathbf{X}_{Q,:})^{-1} \mathbf{X}_{Q,:}^\top \tilde{\mathbf{\Gamma}} \\ &= \tilde{\mathbf{\Gamma}} - \tilde{\mathbf{\Gamma}} \mathbf{X}_{Q,:} (\mathbf{X}^\top (\mathbf{\Gamma} + \mathbf{D}) \mathbf{X})^{-1} \mathbf{X}_{Q,:}^\top \tilde{\mathbf{\Gamma}}. \end{aligned} \quad (92)$$

Hence, by using (91) and (92) we have

$$(\mathbf{X}^\top \mathbf{D} \mathbf{X})^{-1} - (\mathbf{X}^\top \mathbf{D} \mathbf{X} + \mathbf{X}^\top \mathbf{\Gamma} \mathbf{X})^{-1} = \mathbf{A}^{-1} \mathbf{X}^\top (\mathbf{\Gamma} - \mathbf{\Gamma} \mathbf{X} (\mathbf{X}^\top (\mathbf{\Gamma} + \mathbf{D}) \mathbf{X})^{-1} \mathbf{X}^\top \mathbf{\Gamma}) \mathbf{X} \mathbf{A}^{-1}.$$

□

*Proof of Lemma 10.* Let  $\mathbf{A} \triangleq \mathbf{X}^\top \mathbf{D} \mathbf{X}$ , then

$$\begin{aligned} &\left| \mathbf{z}^\top (\mathbf{X}^\top (\mathbf{D} + \mathbf{\Gamma}) \mathbf{X})^{-1} \mathbf{z} - \mathbf{z}^\top (\mathbf{X}^\top \mathbf{D} \mathbf{X})^{-1} \mathbf{z} \right| \\ &\stackrel{1}{=} \left| \mathbf{z}^\top \left( \mathbf{A}^{-1} \mathbf{X}^\top \mathbf{\Gamma} \mathbf{X} \mathbf{A}^{-1} - \mathbf{A}^{-1} \mathbf{X}^\top \mathbf{\Gamma} \mathbf{X} (\mathbf{X}^\top (\mathbf{D} + \mathbf{\Gamma}) \mathbf{X})^{-1} \mathbf{X}^\top \mathbf{\Gamma} \mathbf{X} \mathbf{A}^{-1} \right) \mathbf{z} \right| \\ &\stackrel{2}{\leq} \left| \mathbf{z}^\top \mathbf{A}^{-1} \mathbf{X}^\top \mathbf{\Gamma} \mathbf{X} \mathbf{A}^{-1} \mathbf{z} \right| + \left| \mathbf{z}^\top \mathbf{A}^{-1} \mathbf{X}^\top \mathbf{\Gamma} \mathbf{X} (\mathbf{X}^\top (\mathbf{D} + \mathbf{\Gamma}) \mathbf{X})^{-1} \mathbf{X}^\top \mathbf{\Gamma} \mathbf{X} \mathbf{A}^{-1} \mathbf{z} \right| \\ &\stackrel{3}{\leq} \|\gamma\|_2 \|\mathbf{X} \mathbf{A}^{-1} \mathbf{z}\|_4^2 + \mathbf{z}^\top \mathbf{A}^{-1} \mathbf{X}^\top \mathbf{\Gamma} \mathbf{X} (\mathbf{X}^\top (\mathbf{D} + \mathbf{\Gamma}) \mathbf{X})^{-1} \mathbf{X}^\top \mathbf{\Gamma} \mathbf{X} \mathbf{A}^{-1} \mathbf{z} \\ &\stackrel{4}{\leq} \|\gamma\|_2 \|\mathbf{X} \mathbf{A}^{-1} \mathbf{z}\|_4^2 + \left( \frac{\bar{\omega}_{\max}}{\nu_{\min}} \right) \mathbf{z}^\top \mathbf{A}^{-1} \mathbf{X}^\top \mathbf{\Gamma}^2 \mathbf{X} \mathbf{A}^{-1} \mathbf{z} \\ &\stackrel{5}{\leq} \|\gamma\|_2 \|\mathbf{X} \mathbf{A}^{-1} \mathbf{z}\|_4^2 + \left( \frac{\bar{\omega}_{\max}}{\nu_{\min}} \right) \|\gamma\|_4^2 \|\mathbf{X} \mathbf{A}^{-1} \mathbf{z}\|_4^2 \\ &= \left( \|\gamma\|_2 + \left( \frac{\bar{\omega}_{\max}}{\nu_{\min}} \right) \|\gamma\|_4^2 \right) \|\mathbf{X} \mathbf{A}^{-1} \mathbf{z}\|_4^2, \end{aligned} \quad (93)$$

where  $\stackrel{1}{=}$  is due to Lemma 9,  $\stackrel{2}{\leq}$  is due to the triangle inequality, and the fact that  $\mathbf{X}^\top (\mathbf{D} + \mathbf{\Gamma}) \mathbf{X}$  is positive definite,

and  $\stackrel{3}{\leq}$  and  $\stackrel{5}{\leq}$  are due to Cauchy-Schwartz inequality:

$$\mathbf{x}^\top \text{diag}[\boldsymbol{\gamma}] \mathbf{x} = \sum_{i=1}^n x_i^2 \gamma_i \leq \sqrt{\|\mathbf{x}\|_4^4 \|\boldsymbol{\gamma}\|_2^2} = \|\mathbf{x}\|_4^2 \|\boldsymbol{\gamma}\|_2.$$

Finally,  $\stackrel{4}{\leq}$  is due to (71) and (72). □

*Proof of Lemma 11.* Define the approximate leave- $i$ -out perturbation vector as

$$\hat{\Delta}_{/i} \triangleq \dot{\ell}_i(\hat{\beta}) [\mathbf{J}_{/i}(\hat{\beta}_{/i} - \Delta_{/i}^*)]^{-1} \mathbf{x}_i, \quad (94)$$

where the exact leave- $i$ -out perturbation vector is given by

$$\Delta_{/i}^* \triangleq \hat{\beta}_{/i} - \hat{\beta}. \quad (95)$$

Woodbury lemma yields:

$$\begin{aligned} \mathbf{x}_i^\top \hat{\Delta}_{/i} &= \dot{\ell}_i(\hat{\beta}) \mathbf{x}_i^\top \left( \lambda \text{diag}[\ddot{\mathbf{r}}(\hat{\beta}_{/i} - \Delta_{/i}^*)] + \mathbf{X}_{/i}^\top \text{diag}[\ddot{\ell}_{/i}(\hat{\beta}_{/i} - \Delta_{/i}^*)] \mathbf{X}_{/i} \right)^{-1} \mathbf{x}_i \\ &= \dot{\ell}_i(\hat{\beta}) \mathbf{x}_i^\top \left( \lambda \text{diag}[\ddot{\mathbf{r}}(\hat{\beta})] + \mathbf{X}_{/i}^\top \text{diag}[\ddot{\ell}_{/i}(\hat{\beta})] \mathbf{X}_{/i} \right)^{-1} \mathbf{x}_i \\ &= \dot{\ell}_i(\hat{\beta}) \mathbf{x}_i^\top \left( \lambda \text{diag}[\ddot{\mathbf{r}}(\hat{\beta})] + \mathbf{X}^\top \text{diag}[\ddot{\ell}(\hat{\beta})] \mathbf{X} - \mathbf{x}_i \mathbf{x}_i^\top \ddot{\ell}_i(\hat{\beta}) \right)^{-1} \mathbf{x}_i \\ &= \left( \frac{\dot{\ell}_i(\hat{\beta})}{\ddot{\ell}_i(\hat{\beta})} \right) \frac{\ddot{\ell}_i(\hat{\beta}) \mathbf{x}_i^\top \left( \lambda \text{diag}[\ddot{\mathbf{r}}(\hat{\beta})] + \mathbf{X}^\top \text{diag}[\ddot{\ell}(\hat{\beta})] \mathbf{X} \right)^{-1} \mathbf{x}_i}{1 - \ddot{\ell}_i(\hat{\beta}) \mathbf{x}_i^\top \left( \lambda \text{diag}[\ddot{\mathbf{r}}(\hat{\beta})] + \mathbf{X}^\top \text{diag}[\ddot{\ell}(\hat{\beta})] \mathbf{X} \right)^{-1} \mathbf{x}_i} \\ &= \left( \frac{\dot{\ell}_i(\hat{\beta})}{\ddot{\ell}_i(\hat{\beta})} \right) \frac{H_{ii}}{1 - H_{ii}}, \end{aligned} \quad (96)$$

where  $\mathbf{H} \triangleq \mathbf{X} \left( \lambda \text{diag}[\ddot{\mathbf{r}}(\hat{\beta})] + \mathbf{X}^\top \text{diag}[\ddot{\ell}(\hat{\beta})] \mathbf{X} \right)^{-1} \mathbf{X}^\top \text{diag}[\ddot{\ell}(\hat{\beta})]$ . Define

$$\mathbf{f}_{/i}(\boldsymbol{\theta}) \triangleq \lambda \dot{\mathbf{r}}(\boldsymbol{\theta}) + \mathbf{X}_{/i}^\top \dot{\ell}_{/i}(\boldsymbol{\theta}). \quad (97)$$

The leave-one-out estimate,  $\hat{\beta}_{/i} = \hat{\beta} + \Delta_{/i}^*$ , satisfies  $\mathbf{f}_{/i}(\Delta_{/i}^*) = 0$ . The multivariate mean-value Theorem yields

$$0 = \mathbf{f}_{/i}(\hat{\beta} + \Delta_{/i}^*) = \mathbf{f}_{/i}(\hat{\beta}) + \left( \int_0^1 \mathbf{J}_{/i}(\hat{\beta} + t \Delta_{/i}^*) dt \right) \Delta_{/i}^* \quad (98)$$

where the Jacobean is

$$\mathbf{J}_{/i}(\boldsymbol{\theta}) = \lambda \text{diag}[\ddot{\mathbf{r}}(\boldsymbol{\theta})] + \mathbf{X}_{/i}^\top \text{diag}[\ddot{\ell}_{/i}(\boldsymbol{\theta})] \mathbf{X}_{/i}. \quad (99)$$

Moreover,  $\hat{\beta}$  satisfies

$$0 = \lambda \dot{\mathbf{r}}(\hat{\beta}) + \mathbf{X}^\top \dot{\ell}(\hat{\beta}) = \mathbf{f}_{/i}(\hat{\beta}) + \dot{\ell}_i(\hat{\beta}) \mathbf{x}_i.$$

We get

$$\dot{\ell}_i(\hat{\beta})\mathbf{x}_i = \left( \int_0^1 \mathbf{J}_{/i}(\hat{\beta} + t\Delta_{/i}^*) dt \right) \Delta_{/i}^*,$$

so that

$$\Delta_{/i}^* = \dot{\ell}_i(\hat{\beta}) \left( \int_0^1 \mathbf{J}_{/i}(\hat{\beta} + t\Delta_{/i}^*) dt \right)^{-1} \mathbf{x}_i, \quad (100)$$

leading to the following inequality

$$\|\Delta_{/i}^*\|_2 \leq \left( \frac{|\dot{\ell}_i(\hat{\beta})|}{\nu} \right) \|\mathbf{x}_i\|_2, \quad (101)$$

as a consequence of Assumption 7. Next, we look at the part of  $\Delta_{i,\lambda}^*$  dependent on  $\mathbf{x}_i$ , so we rewrite (100) as

$$\Delta_{/i}^* = \dot{\ell}_i(\hat{\beta}) \left( \int_0^1 \mathbf{J}_{/i}(\hat{\beta}_{/i} - (1-t)\Delta_{/i}^*) dt \right)^{-1} \mathbf{x}_i. \quad (102)$$

Let us rewrite the Jacobean in a more compact form:

$$\mathbf{J}_{/i}(\boldsymbol{\theta}) = \bar{\mathbf{X}}_{/i}^\top \mathbf{D}_{/i}(\boldsymbol{\theta}) \bar{\mathbf{X}}_{/i}, \quad (103)$$

where

$$\bar{\mathbf{X}}_{/i} \triangleq \begin{bmatrix} \mathbf{X}_{/i} \\ \mathbf{I} \end{bmatrix} \in \mathbb{R}^{(n-1+p) \times p}, \quad \mathbf{D}_{/i}(\boldsymbol{\theta}) \triangleq \text{diag} \begin{bmatrix} \ddot{\ell}_{/i}(\boldsymbol{\theta}) \\ \lambda \ddot{\mathbf{r}}(\boldsymbol{\theta}) \end{bmatrix} \in \mathbb{R}^{(n-1+p) \times (n-1+p)}. \quad (104)$$

Define

$$\boldsymbol{\gamma}_{\boldsymbol{\delta}/i}(\boldsymbol{\theta}) \triangleq \begin{bmatrix} \ddot{\ell}_{/i}(\boldsymbol{\theta} + \boldsymbol{\delta}) - \ddot{\ell}_{/i}(\boldsymbol{\theta}) \\ \lambda(\ddot{\mathbf{r}}(\boldsymbol{\theta} + \boldsymbol{\delta}) - \ddot{\mathbf{r}}(\boldsymbol{\theta})) \end{bmatrix} \quad (105)$$

so that

$$\mathbf{J}_{/i}(\boldsymbol{\theta} + \boldsymbol{\delta}) = \mathbf{J}_{/i}(\boldsymbol{\theta}) + \bar{\mathbf{X}}_{/i}^\top \text{diag} [\boldsymbol{\gamma}_{\boldsymbol{\delta}/i}(\boldsymbol{\theta})] \bar{\mathbf{X}}_{/i}, \quad (106)$$

Note that  $\mathbf{J}_{/i}(\boldsymbol{\theta} + \boldsymbol{\delta})$  is positive definite for all  $t \in [0, 1]$ ,  $\boldsymbol{\theta} = \hat{\beta}_{/i}$  and  $\boldsymbol{\delta} = -(1-t)\Delta_{/i}^*$ , due to Assumption 7. The

last steps of the proof are as follows:

$$\begin{aligned}
& \left| \mathbf{x}_i^\top \Delta_{/i}^* - \mathbf{x}_i^\top \hat{\Delta}_{/i} \right| = |\dot{\ell}_i(\hat{\beta})| \left| \mathbf{x}_i^\top \left( \int_0^1 \mathbf{J}_{/i}(\hat{\beta}_{/i} - (1-t)\Delta_{/i}^*) dt \right)^{-1} \mathbf{x}_i - \mathbf{x}_i^\top \mathbf{J}_{/i}^{-1}(\hat{\beta}_{/i} - \Delta_{/i}^*) \mathbf{x}_i \right| \\
& \leq |\dot{\ell}_i(\hat{\beta})| \left| \mathbf{x}_i^\top \left( \int_0^1 \mathbf{J}_{/i}(\hat{\beta}_{/i} - (1-t)\Delta_{/i}^*) dt \right)^{-1} \mathbf{x}_i - \mathbf{x}_i^\top \mathbf{J}_{/i}^{-1}(\hat{\beta}_{/i}) \mathbf{x}_i \right| \\
& + |\dot{\ell}_i(\hat{\beta})| \left| \mathbf{x}_i^\top \mathbf{J}_{/i}^{-1}(\hat{\beta}_{/i}) \mathbf{x}_i - \mathbf{x}_i^\top \mathbf{J}_{/i}^{-1}(\hat{\beta}_{/i} - \Delta_{/i}^*) \mathbf{x}_i \right| \\
& \stackrel{0}{\leq} |\dot{\ell}_i(\hat{\beta})| \left| \mathbf{x}_i^\top \mathbf{J}_{/i}^{-1}(\hat{\beta}_{/i}) \mathbf{x}_i - \mathbf{x}_i^\top \left( \mathbf{J}_{/i}(\hat{\beta}_{/i}) + \bar{\mathbf{X}}_{/i}^\top \text{diag} \left[ \int_0^1 \gamma_{-(1-t)\Delta_{/i}^*/i}(\hat{\beta}_{/i}) dt \right] \bar{\mathbf{X}}_{/i} \right)^{-1} \mathbf{x}_i \right| \\
& + |\dot{\ell}_i(\hat{\beta})| \left| \mathbf{x}_i^\top \mathbf{J}_{/i}^{-1}(\hat{\beta}_{/i}) \mathbf{x}_i - \mathbf{x}_i^\top \left( \mathbf{J}_{/i}(\hat{\beta}_{/i}) + \bar{\mathbf{X}}_{/i}^\top \text{diag} \left[ \gamma_{-\Delta_{/i}^*/i}(\hat{\beta}_{/i}) \right] \bar{\mathbf{X}}_{/i} \right)^{-1} \mathbf{x}_i \right| \\
& \stackrel{1}{\leq} |\dot{\ell}_i(\hat{\beta})| \left( \left\| \int_0^1 \gamma_{-(1-t)\Delta_{/i}^*/i}(\hat{\beta}_{/i}) dt \right\|_2 + \left( \frac{\bar{\omega}_{\max,i}}{\nu} \right) \left\| \int_0^1 \gamma_{-(1-t)\Delta_{/i}^*/i}(\hat{\beta}_{/i}) dt \right\|_4^2 \right) \left\| \bar{\mathbf{X}}_{/i} \mathbf{J}_{/i}^{-1}(\hat{\beta}_{/i}) \mathbf{x}_i \right\|_4^2 \\
& + |\dot{\ell}_i(\hat{\beta})| \left( \left\| \gamma_{-\Delta_{/i}^*/i}(\hat{\beta}_{/i}) \right\|_2 + \left( \frac{\bar{\omega}_{\max,i}}{\nu} \right) \left\| \gamma_{-\Delta_{/i}^*/i}(\hat{\beta}_{/i}) \right\|_4^2 \right) \left\| \bar{\mathbf{X}}_{/i} \mathbf{J}_{/i}^{-1}(\hat{\beta}_{/i}) \mathbf{x}_i \right\|_4^2 \\
& \stackrel{2}{\leq} |\dot{\ell}_i(\hat{\beta})| \left( \left\| \int_0^1 \gamma_{-(1-t)\Delta_{/i}^*/i}(\hat{\beta}_{/i}) dt \right\|_2 + \left( \frac{\bar{\omega}_{\max,i}}{\nu} \right) \left\| \int_0^1 \gamma_{-(1-t)\Delta_{/i}^*/i}(\hat{\beta}_{/i}) dt \right\|_2^2 \right) \left\| \bar{\mathbf{X}}_{/i} \mathbf{J}_{/i}^{-1}(\hat{\beta}_{/i}) \mathbf{x}_i \right\|_4^2 \\
& + |\dot{\ell}_i(\hat{\beta})| \left( \left\| \gamma_{-\Delta_{/i}^*/i}(\hat{\beta}_{/i}) \right\|_2 + \left( \frac{\bar{\omega}_{\max,i}}{\nu} \right) \left\| \gamma_{-\Delta_{/i}^*/i}(\hat{\beta}_{/i}) \right\|_2^2 \right) \left\| \bar{\mathbf{X}}_{/i} \mathbf{J}_{/i}^{-1}(\hat{\beta}_{/i}) \mathbf{x}_i \right\|_4^2 \\
& \stackrel{3}{\leq} 4c_1(n)c_2(n) \left\| \Delta_{/i}^* \right\|_2 \left( 1 + 2c_2(n) \left\| \Delta_{/i}^* \right\|_2 \left( \frac{\bar{\omega}_{\max,i}}{\nu} \right) \right) \left\| \bar{\mathbf{X}}_{/i} \mathbf{J}_{/i}^{-1}(\hat{\beta}_{/i}) \mathbf{x}_i \right\|_4^2 \\
& \stackrel{4}{\leq} 4 \left\| \mathbf{x}_i \right\|_2 \left( \frac{c_1^2(n)c_2(n)}{\nu} \right) \left( 1 + \frac{2c_1(n)c_2(n)\bar{\omega}_{\max,i}}{\nu^2} \left\| \mathbf{x}_i \right\|_2 \right) \left\| \bar{\mathbf{X}}_{/i} \mathbf{J}_{/i}^{-1}(\hat{\beta}_{/i}) \mathbf{x}_i \right\|_4^2 \\
& \stackrel{5}{\leq} \underbrace{4 \left\| \mathbf{x}_i \right\|_2 \left( \frac{c_1^2(n)c_2(n)}{\nu} \right) \left( 1 + \frac{2c_1(n)c_2(n)(1+\omega_{\max,i})}{\nu^2} \left\| \mathbf{x}_i \right\|_2 \right)}_{\triangleq \bar{C}_i} \sqrt{\left\| \mathbf{X}_{/i} \mathbf{J}_{/i}^{-1}(\hat{\beta}_{/i}) \mathbf{x}_i \right\|_4^4 + \left\| \mathbf{J}_{/i}^{-1}(\hat{\beta}_{/i}) \mathbf{x}_i \right\|_4^4},
\end{aligned}$$

where

- $\stackrel{0}{\leq}$  is due (106).
- $\stackrel{1}{\leq}$  is due to Assumption 7, and Lemma 10, where  $\bar{\omega}_{\max,i} \triangleq \sigma_{\max}(\bar{\mathbf{X}}_{/i} \bar{\mathbf{X}}_{/i}^\top)$ .
- $\stackrel{2}{\leq}$  is due the fact that for any  $\gamma$  we have  $\|\gamma\|_4^2 \leq \|\gamma\|_2^2$ ,
- $\stackrel{3}{\leq}$  is due to Assumption 6 as illustrated below

$$\begin{aligned}
\left\| \gamma_{-\Delta_{/i}^*/i}(\hat{\beta}_{/i}) \right\|_2 & \leq \left\| \ddot{\ell}_{/i}(\hat{\beta}_{/i} - \Delta_{/i}^*) - \ddot{\ell}_{/i}(\hat{\beta}_{/i}) \right\|_2 + \left\| \lambda(\ddot{\mathbf{r}}(\hat{\beta}_{/i} - \Delta_{/i}^*) - \ddot{\mathbf{r}}(\hat{\beta}_{/i})) \right\|_2 \\
& \leq 2c_2(n) \left\| \Delta_{/i}^* \right\|_2.
\end{aligned}$$

Likewise,

$$\begin{aligned}
\left\| \int_0^1 \gamma_{-(1-t)\Delta_{/i}^*/i}(\hat{\beta}_{/i}) dt \right\|_2 & \leq \int_0^1 \left\| \gamma_{-(1-t)\Delta_{/i}^*/i}(\hat{\beta}_{/i}) \right\|_2 dt \\
& \leq \int_0^1 \left\| \ddot{\ell}_{/i}(\hat{\beta}_{/i} - (1-t)\Delta_{/i}^*) - \ddot{\ell}_{/i}(\hat{\beta}_{/i}) \right\|_2 dt \\
& + \int_0^1 \left\| \lambda(\ddot{\mathbf{r}}(\hat{\beta}_{/i} - (1-t)\Delta_{/i}^*) - \ddot{\mathbf{r}}(\hat{\beta}_{/i})) \right\|_2 dt \\
& \leq 2c_2(n) \left\| \Delta_{/i}^* \right\|_2.
\end{aligned} \tag{107}$$

Here we should emphasize that this is the main place in which we have used the smoothness of second derivatives of the loss and regularizer in Assumption 6. <sup>6</sup>

- $\stackrel{4}{\leq}$  is due to inequality (101), and Assumption 6.
- $\stackrel{5}{\leq}$  is due to (104), and

$$\begin{aligned}\bar{\omega}_{\max,i} &= \sigma_{\max}(\bar{\mathbf{X}}_{/i}\bar{\mathbf{X}}_{/i}^\top) = \sigma_{\max}(\bar{\mathbf{X}}_{/i}^\top\bar{\mathbf{X}}_{/i}) = \sigma_{\max}\left(\begin{bmatrix} \mathbf{X}_{/i} \\ \mathbf{I} \end{bmatrix}^\top \begin{bmatrix} \mathbf{X}_{/i} \\ \mathbf{I} \end{bmatrix}\right) \\ &= \sigma_{\max}(\mathbf{I} + \mathbf{X}_{/i}^\top\mathbf{X}_{/i}) \leq 1 + \sigma_{\max}(\mathbf{X}_{/i}^\top\mathbf{X}_{/i}) = 1 + \omega_{\max,i}.\end{aligned}\quad (110)$$

The final result follows the basic inequality:  $\sqrt{a^2 + b^2} \leq |a| + |b|$ .  $\square$

*Proof of Lemma 12.* First, we prove

$$\Pr\left[\|\mathbf{x}\|_\infty > \rho_{\max}\sqrt{2(1+c)\log p}\right] \leq \frac{2}{p^c} \quad (111)$$

as follows

$$\Pr[\|\mathbf{x}\|_\infty > t] \leq \sum_{i=1}^p \Pr[|x_i| > t] \leq 2 \sum_{i=1}^p e^{-\frac{t^2}{2\Sigma_{ii}}} \leq 2pe^{-\frac{t^2}{2\max_{i=1,\dots,p}\Sigma_{ii}}} \leq 2e^{\log p - \frac{t^2}{2\rho_{\max}}},$$

where  $t = \rho_{\max}\sqrt{2(1+c)\log p}$  and  $\max_{i=1,\dots,p}\Sigma_{ii} \leq \rho_{\max}$ . Second, we prove

$$\Pr[\|\mathbf{x}\|_4^2 > 2(1+c)\rho_{\max}\sqrt{p}\log p] \leq \frac{2}{p^c} \quad (112)$$

in the following way:

$$\begin{aligned}\Pr\left[\sqrt{\sum_{i=1}^p x_i^4} > t\right] &= \Pr\left[\sum_{i=1}^p x_i^4 > t^2\right] \leq \Pr\left[p \max_{i=1,\dots,p} x_i^4 > t^2\right] \\ &\leq \Pr\left[\|\mathbf{x}\|_\infty > \left(\frac{t^2}{p}\right)^{1/4}\right] \leq 2e^{\log p - \frac{t}{2\rho_{\max}\sqrt{p}}},\end{aligned}\quad (113)$$

where  $t = 2(1+c)\rho_{\max}\sqrt{p}\log p$  yields the desired result. Let  $\mathbf{z} \triangleq \mathbf{J}^{-1}\mathbf{x}$  and  $\mathbf{u} \triangleq \mathbf{X}\mathbf{J}^{-1}\mathbf{x}$ , then  $\mathbf{z}$  is zero mean Gaussian with covariance  $\Sigma_{\mathbf{z}} = \mathbf{J}^{-1}\Sigma\mathbf{J}^{-1}$  and  $\Sigma_{\mathbf{u}} = \mathbf{X}\mathbf{J}^{-1}\Sigma_{\mathbf{x}}\mathbf{J}^{-1}\mathbf{X}^\top$ , leading to

$$\sigma_{\max}(\Sigma_{\mathbf{z}}) = \sigma_{\max}(\mathbf{J}^{-1}\Sigma\mathbf{J}^{-1}) \leq \frac{\rho_{\max}}{\nu_{\min}^2}, \quad (114)$$

$$\sigma_{\max}(\Sigma_{\mathbf{u}}) = \sigma_{\max}(\mathbf{X}\mathbf{J}^{-1}\Sigma\mathbf{J}^{-1}\mathbf{X}^\top) \leq \frac{\rho_{\max}}{\nu_{\min}^2}\omega_{\max}. \quad (115)$$

---

<sup>6</sup>Note that by checking the derivation, it is clear that we can replace Assumption 6 with the following weaker assumptions:

$$c_2(n) > \sup_{t \in [0,1]} \frac{\|\ddot{\ell}_{/i}((1-t)\hat{\beta}_{/i} + t\hat{\beta}) - \ddot{\ell}_{/i}(\hat{\beta})\|_2}{\left\|\hat{\beta}_{/i} - \hat{\beta}\right\|_2^\zeta} \quad (108)$$

$$c_2(n) > \sup_{t \in [0,1]} \frac{\|\ddot{\mathbf{r}}((1-t)\hat{\beta}_{/i} + t\hat{\beta}) - \ddot{\mathbf{r}}(\hat{\beta})\|_2}{\left\|\hat{\beta}_{/i} - \hat{\beta}\right\|_2^\zeta} \quad (109)$$

for some  $\zeta > 0$ , and still find an (weaker) upper bound for  $\left|\mathbf{x}_i^\top \Delta_{/i}^* - \mathbf{x}_i^\top \hat{\Delta}_{/i}\right|$  that converges to zero as  $n, p \rightarrow \infty$ .

Therefore, we have

$$\begin{aligned} & \Pr \left[ \|\mathbf{J}^{-1}\mathbf{x}\|_4^2 > 2(1+c) \left( \frac{\rho_{\max}}{\nu_{\min}^2} \right) \sqrt{p} \log p \right] \\ & \leq \Pr \left[ \|\mathbf{J}^{-1}\mathbf{x}\|_4^2 > 2(1+c) \sigma_{\max}(\mathbf{\Sigma}_{\mathbf{z}}) \sqrt{p} \log p \right] \leq \frac{2}{p^c}, \end{aligned}$$

and

$$\begin{aligned} & \Pr \left[ \|\mathbf{X}\mathbf{J}^{-1}\mathbf{x}\|_4^2 > 2(1+c) \left( \frac{\rho_{\max}}{\nu_{\min}^2} \omega_{\max} \right) \sqrt{m} \log m \right] \\ & \leq \Pr \left[ \|\mathbf{X}\mathbf{J}^{-1}\mathbf{x}\|_4^2 > 2(1+c) \sigma_{\max}(\mathbf{\Sigma}_{\mathbf{u}}) \sqrt{m} \log m \right] \leq \frac{2}{m^c}. \end{aligned}$$

□

*Proof of Lemma 14.* Since  $\mathbf{X} \in \mathbb{R}^{n \times p}$  is composed of independently distributed  $\mathcal{N}(0, \mathbf{\Sigma})$  rows, then

$$\begin{aligned} & \Pr [\sigma_{\max}(\mathbf{X}\mathbf{X}^\top) \geq \sigma_0] = \Pr [\sigma_{\max}(\mathbf{X}^\top\mathbf{X}) \geq \sigma_0] \\ & = \Pr \left[ \max_{\|\mathbf{u}\|_2^2 \leq 1} \|\mathbf{X}\mathbf{u}\|_2^2 \geq \sigma_0 \right] = \Pr \left[ \max_{\|\mathbf{u}\|_2^2 \leq 1} \|\mathbf{Z}\mathbf{\Sigma}^{1/2}\mathbf{u}\|_2^2 \geq \sigma_0 \right] \\ & = \Pr \left[ \max_{\|\mathbf{\Sigma}^{-1/2}\mathbf{u}\|_2^2 \leq 1} \|\mathbf{Z}\mathbf{u}\|_2^2 \geq \sigma_0 \right] \leq \Pr \left[ \max_{\|\frac{\mathbf{u}}{\sqrt{\rho_{\max}}}\|_2^2 \leq 1} \|\mathbf{Z}\mathbf{u}\|_2^2 \geq \sigma_0 \right] \\ & = \Pr \left[ \max_{\|\mathbf{u}\|_2^2 \leq 1} \|\mathbf{Z}\mathbf{u}\|_2^2 \geq \frac{\sigma_0}{\rho_{\max}} \right] = \Pr \left[ \sqrt{\sigma_{\max} \left( \frac{\mathbf{Z}^\top\mathbf{Z}}{n} \right)} \geq \sqrt{\frac{\sigma_0}{n\rho_{\max}}} \right], \end{aligned} \quad (116)$$

where  $\mathbf{Z} \in \mathbb{R}^{n \times p}$  is composed of independently distributed  $\mathcal{N}(0, 1/n)$  entries. As a consequence of Lemma 13, and letting  $\sigma_0 = n\rho_{\max} (1 + \sqrt{\frac{p}{n}} + t)^2$ , we get

$$\Pr \left[ \sigma_{\max}(\mathbf{X}\mathbf{X}^\top) \geq n\rho_{\max} \left( 1 + \sqrt{\frac{p}{n}} + t \right)^2 \right] \leq e^{-nt^2/2}. \quad (117)$$

Finally, let  $t = \sqrt{\frac{2p}{n}}$ , yielding

$$\Pr \left[ \sigma_{\max}(\mathbf{X}\mathbf{X}^\top) \geq n\rho_{\max} \left( 1 + 3\sqrt{\frac{p}{n}} \right)^2 \right] \leq e^{-p}.$$

□

## A.6 Ridge example

In Section 4, we claimed that under the asymptotic setting  $n/p \rightarrow \delta_o$  for some  $\delta_o$  bounded away from zero, a refinement of the arguments presented in [El Karoui, 2018, Donoho and Montanari, 2016, Donoho et al., 2011, Bayati and Montanari, 2012, Weng et al., 2018] will offer  $C_o = O(\text{poly log } n)$ . The main objective of this section is to confirm this claim. Toward this goal we offer bounds on parameters  $\rho_{\max}$ ,  $c_1(n)$ ,  $c_2(n)$ , and  $\nu$  that appear in the expression of  $C_o$ . To demonstrate our argument, we focus on a simple example in which the regularizer is  $r(\boldsymbol{\beta}) = \|\boldsymbol{\beta}\|_2^2$ .

### A.6.1 Model

Suppose that in finding  $\hat{\beta}$  and  $\hat{\beta}_{/i}$ , in (1) and (4) respectively, we set  $\ell(y|\mathbf{x}^\top\beta) = \omega(y - \mathbf{x}^\top\beta)$  where the cost function  $\omega(\cdot)$  is three times differentiable and its third derivative satisfies  $\ddot{\omega}(|z|) \leq K_1|z|^{m_1}$  for some fixed numbers  $K_1$  and  $m_1$ . Furthermore, we assume that  $\dot{\omega}(z) \leq K_2|z|^{m_2}$  for fixed numbers  $K_2$  and  $m_2$ . Moreover let  $r(\beta) = \|\beta\|_2^2$ . The ridge regression problem

$$\sum_{i=1}^n \omega(y_i - \mathbf{x}_i^\top\beta) + \lambda\|\beta\|_2^2, \quad (118)$$

has been extensively studied in [El Karoui, 2018], under the following data generation model:

$$y_i = \mathbf{x}_i^\top\beta^* + \epsilon_i,$$

where the entries of  $\mathbf{x}_i$  are IID  $N(0, \mathbf{I})$  random vectors,  $\epsilon_i \sim N(0, \sigma^2)$  and  $\|\beta^*\|_2^2$  remains bounded. With a standard rescaling argument, assuming  $n/p = \Theta(1)$ , we look at the equivalent problem where  $\mathbf{x}_i$  are IID  $N(0, \frac{\mathbf{I}}{n})$  random vectors,  $\epsilon_i \sim N(0, \sigma^2)$  and  $\|\beta^*\|_2^2 = \Theta(p)$ . Specifically, we assume that the empirical distribution of the elements of  $\beta^*$  are converging weakly to a non-degenerate distribution  $p_\beta$ . Furthermore, suppose that  $\frac{1}{p} \sum (\beta_i^*)^2 \rightarrow \int t^2 dp_\beta(t) < \infty$ . Note that the scaling of  $\mathbf{x}_i$  and  $\beta^*$  ensures that the signal-to-noise ratio of each observation is bounded away from zero or infinity. This ensures that the optimal choice of  $\lambda$ , that minimizes the out-of-sample prediction error, converges to fixed number away from 0 and  $\infty$ . For more evidence on this claim, refer to [Mousavi et al., 2018]. Before, proceeding to the calculation of  $c_1(n)$ ,  $c_2(n)$ , and  $\rho_{\max}$  we would like to explain the reason for some of the assumptions we have made above. In particular, it usually seems more natural to assume  $\mathbf{x}_i \sim N(\mathbf{0}, \mathbf{I})$ , rather than  $\mathbf{x}_i \sim N(\mathbf{0}, \mathbf{I}/n)$ . Then, the question is why have we chosen the scaling  $\mathbf{I}/n$ ? The answer lies in the following simple observation. Suppose that we use the scaling  $\mathbf{x}_i \sim N(\mathbf{0}, \mathbf{I})$ . Then, it is straightforward to see that  $\text{var}(\mathbf{x}_i^\top\beta) = \Theta(p)$ . Since the variance of  $\epsilon_i$  is a fixed number, as the dimension of the problem increases, the signal-to-noise ratio in each observation goes to infinity, which is statistically a simple regime. On the other hand, under the scaling considered in this paper, the signal-to-noise ratio per observation is fixed, and the optimal choice of  $\lambda$  converges to a finite non-zero number [Mousavi et al., 2018].

In the next two sections, for this setup we obtain upper bounds for  $c_1(n)$ ,  $c_2(n)$ , and  $\rho_{\max}$ , and a lower bound for  $\nu$ , thereby addressing Assumptions 5, 6, and 7.

### A.6.2 Discussion of Assumption 6

The following theorem, a simple corollary of Theorem 3.9 of [El Karoui, 2018], provides bounds on  $c_1(n)$  and  $c_2(n)$ .<sup>7</sup>

**Theorem 6.** *Under the assumptions discussed in Section A.6.1, we have*

$$\begin{aligned} \sup_j |y_j - \mathbf{x}_j^\top\hat{\beta}| &= O_p(\text{poly log } n), \\ \sup_{1 \leq i \leq n} \sup_j |y_j - \mathbf{x}_j^\top\hat{\beta}_{/i}| &= O_p(\text{poly log } n). \end{aligned} \quad (119)$$

Now we can use this result to prove our main claim.

---

<sup>7</sup>We should emphasize that the scaling that is used in [El Karoui, 2018] is slightly different from the one we consider in this section. In particular, [El Karoui, 2018] uses  $\mathbf{x}_i \sim N(0, \mathbf{I})$ , but assumes that  $\beta^* = O_p(1)$ . Nevertheless, since this is a simple change of scaling, it is straightforward to transfer their results to our scaling as well.

**Theorem 7.** *Under the assumptions discussed in Section A.6.1, we have*

$$\sup_{t \in [0,1]} \sup_i \frac{\|\ddot{\ell}_{/i}((1-t)\hat{\beta}_{/i} + t\hat{\beta}) - \ddot{\ell}_{/i}(\hat{\beta})\|_2}{\|\hat{\beta}_{/i} - \hat{\beta}\|_2} = O_p(\text{poly log } n).$$

*Proof.* Define  $\chi_n = \max(\sup_j |y_j - \mathbf{x}_j^\top \hat{\beta}|, \sup_{1 \leq i \leq n} \sup_j |y_j - \mathbf{x}_j^\top \hat{\beta}_{/i}|)$ . Note that according to Theorem 6, we have  $\chi_n = O_p(\text{poly log } n)$ . By using the mean value theorem, we have

$$\ddot{\ell}_j((1-t)\hat{\beta}_{/i} + t\hat{\beta}) - \ddot{\ell}_j(\hat{\beta}) = \ddot{\omega}(\tilde{y}_{ij})(1-t)(\mathbf{x}_j^\top (\hat{\beta}_{/i} - \hat{\beta})), \quad (120)$$

where  $\tilde{y}_{ij}$  belongs to the interval between  $y_j - \mathbf{x}_j^\top \hat{\beta}$  and  $y_j - \mathbf{x}_j^\top ((1-t)\hat{\beta}_{/i} + t\hat{\beta})$ . Hence, if we define  $\ddot{\mathbf{W}}^i = \text{diag}([\ddot{\omega}(\tilde{y}_{i1}), \dots, \ddot{\omega}(\tilde{y}_{i,i-1}), \ddot{\omega}(\tilde{y}_{i,i+1}), \dots, \ddot{\omega}(\tilde{y}_{i,n})])$ , then

$$\begin{aligned} \sup_i \frac{\|\ddot{\ell}_{/i}((1-t)\hat{\beta}_{/i} + t\hat{\beta}) - \ddot{\ell}_{/i}(\hat{\beta})\|_2}{\|\hat{\beta}_{/i} - \hat{\beta}\|_2} &= \sup_i (1-t) \frac{\|\ddot{\mathbf{W}}^i \mathbf{X}_{/i}(\hat{\beta}_{/i} - \hat{\beta})\|_2}{\|\hat{\beta}_{/i} - \hat{\beta}\|_2} \\ &\leq \sup_i (1-t) \sup_{j \neq i} |\ddot{\omega}(\tilde{y}_{ij})| \sigma_{\max}(\mathbf{X}_{/i}) \\ &\leq \sup_i \sup_{j \neq i} |\ddot{\omega}(\tilde{y}_{ij})| \sigma_{\max}(\mathbf{X}). \end{aligned} \quad (121)$$

Note that according to Lemma 13 with probability  $1 - e^{-\frac{n}{2}}$ , we have  $\sigma_{\max}(X) \leq 2 + \sqrt{\frac{p}{n}}$ . Furthermore, given that  $\sup_i \sup_{j \neq i} |\tilde{y}_{ij}| \leq \chi_n$ , and the third derivative of  $\omega$  grows at most polynomially, by using Theorem 6 we have

$$\sup_i \sup_{j \neq i} |\ddot{\omega}(\tilde{y}_{ij})| = O_p(\text{poly log } n). \quad (122)$$

Combining (122) and (121) establishes the result.  $\square$

Note that since  $\dot{\omega}(z)$  has polynomial growth, it is straightforward to use Theorem 6 and show that

$$\|\dot{\ell}(\hat{\beta})\|_\infty = O_p(\text{poly log } n).$$

Hence, we have  $c_1(n) = O_p(\text{poly log } n)$ .

### A.6.3 Discussion of Assumption 5 and 7

For the model described in Section A.6.1 the covariance matrix  $\Sigma = \text{diag}([1/n, 1/n, \dots, 1/n])$ . Hence,  $\rho_{\max} = 1/n$ . Since  $p$  is growing with  $n$ , to keep the signal to noise ratio of each response variable fixed, we have set the variance of each element of the design matrix to  $1/n$ . Finally, note that the ridge penalty  $r(\beta) = \|\beta\|_2^2$  implies that  $\text{diag}[\ddot{r}(\beta)] = \mathbf{I}_{p \times p}$ , leading to  $\nu > \lambda$ .

### A.6.4 Summary

By plugging the bounds we derived for  $\nu$ ,  $\rho_{\max}$ ,  $c_1(n)$  and  $c_2(n)$  in Sections A.6.2 and A.6.3 in (26) we obtain  $C_o = O_p(\text{poly log } n)$ .



## A.7 ALO and LO in the $p$ fixed and large $n$ regime

As we discussed so far, our main concern in this paper is high-dimensional settings in which  $n$  is proportional to  $p$ . However, to present a complete picture about ALO, in this section, we study it in the classical asymptotic regime where  $n$  is large and  $p$  is fixed. The assumptions presented here will be used throughout Section A.7 only. Let

$$\hat{\beta}_{\lambda_n} \triangleq \arg \min_{\beta \in \mathbb{R}^p} \left\{ \sum_{i=1}^n \ell(y_i | \mathbf{x}_i^\top \beta) + \lambda_n r(\beta) \right\}.$$

We also assume that the samples  $\{(\mathbf{x}_i, y_i)\}_{i=1}^n$  are independent and identically distributed, and that  $\frac{\lambda_n}{n} \rightarrow \lambda^*$ . Define,

$$\beta^* = \arg \min_{\beta} \mathbb{E} \ell(y_i | \mathbf{x}_i^\top \beta) + \lambda^* r(\beta).$$

Also, define

$$\begin{aligned} \mathbf{R} &\triangleq \mathbb{E} \left\{ \dot{\ell}(y | \mathbf{x}^\top \beta^*) \dot{\phi}(y, \mathbf{x}^\top \beta^*) \mathbf{x} \mathbf{x}^\top \right\}, \\ \mathbf{K} &\triangleq \mathbb{E} \left\{ \ddot{\ell}(y | \mathbf{x}^\top \beta^*) \mathbf{x} \mathbf{x}^\top + \lambda^* \text{diag}[\ddot{\mathbf{r}}(\beta^*)] \right\}. \end{aligned} \quad (123)$$

For the sake of brevity, we follow [Stone, 1977] and make the following assumptions that enable us avoid repeating standard asymptotic arguments that can be found elsewhere, e.g. in [Van der Vaart, 2000]:

(B.1) As  $n \rightarrow \infty$   $\hat{\beta}_{\lambda_n} \xrightarrow{p} \beta^*$ .

(B.2)  $\sup_i \|\hat{\beta}_{\lambda_n/i} - \beta^*\|_2 \xrightarrow{p} 0$ .

(B.3) Define  $\Delta_{/i} \triangleq \hat{\beta}_{\lambda_n} - \hat{\beta}_{\lambda_n/i}$ . Let  $b_1, b_2, \dots, b_n$  and  $c_1, c_2, \dots, c_n$  denote  $2n$  numbers between  $[0, 1]$  that may depend on the dataset  $\mathcal{D}$ . Then, we assume that

$$\frac{\mathbf{X} \text{diag} \left[ \ddot{\ell}(\hat{\beta}_{\lambda_n} + b_i \Delta_{/i}) \right] \mathbf{X}^\top + \lambda_n \text{diag}[\ddot{\mathbf{r}}(\hat{\beta}_{\lambda_n} + c_i \Delta_{/i})]}{n} \xrightarrow{p} \mathbf{K}.$$

(B.4) Let  $a_1, \dots, a_n$  denote  $n$  number between  $0, 1$  that may depend on dataset  $\mathcal{D}$ . Then, assume that

$$\frac{1}{n} \sum_{i=1}^n \mathbf{x}_i \mathbf{x}_i^\top \dot{\ell}_i(\hat{\beta}_{\lambda_n/i}) \dot{\phi} \left( y_i, \mathbf{x}_i^\top \hat{\beta}_{\lambda_n} + a_i \mathbf{x}_i^\top \Delta_{/i} \right) \xrightarrow{p} \mathbf{R}.$$

(B.5) Note that

$$H_{ii} = \mathbf{x}_i^\top \left( \mathbf{X} \text{diag}[\ddot{\ell}(\hat{\beta}_{\lambda_n})] \mathbf{X}^\top + \lambda \text{diag}[\ddot{\mathbf{r}}(\hat{\beta}_{\lambda_n})] \right)^{-1} \mathbf{x}_i \ddot{\ell}_i(\hat{\beta}_{\lambda_n}).$$

Hence, we also assume that  $H_{ii} \xrightarrow{p} 0$ .

(B.6) Let  $d_1, d_2, \dots, d_n$  denote  $n$  numbers between  $[0, 1]$ . Note that we have already assumed that  $\sup_i H_{ii} \xrightarrow{p} 0$ .

We further assume that

$$\sum_{i=1}^n \left( \frac{\mathbf{x}_i \mathbf{x}_i^\top}{n} \right) \left( \frac{\dot{\ell}_i(\hat{\beta}_{\lambda_n})}{1 - H_{ii}} \right) \dot{\phi} \left( y_i, \mathbf{x}_i^\top \hat{\beta} + d_i \left( \frac{\dot{\ell}_i(\hat{\beta}_{\lambda_n})}{\dot{\ell}_i(\hat{\beta}_{\lambda_n})} \right) \left( \frac{H_{ii}}{1 - H_{ii}} \right) \right) \xrightarrow{p} \mathbf{R}.$$

It should be clear that all these assumptions can be proved under appropriate regularity conditions on the loss function and the regularizer. Note that according to this theorem the error between ALO and LO is  $o_p(1/n)$ .

**Theorem 8.** Under assumptions (B.1), (B.2), ..., (B.6), we have  $n(\text{ALO}_{\lambda_n} - \text{LO}_{\lambda_n}) \xrightarrow{P} 0$ , as  $n \rightarrow \infty$ .

*Proof.* For notational simplicity instead of using  $\lambda_n$  we use  $\lambda$  in our formulas. However, the reader should note that  $\lambda/n \rightarrow \lambda^*$ . First note that the gradient condition implies that

$$\mathbf{X}_{/i} \dot{\boldsymbol{\ell}}_{/i}(\hat{\boldsymbol{\beta}}_{/i}) + \lambda \dot{\mathbf{r}}(\hat{\boldsymbol{\beta}}_{/i}) = 0.$$

Hence,

$$\mathbf{X} \dot{\boldsymbol{\ell}}(\hat{\boldsymbol{\beta}}_{/i}) + \lambda \dot{\mathbf{r}}(\hat{\boldsymbol{\beta}}_{/i}) = \dot{\ell}_i(\hat{\boldsymbol{\beta}}_{/i}) \mathbf{x}_i. \quad (124)$$

Furthermore, we can use the fact that  $\mathbf{X} \dot{\boldsymbol{\ell}}(\hat{\boldsymbol{\beta}}) + \lambda \dot{\mathbf{r}}(\hat{\boldsymbol{\beta}}) = 0$  to obtain

$$\mathbf{X} \dot{\boldsymbol{\ell}}(\hat{\boldsymbol{\beta}}_{/i}) + \lambda \dot{\mathbf{r}}(\hat{\boldsymbol{\beta}}_{/i}) - \mathbf{X} \dot{\boldsymbol{\ell}}(\hat{\boldsymbol{\beta}}) - \lambda \dot{\mathbf{r}}(\hat{\boldsymbol{\beta}}) = \dot{\ell}_i(\hat{\boldsymbol{\beta}}_{/i}) \mathbf{x}_i$$

Since both the loss function and the regularizer are assumed to be twice continuously differentiable, we can use the mean value theorem to simplify this expression to

$$\left( \mathbf{X} \text{diag} \left[ \ddot{\boldsymbol{\ell}} \left( \hat{\boldsymbol{\beta}} + b_i \boldsymbol{\Delta}_{/i} \right) \right] \mathbf{X}^\top + \lambda \text{diag} \left[ \ddot{\mathbf{r}} \left( \hat{\boldsymbol{\beta}} + c_i \boldsymbol{\Delta}_{/i} \right) \right] \right) \boldsymbol{\Delta}_{/i} = \dot{\ell}_i(\hat{\boldsymbol{\beta}}_{/i}) \mathbf{x}_i, \quad (125)$$

where all  $b_i$ s and  $c_i$ s are in  $[0, 1]$ . Furthermore, if  $\phi$  is continuously differentiable, then we can again use the mean value theorem to obtain

$$\begin{aligned} \text{LO} &= \frac{1}{n} \sum_{i=1}^n \phi(y_i, \mathbf{x}_i^\top \hat{\boldsymbol{\beta}}) + \frac{1}{n} \sum_{i=1}^n \mathbf{x}_i^\top \boldsymbol{\Delta}_{/i} \dot{\phi} \left( y_i, \mathbf{x}_i^\top \hat{\boldsymbol{\beta}} + a_i \mathbf{x}_i^\top \boldsymbol{\Delta}_{/i} \right) = \frac{1}{n} \sum_{i=1}^n \phi(y_i, \mathbf{x}_i^\top \hat{\boldsymbol{\beta}}) \\ &+ \frac{1}{n} \sum_{i=1}^n \mathbf{x}_i^\top \left( \mathbf{X} \text{diag} \left[ \ddot{\boldsymbol{\ell}} \left( \hat{\boldsymbol{\beta}} + b_i \boldsymbol{\Delta}_{/i} \right) \right] \mathbf{X}^\top + \lambda \text{diag} \left[ \ddot{\mathbf{r}} \left( \hat{\boldsymbol{\beta}} + c_i \boldsymbol{\Delta}_{/i} \right) \right] \right)^{-1} \mathbf{x}_i \\ &\times \dot{\ell}_i(\hat{\boldsymbol{\beta}}_{/i}) \dot{\phi} \left( y_i, \mathbf{x}_i^\top \hat{\boldsymbol{\beta}} + a_i \mathbf{x}_i^\top \boldsymbol{\Delta}_{/i} \right). \end{aligned}$$

Hence,

$$\begin{aligned} \text{LO} &- \frac{1}{n} \sum_{i=1}^n \phi(y_i, \mathbf{x}_i^\top \hat{\boldsymbol{\beta}}) \\ &= \frac{1}{n} \sum_{i=1}^n \text{trace} \left[ \left( \mathbf{X} \text{diag} \left[ \ddot{\boldsymbol{\ell}} \left( \hat{\boldsymbol{\beta}} + b_i \boldsymbol{\Delta}_{/i} \right) \right] \mathbf{X}^\top + \lambda \text{diag} \left[ \ddot{\mathbf{r}} \left( \hat{\boldsymbol{\beta}} + c_i \boldsymbol{\Delta}_{/i} \right) \right] \right)^{-1} \mathbf{x}_i \mathbf{x}_i^\top \right] \\ &\times \dot{\ell}_i(\hat{\boldsymbol{\beta}}_{/i}) \dot{\phi} \left( y_i, \mathbf{x}_i^\top \hat{\boldsymbol{\beta}} + a_i \mathbf{x}_i^\top \boldsymbol{\Delta}_{/i} \right). \end{aligned}$$

It is then straightforward to use Assumptions (B.3) and (B.4) to claim that

$$n(\text{LO} - \frac{1}{n} \sum_{i=1}^n \phi(y_i, \mathbf{x}_i^\top \hat{\boldsymbol{\beta}})) \xrightarrow{P} \text{trace}(\mathbf{K}^{-1} \mathbf{R}).$$

Similarly, we can use the mean value theorem to argue that

$$\begin{aligned}
\text{ALO} &= \frac{1}{n} \sum_{i=1}^n \phi(y_i, \mathbf{x}_i^\top \hat{\boldsymbol{\beta}}) \\
&+ \frac{1}{n} \sum_{i=1}^n \left( \frac{H_{ii}}{\ddot{\ell}_i(\hat{\boldsymbol{\beta}})} \right) \times \left( \frac{\dot{\ell}_i(\hat{\boldsymbol{\beta}})}{1 - H_{ii}} \right) \dot{\phi} \left( y_i, \mathbf{x}_i^\top \hat{\boldsymbol{\beta}} + d_i \left( \frac{\dot{\ell}_i(\hat{\boldsymbol{\beta}})}{\ddot{\ell}_i(\hat{\boldsymbol{\beta}})} \right) \left( \frac{H_{ii}}{1 - H_{ii}} \right) \right) \\
&= \frac{1}{n} \sum_{i=1}^n \phi(y_i, \mathbf{x}_i^\top \hat{\boldsymbol{\beta}}) + \frac{1}{n} \text{trace} \left[ \left( \frac{\mathbf{X} \text{diag}[\ddot{\boldsymbol{\ell}}(\hat{\boldsymbol{\beta}})] \mathbf{X}^\top + \lambda \text{diag}[\ddot{\mathbf{r}}(\hat{\boldsymbol{\beta}})]}{n} \right)^{-1} \right. \\
&\times \left. \sum_{i=1}^n \left( \frac{\mathbf{x}_i \mathbf{x}_i^\top}{n} \right) \left( \frac{\dot{\ell}_i(\hat{\boldsymbol{\beta}})}{1 - H_{ii}} \right) \dot{\phi} \left( y_i, \mathbf{x}_i^\top \hat{\boldsymbol{\beta}} + d_i \left( \frac{\dot{\ell}_i(\hat{\boldsymbol{\beta}})}{\ddot{\ell}_i(\hat{\boldsymbol{\beta}})} \right) \left( \frac{H_{ii}}{1 - H_{ii}} \right) \right) \right]
\end{aligned}$$

with  $|d_i| \leq 1$ ,  $i = 1, \dots, n$ . Again it is straightforward to use Assumptions (B.3) and (B.6) to show that

$$n(\text{ALO} - \frac{1}{n} \sum_{i=1}^n \phi(y_i, \mathbf{x}_i^\top \hat{\boldsymbol{\beta}})) \xrightarrow{P} \text{trace}(\mathbf{K}^{-1} \mathbf{R}). \quad (126)$$

□